Abstract

Title of dissertation RAPID ADAPTIVE PLASTICITY IN AUDITORY CORTEX

Serin Atiani, PhD 2010

Directed by Dr. Shihab Shamma, Electrical and Computer Engineering Department

Navigating the acoustic environment entails actively listening for different sound sources, extracting signal from a background of noise, identifying the salient features of a signal and determining what parts of it are relevant. Humans and animals in natural environments perform such acoustic tasks routinely, and have to adapt to changes in the environment and features of the acoustic signals surrounding them in real time. Rapid plasticity has been reported to be a possible mechanism underling the ability to perform these tasks. Previous studies report that neurons in primary auditory cortex (A1) undergo changes in spectro-temporal tuning that enhance the discriminability between different sound classes, modulating their tuning to enhance the task relevant feature. This thesis investigates rapid task related plasticity in two distinct directions; first I investigate the effect of manipulating task difficulty on this type of plasticity. Second I expand the investigation of rapid plasticity into higher order auditory areas. With increasing task difficulty, A1 neurons' response is altered to increasingly suppress the representation of the noise while enhancing the representation of the signal. Comparing adaptive plasticity

in secondary auditory cortex (PEG) to A1, PEG neurons further enhance the discriminability of the sound classes by an even greater enhancement of the target response. Taken together these results indicate that adaptive neural plasticity is a plausible mechanism that underlies the performance of novel auditory behaviors in real time, and provide insights into the development of behaviorally significant representation of sound in auditory cortex.

Rapid Adaptive Plasticity in Auditory Cortex

by

Serin Atiani

Dissertation to be submitted to the Faculty of the Graduate School of the
University of Maryland, College Park, in partial fulfillment
of the requirements for the degree of
Doctor of Philosophy
2010

Advisory Committee:
Dr. Shihab Shamma, Chair
Dr. Jonathan Simon
Dr. David Poeppel
Dr. Robert Dooling
Dr. Cynthia Moss

Acknowledgements

My work towards this thesis has been a great learning process, one that started on day one and hasn't ended yet. I have been blessed for having so many people whose help, insights, contributions, and support went into making this process a rich life experience.

A great deal of thanks goes to Dr. Shihab Shamma, whose mentorship, insights, science and more importantly belief put me on the right track and supported me through a long process that I hope will be first step in a long career. Many thanks go Dr. Jonathan Simon for his help, direction and many important conversations along the way. Many thanks go to Dr. David Poeppel for the scientific discussions, and for teaching me to question the conventional. And many thanks to Dr. Bob Dooling and Dr. Cindy Moss for accepting to be members of this committee and for their help and support for me as student through these years. Special thanks goes to Dr. Jonathan Fritz for his critical eye and for teaching me how to do physiological experiments; to Dr. Pingbo Yin, whose long patient teachings helped me become the physiologist that I am, and to Dr. Mounya El-Hilali and Dr. Stephen David for their guidance, support and many critical insights into my work that helped make it better

I would like to thank members of Neural Systems Laboratory and the NACS program, for their friendship and support. To Nima, Ling, Kevin, Anu, Phill, Baily, Majid, and everybody else: your wonderful company and support gave graduate school the human dimension that makes it an better learning experience.

These past years wouldn't have been possible without the friends that have been family away from family in the US. And non of what I am would have been possible with

out my loving cherishing family, my mother Maha Abu Issa, my father Ibrahim Atiani and my brother Samer Atiani, who planted in me ambition and supported and believed in me through all my dreams, my good and bad choices. And this thesis wouldn't have been completed if it wasn't for the love, support and encouragement of my love and life partner Osama Qasem, whose love, support and belief helped me through the last and most critical months, and for that I will always be grateful!

College Park,

April 2010

Serin

Table of contents

List of Tables:

List of Figures

Chapter 1: Introduction

The auditory cortex is essential for the perception and localization of complex sounds (Gerstein and Kiang 1964, Whitfield and Evans 1965, Brugge et al 1973, Whitfield 1980, Middlebrooks et al 1980, Schreiner et al. 1995, Wang et al. 1995, Wang 2000, Eggermont 2001, Sutter 2005, Recanzone and Sutter 2007, Kanwal and Rauschecker 2007). While its precise role in carrying out these functions remains uncertain, extensive neurophysiological experiments over the last couple of decades have shed new light on the neural responses and patterns of activity by which it encodes sound. In particular, it has become evident that cortical units exhibit dynamic responses and adaptive receptive fields.

Understanding the adaptive and dynamic nature of cortical units is critical to reaching a better understanding of their rich and diverse functions. Research over the last two decade has demonstrated that sensory receptive fields and cortical response maps can be modified throughout adulthood in mammals. Moreover, these changes can occur at any time scale; slowly over days and months during recovery from injury or during extended training to rapidly (seconds to minutes) while the animal engages in a behavioral task. One common term that has been consistently used to describe these changes is plasticity. Moucha and Kilgard define plasticity as “the remarkable ability of developing, adult, and aging brains to adapt to a changing world”. As described, plasticity occurs in sensory and motor systems following deprivation of input or overstimulation, increased or decreased usage, learning of new skills, and injury. These experience-dependent changes can be as subtle as a change in neuronal excitability (Engineer et al., 2004) or as dramatic as the rewiring of auditory cortex to

process visual information (Sur et al., 1988). Topographic maps, receptive field size, neuronal firing rate, temporal precision, and combination sensitivity can all be modified by our experiences. The types of plasticity activated by specific situations depend on the nature of the experiences, the behavioral significance and the characteristics of the stimuli.

As such auditory experience can have profound global effects by reshaping cortical maps and significant local effects by transforming receptive field properties of neurons in auditory cortex (Edeline 1999, Weinberger 2007). The type and form plasticity is highly dependent on the type of auditory experience or task at hand, the salience of spectrotemporal charachteristic of the stimuli and the time scale investigated. Injury induced plasticity studies have focused on the reorganization of cortical maps and recovery of function after injury. Lesion studies were conducted to probe the type of plasticity that takes place during recovery, and the effect that training has on plasticity and recovery of function (Jenkins and Merzenich, 1987, Nudo et al., 1996) demonstrating that sensorimotor experience is instrumental in directing plasticity towards a more complete recovery.

The majority of plasticity research in the auditory modality has focused on receptive field conditioning and long terms changes in auditory cortex. Animals were trained in a feature specific detection or discrimination paradigm that involved extended training on specific inputs inducing long-term perceptual learning (Recanzone et al., 1993, Blake et al., 2002, Brown et al., 2004, Irvine et al., 2004). Animals were trained to practice a task that engages a limited region of the sensory epithelium, resulting in enlargement in the regions responding to the trained stimulus

characteristics in the cortical map. Cortical receptive fields narrowed or broadened and response latency increased or decreased depending on the spectral and temporal characteristic of the conditioned stimuli. (Edeline and Weinberger, 1993, Recanzone et al., 1993). Owl monkeys trained on a tone frequency discrimination task have A1 neurons with enlarged representation of the trained frequency in the cortical map, narrower RFs and longer response latencies than untrained controls (Recanzone et al., 1993). This experimental paradigm allowed investigation of long term effects of perceptual learning, taking a static look at plasticity after training is finished and in most of these studies (with the exception of Ohl and Scheich, 1996, and Ohl et. al 2001) while the animal is under anesthesia.

In the last few years an experimental protocol was developed that facilitated the study of the neural basis of active listening and a shorter time scale of plasticity, Which is investigated during the engagement in a task. These experiments studied task dependent changes that emerge *during* the performance of the task, i.e. changes that emerge on the time scale of seconds to minutes as the subject is engaged in task performance (Fritz et al 2003, 2005, 2007). While this type of plasticity is the result of training, it requires active engagement of the task. Animals were trained on a behavioral paradigm that relied on rule based tasks making certain features of the stimuli more or less relevant during the performance of the task. The reliance of this paradigm on a task rule, and the ability to observe the changes during the performance of the task allowed for the expansion of the training to larger stimulus sets, varying the relevant features, rather than training on a specific frequency or specific temporal feature.

When the animals were trained to distinguish between different stimuli from different sound classes, neural receptive fields in A1 adapted to enhance the representation of features of the relevant stimuli and suppress those that are irrelevant (Fritz et al., 2003, 2005, 2007). This work has resulted in the hypothesis that rapid plasticity is an ongoing process that dynamically adapts cortical receptive fields in response to changing environments. Cortical receptive fields are situated at the focal juncture of this process, depicted by the highly schematized diagram in Figure 1.1. During the performance of the task in a trained animal, receptive fields adapt to enhance behavioral performance, monitored through external (reward or aversive) feedback signals. The auditory cortex receives acoustic relevant and irrelevant input cues, and generates corresponding sensory representations that are ultimately associated with, or mapped to motor behavior. The formation of a specific sensory-motor map defines a specific learnt task or behavioral context (Firtz et al 2005, Blake et al 2006). This process is hypothesized to involve a network including auditory, parietal and frontal cortex.

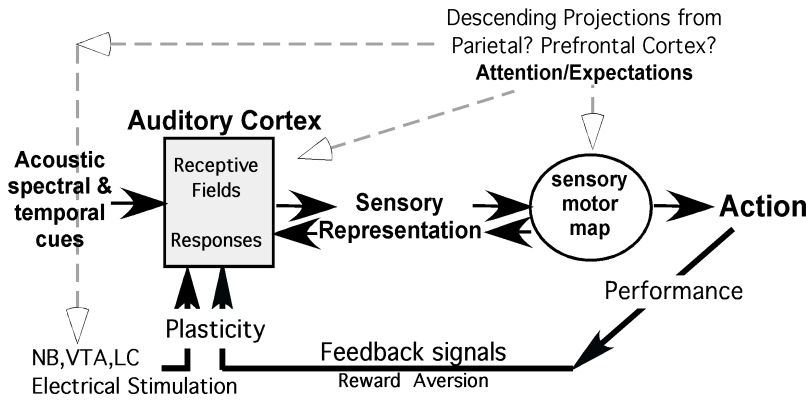

Figure 1.1 Schematic of areas and pathways critical for task performance

Given this hypothesis I expect a direct correlation between the task difficulty and the magnitude and form of induced adaptive cortical plasticity. Increased task difficulty requires higher level of attentional resources to solve the task whose difficulty is manifested by a reduction in the space between the classes of stimuli that the animal is required to distinguish. Another prediction from the above hypothesis is that the adaptation of the cortical receptive fields in higher order cortical areas should take a form and magnitude that diverges from direct representation of physical features of the stimuli and more of their the behavioral significance. Therefore I expect that plasticity in higher order auditory areas is larger in magnitude and closer in form to the representation of the behaviorally relevant signal in executive and motor areas of the brain which directly underlie the behavior of the animal.

This thesis expands on previous work from our lab to investigate first: the effect of task difficulty on rapid plasticity, second: rapid plasticity in higher order cortical areas.

To study the effect of task difficulty on rapid plasticity the experiments I conducted increased task difficulty by imbedding a pure tone in a noise like stimulus and manipulating the difficulty by varying the level of the tone while keeping the level of the noise constant. I explored the effect of varying task difficulty and on this type of plasticity. Results are reported in chapter 3

To study plasticity in higher order auditory areas, I employed a similar experimental paradigm with a slightly altered task, and recorded from primary and secondary auditory areas in the awake behaving ferret. I present the data from secondary auditory areas in comparison to the data collected under the same

conditions and stimuli in primary auditory cortex. This allowed for a direct comparison of rapid plasticity in these two different auditory cortical areas. Results are reported in chapter 4

A last small study of tuning properties is included in chapter 5 investigating tuning properties of local field potentials (LFP) in comparison with tuning properties of the spiking activity of multi units in auditory cortex. I analyze the tuning properties of the aggregate LFP signal and 4 of its components frequency bands: alpha, beta, gamma and high gamma and compare their tuning properties to those of the multi unit from the same recording site. I study these properties in response to narrow, band pass and broad band signal. This study was conducted as a prerequisite to studying the imprint of rapid plasticity on the LFP signal.

Chapter 2: Review of the auditory system

The auditory system consists of the ear and parts of the central nervous system (CNS). Technically, the term ear refers to the entire peripheral auditory apparatus including the outer, middle, and inner ear. Sound information is then projected along a multitude of channels making up the main auditory pathway. In the following section, we briefly review the structure of the different auditory nuclei and review basic knowledge about their role in sound perception.

1.1 Auditory periphery

Incoming sound waves entering the ear make the eardrum vibrate. The sound energy is then converted into mechanical energy, which produces a complex spatio-temporal pattern of vibrations along the basilar membrane of the cochlea (Figure 2). The maximal displacement at each cochlear point corresponds to a distinct tone frequency in the stimulus, creating a tonotopically ordered response axis along the length of the cochlea (Durrant, and Lovrinic 1995, Yost 2000).

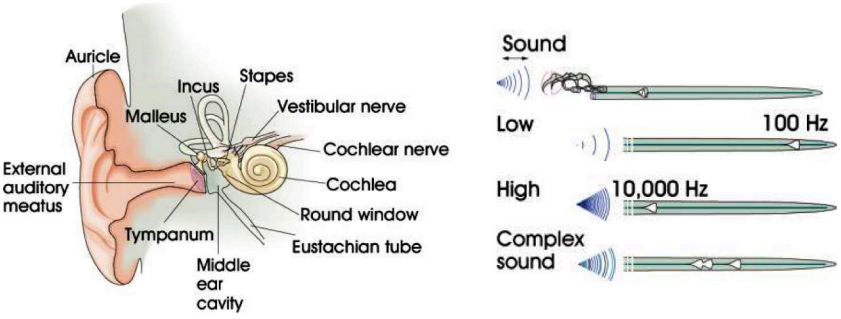

Figure 2.1: Ear and cochlea (Kandel et al 2000).

Following the cochlear stage, the stimulus frequency and intensity are then encoded at the level of the cochlear nerve fibers through innervation of the inner hair cells.

While the activity of the nerve fibers is thought to be relatively homogeneous in terms of vibration patterns (Moore 1995), the next relay station -the cochlear nucleus, appears to be more intricate. Various projections within the cochlear nucleus constitute parallel pathways for analyzing different sound attributes. Present evidence suggests a role of the cochlear nucleus in enhancing and sharpening the features of the neural patterns, prior to relaying them to more central areas via the superior olivary complex (SOC) and the inferior colliculus (IC) (Palmer et. al 1995).

1.2 Central pathways

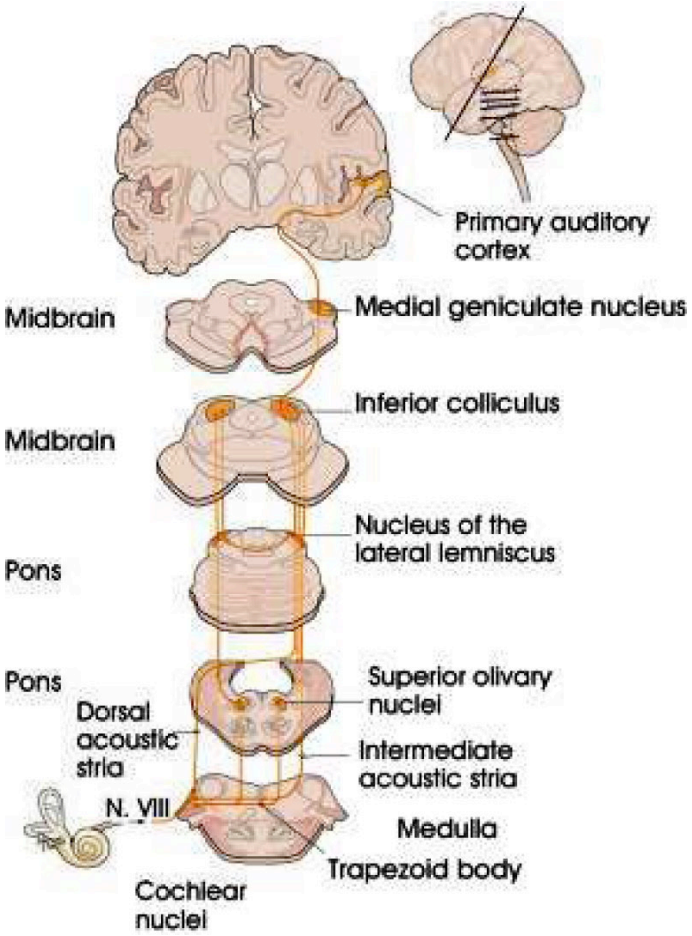

Figure 2.2: The central auditory pathway (Kandel et al 2000).

At this stage along the auditory pathway, the acoustic waveform is converted into

a pattern of neural activity that faithfully maps the temporal and spectral attributes of the incoming sound. The following stages begin the process of temporal integration and the formation of a coherent auditory image. Nuclei of the midbrain, the Inferior Colliculus (IC) in particular is believed to be the first stage in the system where all the acoustic information converges together, coming through projections from the superior olivary complex and the lateral lemniscus (Kandel et al. 2000) (Figure 2.3). The IC appears to act both as an integrative station as well as a switchboard to higher auditory and multi-modal sensory areas. It also plays a key role in binaural hearing and thus in sound localization (Eggermont 2001).

If the IC is believed to be the last station in the auditory pathway whose function is directed towards the formation of auditory images, the subsequent auditory nuclei are thought to play a role in the analysis of this auditory image and hence in the perception of sound (Eggermont 2001). The nuclei beyond IC, including the auditory thalamus (Medial Geniculate Body, MGB) and auditory cortex are hence involved in the process of auditory pattern recognition, where the features of the auditory image are sharpened and grouped together into streams, mediated by auditory memory and contextual information. Present evidence seems to favor a role of cortical circuitry in auditory pattern recognition. As most of the interesting auditory features are already extracted by the level of the IC, it is suggested that the auditory cortex is playing a role in organizing these features in terms of auditory objects (Nelken 2004a)

It is, however, very important to stress that the structure and function of the central auditory nervous system is far less understood than the periphery. The anatomical complexity of the pathways, the neural morphology of cells and circuitry, as well as the unknown nature of the neural code have made it very difficult to study the central pathways of the auditory system. Our current knowledge of the auditory functions mediated by the different nuclei is very limited, and greatly speculative. Nonetheless, evidence from imaging as well as physiological and anatomical studies are laying the grounds for a better understanding of the function of the central auditory system and the neural strategies of sound perception.

1.3 Neural receptive fields

As we try to understand how the acoustic environment and auditory experiences are represented in auditory cortex, a natural step is to characterize the selectivity of auditory neurons to external stimuli. Clearly, different neurons respond variably to different stimulus patterns, and a functional description of each cell's behavior is its receptive field. A receptive field is a description of the optimal input that elicits the strongest response in a neuron. In the case of auditory neurons, the receptive field is generally described as a one-dimensional (spectral) or a two-dimensional (spectral and temporal) function called STRF (Spectro-Temporal Receptive Field), which acts as a time-dependent spectral transfer function, or a frequency-dependent dynamical filter (DeCharm st al.1998, Klien et al 2000, Theunissen et al. 2000).

STRFs are a linear mapping from the sound spectrogram $s(f, t)$ to the neural response $r(t)$. The convolution of the receptive field with the spectrotemporal

representation *s(f, t)* of a stimulus captures the linear component of the response of the neuron *r(t)* as demonstrated in equation [1]. Taking the applying the fourier transform to equation [1] gives us equation [2].

$$r(t) = \int s(f,t) \cdot STRF(f, t-\tau)\, d\tau \qquad \ldots [1]$$

$$F\{r(t)\} \Rightarrow R(\omega) = \sum_{f} S(f,\omega) \cdot H(f,\omega) \ldots [2]$$

STRFs are measured by reverse correlating with the dynamic spectra of the stimuli, which in this case are 30 different instances of temporally orthogonal ripple combinations (TORCs)

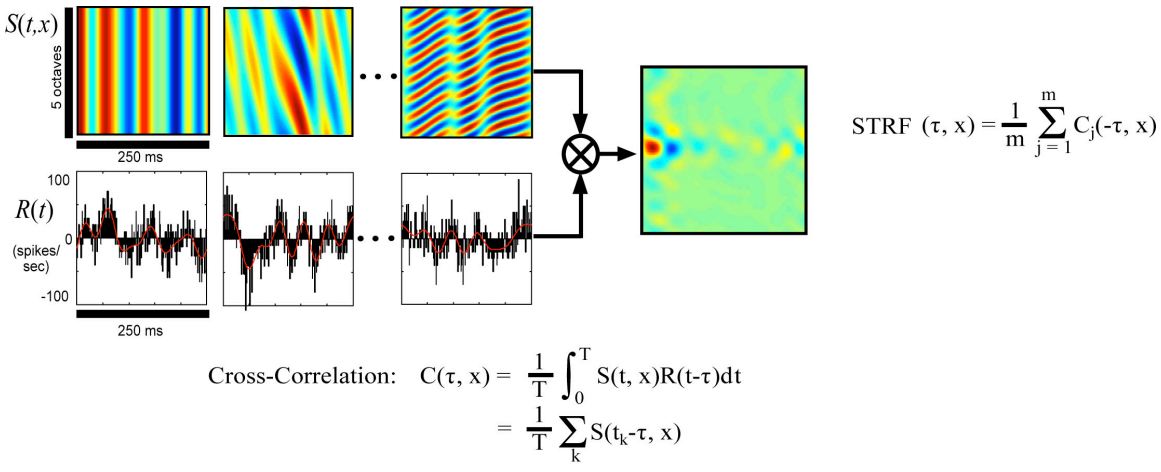

Figure 2.3 STRF estimation

STRFs have been very instrumental in understanding the behavior of neurons in the auditory system, especially at the cortical level. They offer a quantitative linear description of the neurons' selectivity to specific stimulus patterns, and hence led to a better understanding of cortical processing. However as a model the STRF is limited because it is a linear model describing a non-linear system. Therefore STRFs can be thought of as a linear snapshot of a non-linear system. STRF estimation are not effective in measuring the receptive field of neurons in higher order cortical areas

where the responses are temporally sluggish and where neural response fail to phase lock to the envelop of TORCs which results in low yield STRFs. This requires a different measure to estimate receptive field in these areas. In Chapter 4 we use one dimensional spectral estimation of the receptive field of the probed cells. This as we explain in due course doesn't convey information about the temporal dynamics of the neural response, however it presents a robust measure for the estimation receptive fields in primary and secondary auditory cortex, which is necessary for direct comparison of tuning properties and plasticity in these areas.

Chapter3: Effect of task difficulty on receptive fields in A1

3.1 Introduction

Humans and animals commonly navigate noisy auditory scenes in which distracters and loud background sounds obscure foreground signals of interest. The mechanisms that give rise to the ability to discern and extract targeted auditory signals from noise are multifaceted, including simple adaptation to steady background noise, the perception of pitch that facilitates segregation of simultaneous speakers, and the localization and selective attention to one among spatially distributed sound sources. One process that may underlie some of these abilities is real-time adaptive plasticity in which the auditory system changes its filter properties in order to optimize its ability to discriminate foreground from background. Reports have previously described a form of rapid cortical plasticity in which the spectro-temporal receptive fields (STRFs) in primary auditory cortex (A1) adapt *during* the task in a manner that maximizes the discrimination of the target (foreground) relative to reference (background) signals (Fritz et al., 2003). Different aspects of this process have been recently explored in a series of experiments in which animals were trained to discriminate tones or tone-complexes from broadband noise, or discriminate between two tones of different frequencies (Fritz et al., 2005, 2007b). In all these experiments, the pattern of STRF changes that emerged followed a simple model in which the acoustic features of the foreground were enhanced and those of the background suppressed, a hypothesis called a "contrast matched filter" (Fritz et al., 2007a). Such changes matched the signals' spectra, so as to enhance the STRF

responsiveness to the target relative to the reference. For instance, when a target tone is discriminated from a broadband noise reference, an excitatory region at the frequency of the tone emerges in the STRFs, surrounded by a region of suppression; but when the target tone is discriminated from a different reference tone (Fritz et al., 2005), the enhanced target excitation now becomes contrasted with suppression at the frequency of the reference tone.

However, an important and previously unresolved question is whether the magnitude of these changes is influenced by task difficulty, or more specifically, by the perceptual difference between the target and reference signals that the animal must discriminate. Furthermore, it is unknown how exactly the underlying receptive fields change under these circumstances, i.e., whether they simply exhibit a modulated gain, or alternatively, a change of shape such as tuning or bandwidth. A handful of previous studies of visual processing have demonstrated that increased task difficulty generally enhances allocation of attention and the magnitude of its neural correlates in cortical responses (Boudreau et al., 2006; Spitzer et al., 1988; Spitzer and Richmond, 1991). These measurements, however, did not distinguish receptive field gain from shape changes, and how increased task difficulty affected them differentially.

This study explores these issues using an auditory detection task in which a target tone was embedded in broadband noise of fixed amplitude, and task difficulty was modulated by varying the signal-to-noise ratio of the target (SNR). As target SNR decreased, distinguishing the target from the reference noise became more difficult, requiring more attention or effort, which, I predicted, could cause larger

adaptive changes in the STRF. To explore this hypothesis, ferrets were trained to perform this task in a paradigm that was identical to one that used by Fritz et al. 2003, replacing the pure tone target with pure tone embedded in broad band noise. In such a paradigm, the reference broadband noise was one of a set of 30 specially designed spectrotemporally modulated broadband noisy sounds - called TORCs - that were used to measure the STRF of the cell while the animal performed the task (Klein et al., 2000). The target tone here was simply embedded in the last of a sequence of TORCs, with a variable SNR that ranged from +15 to -10 dB. This approach allowed for the measure of full STRF of the cell rather than just its firing rates in response to a stimulus within its receptive field. Such a broad view enabled assessment of a variety of adaptive gain and tuning changes that might otherwise be difficult to detect.

The key feature of the tone-in-noise task is that, unlike the case with pure-tone targets, the TORCs appeared not only as reference stimuli but also as maskers *in* the target stimulus, thus reducing the perceptual difference between target and reference signals. The animal presumably had to actively suppress the noise so as to enhance the detectability of the embedded target tone. This chapter describes how rapid A1 plasticity in this task depended on three key factors: (i) task difficulty as reflected by the SNR of the target (i.e., *high, medium,* or *low SNR),* and (ii) cell's BF relative to the frequency of the target tone (i.e., *near* or *far*), (iii) the performance of the animal.

3.2 Methods

Stimuli

Reference stimuli were randomly chosen from a set of 30 TORCS (temporally orthogonal ripple combinations (Klein et al., 2000)), broadband stimuli that spectrally span 5 octaves. Each of the 30 TORCs was a broadband noise with a dynamic spectral profile that is the superposition of the envelopes of 6 ripples. A single ripple has a sinusoidal spectral profile, with peaks equally spaced at 0 (flat) to 1.2 peaks-per-octave; the envelope drifted temporally up or down the logarithmic frequency axis at a constant velocity from 4 Hz up to 24 Hz (Depireux et al., 2001; Klein et al., 2000; Kowalski et al., 1996; Miller et al., 2002). Targets consisted of 1.5 sec tones embedded in one of the set of 30 TORCs used as references. Target tone frequency was chosen based on the best frequency (BF) of one of the isolated units. The amplitude of the tone (and hence SNR) was set for a given experiment. However across experiments tone amplitude ranged from -10 dB to +15 dB relative to the amplitude of the TORCs (Depireux et al., 2001; Klein et al., 2000). The ratio of the amplitude of the tone to that of TORCs is referred to as signal-to-noise ratio (SNR) of the target sound.

A trial consisted of a sequence of reference stimuli (ranging from 1-7 TORCs) followed by a target (except on catch trials in which 7 reference stimuli were presented with no target). A target was equiprobable for every position (2-7) in the sequence (~20%).

During most of training and all active physiological measurements, the acoustic stimuli were 1.5 seconds in duration. In passive STRF measurements, TORC stimuli

were longer (3 seconds), which allowed for more rapid receptive field measurements. During physiological recording from contralateral A1, the computer-generated stimuli were monaurally delivered through an inserted earphone (Etymotic) that was calibrated *in-situ* at the beginning of each experiment. The amplitude of TORC stimuli was set at a value in the range between 60-75 dB (set for a given experiment) during physiological recording.

Training paradigm and procedure

Three adult ferrets were trained on the tone-in-noise detection task using a conditioned avoidance procedure (Fritz et al., 2003; Heffner and Heffner, 1995). Ferrets licked water from a spout while listening to a sequence of reference stimuli until they heard a target sound consisting of a tone embedded in one of the reference stimuli. Length of reference and target stimuli was always the same, and for most of training and all recording sessions stimulus length was 1.5 seconds. When presented with a target, the animals were trained to briefly stop licking, in order to avoid a mild shock.

We started behavioral training by initially training the ferrets on a pure tone detection task (Fritz et al., 2003) until the animal reached criterion, defined as consistent performance on the detection task pure tone targets for two sessions with >80% hit rate accuracy and >80% safe rate for a discrimination rate > 0.65, where the safe rate is (1- false alarm rate). Safe rate was measured from the response rate during the reference (safe stimuli). Safe rate for a trial is measured by averaging the response of the animal for all the references in that trial.

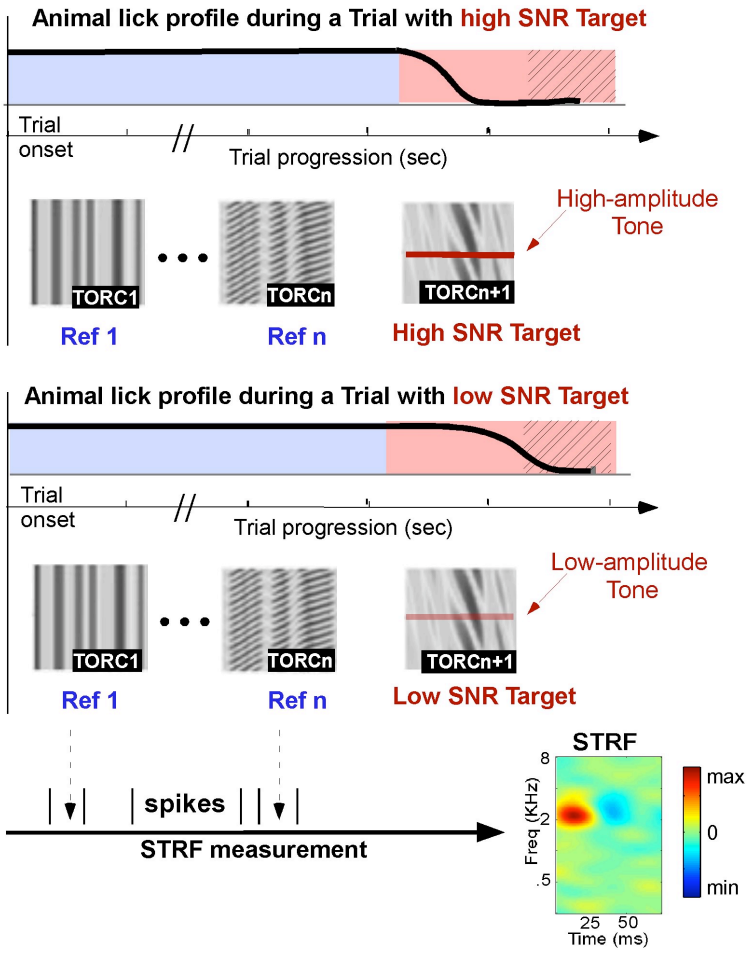

Figur 3.1 Schematic of the experimental stimuli and data e analysis. A series of spectrotemporal modulated noise bursts (TORC1,TORC2, ...TORCn) (where n=1 or 2 …or 6, in catch trials there were 7 references with no target) served as *referenc* sounds that ended with an *e* embedded *targe* tone whose level relative to *t* the noise was adjusted in different tasks to range from *high SNR (>=0 dB), mid SNR (<-5 dB >= to <0 dB), low SNR (<-5 dB).* Animals licked water from a spout during the *referenc* bursts (blue region), and were trained to withhold licking upon hearing *e* the *targe* tone (pink region). The response latency to the target was shorter in high *t* SNR (top panel) than in low SNR tasks (bottom panel). STRF measurements were made only from responses during presentation of the *referenc* TORCs, *e* no *t* from target

Once the criterion for pure tone performance was reached, we started adding noise (a TORC) to the tone in the target sound, initially with high SNR. Once the animal reached the behavioral criterion for that SNR we continued to decrease the SNR in subsequent sessions to as low as -10dB SNR Animals were not reliably able to reach behavioral criterion at levels below –10dB SNR.

The ferrets were trained daily (~60 trials/session) in a sound-attenuating chamber (IAC Isolation Booth). Initial training on pure tone detection in the free-running test box took about 4 weeks for each ferret to reach criterion. Subsequent training on the tone-in-noise detection task took an additional 4-6 weeks. Ferrets trained on the tone-in-noise task were further tested on the task with different SNRs ranging from -10dB SNR to +15dB SNR in 5dB steps, and tone frequencies ranging from 125Hz to 16000Hz. We also tested the ferrets on the pure tone detection task as an extreme case of the tone-in-noise task with an infinite SNR. In each training session the target tone frequency was fixed and the animal was trained for 4 to 6 training blocks of 10 trials each. For each training block the target SNR was fixed, but was randomly varied between successive blocks.

During the physiological experiments, the animals performed from one to three separate task sessions, each consisting of about 40 trials. Within each task session, the target frequency and SNR were held constant, but were varied across successive task sessions.

Surgery

To secure stability for electrophysiological recording, a stainless steel head-post was surgically implanted on the skull. During surgery, the ferrets were

anaesthetized with a combination of Ketamine-Xylazine for induction, and isoflurane (1-2%) for maintenance of deep anesthesia throughout the surgery. Using sterile procedure, the skull was surgically exposed and the head-post was mounted using bone cement, leaving clear access to primary auditory cortex in both hemispheres. Antibiotics and post-surgery analgesics were administered as needed following surgery.

Post-surgical habituation and training

After recovery from head-post implantation (2 weeks), the ferrets were habituated to head restraint in a customized Lucite horizontal holder over a period of 1-2 weeks, Animal performance suffered from the transition from a performance of the task with free movement in the initial training period to performance under head fixed condition, therefore animals were re-trained on the task for an additional 2 to 3 weeks while restrained in the holder (further details in (Fritz et al., 2005)). The task-naive control ferret received no behavioral training on the discrimination task, but like the other head-post implanted ferrets, also received gradual habituation to head restraint in the holder, before physiological recording commenced.

Neurophysiological recording

Experiments were conducted in a double-walled, sound-attenuation chamber (IAC). Small craniotomies (1-2 mm in diameter) were made over primary auditory cortex prior to recording sessions that lasted 6-8 hours. We used single and multiple independently moveable electrodes (AlphaOmega). In our standard electrode

configuration, there were up to 4 recording electrodes separated by ~500 microns from their nearest neighbor. Single units (typically 1-4 neurons/electrode) were isolated using off-line spike sorting techniques with custom-designed MATLAB software. In each individual recording session we slowly advanced electrodes until we had isolated cells on all separate electrodes. The range of best frequencies in a given experiment varied from 0.5- 2.5 octaves. This allowed us to simultaneously test the effect of the target tone frequency on different cells whose BFs were at different spectral distances from the target tone. BF was defined as the frequency of the largest excitatory peak in the STRF.

Responses from each microelectrode were recorded and then stored, filtered and spike-sorted off-line. Multiunit records were constructed by thresholding responses to obtain spikes, by triggering at a level four standard deviations (4σ) above baseline variation in the raw trace. Electrode location in A1 was based on the presence of distinctive A1 physiological characteristics such as latency and tuning (Bizley et al., 2005; Nelken et al., 2004; Shamma et al., 1993).

STRF Analysis

STRFs were measured using reverse correlation (Klein et al., 2000). Response variance (σ) was estimated using a bootstrap procedure (Depireux et al., 2001; Efron and Tibshirani, 1993) and an overall signal-to-noise ratio (SNR_{STRF}) was computed for each STRF. STRFs with an $SNR_{STRF} < 0.4$ were excluded from further analysis. Each STRF plot was therefore associated with a particular variance (σ). Excitatory (positive) and inhibitory (negative) fluctuations from the mean of the STRF were deemed significant only if they exceeded a level of 2σ. This analysis and

criteria also applied in determining the significant changes between two STRFs, i.e., in the $STRF_{diff}$. Thus, a significant STRF change refers to a suppressive or facilitative region in the $STRF_{diff}$ that exceeded the 2σ criterion.

To measure the STRF with a reliable SNR_{STRF} we collected neural responses to multiple repetitions of the set of stimuli used, each repetition consisted of 30 TORCs. To measure the population effect of the task, we first computed the $STRF_{diff}$ for each unit. We then located the maximum point of each $STRF_{diff}$ in a band +/- 0.2 octaves around the BF of the cell and within the first 1-25 ms of the STRF. Each $STRF_{diff}$ was then aligned at the local maximum points to measure the average effect across the population. To compare the population effects in behaving and in naïve animals (Fig.SD-2), we accumulated the $STRF_{diff}$ for units that showed significant changes in the spectrotemporal window defined above and divided the sum by the total number of units in that set of STRFs. To determine changes in the sharpness of tuning of the cell, we measured the bandwidth of the tuning of the cell. STRF bandwidth was defined as the width of excitatory area around the BF peak, measured at the frequencies where the amplitude decreased to 20% of the BF peak.

Gain and *shape* changes in STRFs were computed in two distinct ways to provide a counter check of the results. In the **first method**, we defined the *active* (during-behavior) *STRF* ($\mathbf{S_d}$) as the sum of a scaled pre-task *passive STRF* ($\mathbf{S_b}$) and a task-dependent change in the shape of the STRF, i.e.:

$$\mathbf{S_d} = g.\mathbf{S_b} + \delta,$$

where g is the *gain* that reflects the fraction of the STRF that maintained its original shape, and δ is the remaining (orthogonal) portion of the STRF that could not be

captured by scaling $\mathbf{S_b}$. We also assumed that our measurements of the $\mathbf{S_b}$ and $\mathbf{S_d}$ were contaminated by corresponding noise terms (e.g., $\mathbf{n_b}$ and $\mathbf{n_d}$, with $\mathbf{S_b} = \mathbf{S_b^o} + \mathbf{n_b}$, $\mathbf{S_d} = \mathbf{S_d^o} + \mathbf{n_d}$, and $\mathbf{S_b^o}$, $\mathbf{S_d^o}$ are the ideal STRFs). Taking the inner-product with $\mathbf{S_b}$ on both sides of the equation, and having (by orthogonality) $< \delta, \mathbf{S_b} > = 0$, then

$$gain = g = <\mathbf{S_d},\mathbf{S_b}> / (\sigma_b^2 - \sigma_{nb}^2)$$

where < , > is inner product between the two STRFs, and σ_b^2 is the power of the initial STRF (or $<\mathbf{S_b},\mathbf{S_b}>$), σ_{nb}^2 is the power in the noise of the initial STRF . Pure *shape* changes were therefore expressed as: $\delta = \mathbf{S_d} - g.\mathbf{S_b}$, and this δ was used in generating Fig.3.7C.

The second method employed a *gain fitting STRF model* (David et al., 2008). The model measured the STRF from responses to TORCs presented in the passive pre-behavioral, active behavioral, and passive post-behavioral epochs. This average STRF was then used to predict the response of the neuron to the TORCs, which was then compared to the actual neural responses observed during each of the three epochs. Predicted responses were then adjusted by a scalar gain so as minimize the mean-square error separately for each of the three epochs, mentioned above. The ratio of the scalars computed during behavior and pre-behavior was used as the gain shown in Figs.SD-3B (which is analogous to those in Fig SD-3A and Figs.3.7B using the previous method). This approach allowed for an independent estimate of gain that reflected the response properties of the neurons and the variability of the responses between the three different epochs.

3.3 Results

3.3.1 Behavioral Tasks and Results

Figure 3.1 illustrates the basic task, in which ferrets learned to lick a spout for liquid reward during a number (1-7) of reference sounds, but to refrain from licking during target sounds, using a conditioned avoidance paradigm (Fritz et al., 2003; Heffner and Heffner, 1995). The top and bottom panels illustrate the spectra of the noise (TORC) reference and target tone stimuli, respectively, in *high* and *low SNR* conditions. The noise added to the target was randomly chosen from the set of 30 possible spectro-temporally modulated and broadband TORCs, delivered at the same level as the reference TORCs. The target tone SNR was then adjusted by varying the level of the embedded tone. As indicated, ferrets recognized and responded more quickly to high-SNR than to low-SNR targets.

Figure 3.2A illustrates the typical average licking profile in one animal for a behavioral block of trials. The ferret consistently licked during the reference TORC stimuli (top panel), but decreased its licking when it recognized the target (bottom panel). This decrease in target licking occurred at different latencies and rates, reflecting the SNR of the target tone-in-noise. Thus, when the target tone was pure, the average lick rate dropped quickly after target recognition and approached zero in the post-stimulus decision interval (1500-1800 ms) just prior to the shock interval (cross-hatched interval of 1800-2200 ms). As the task became progressively more difficult at lower SNRs, lick rate decreased more gradually following target stimulus onset and crossed into the shock interval at rates that were inversely proportional to the detectability of the tone. Licking during the shock interval constituted an error

response, and therefore, reflected the decrement in performance of the animal at low SNRs.

In order to develop a quantitative behavioral index of task difficulty, the average lick withdrawal time (LWT) of the animal was measured, which we defined to be the time after target onset when the animal decreased its lick rate to half its average lick rate during the reference stimuli (i.e., down to 40% from 80% in Figure 3.2A). All three ferrets responded to pure tone targets quickly and suppressed licking with a minimum latency of ~200 ms, as shown by the inflection point in the bottom panel of Fig.3.2A. For the pure tone detection task, the LWT was 350 ms from the onset of the target tone. However, when TORCs were added to the target and SNR decreased, ferrets' LWT increased, as shown in Fig.3.2B, for all three animals tested. This trend resembles the increasing reaction time at lower SNRs seen in detection of tone-in-noise with human subjects (Kemp, 1984).

To test the idea that more vigilance was required during the difficult (low SNR) tasks than during easy (high SNR) tasks, the task structure was modified by randomly inserting probe trials (25%) of intermediate difficulty during a block of difficult or easy trials (75%). Reasoning that if detection levels of the rarer probes reflected the overall vigilance or attention level of the animal during the task that increased with task difficulty, then performance on the probe trials should be better during difficult tasks than during easy tasks (Boudreau et al., 2006; Spitzer et al., 1988). Behavioral experiments with four blocks of easy tasks (SNR = +10 dB), and four blocks of difficult tasks (SNR = - 10 dB) tasks were carried out using intermediate probes of SNR = 0 dB. As predicted, the animal's detection of the probe

was higher when presented with in a block of a difficult task, while detection of the same probe was worse when the probe was presented with in blocks of easy tasks.

The animal's safe rate was lower during the difficult blocks than during the easy blocks. The safe rate as defined in our behavioral protocol is inversely correlated with the false alarm rate during a behavioral session. During the difficult tasks the false alarm rate of the animals was higher than during the easier task. This is worth noting because the difference observed in the animal's detection of the probe between the difficult and easy task can also be due to a shift in the animal's detection criterion in a given block of easy or difficult tasks, which would result in a lower or higher detection rate for the probe respectively.

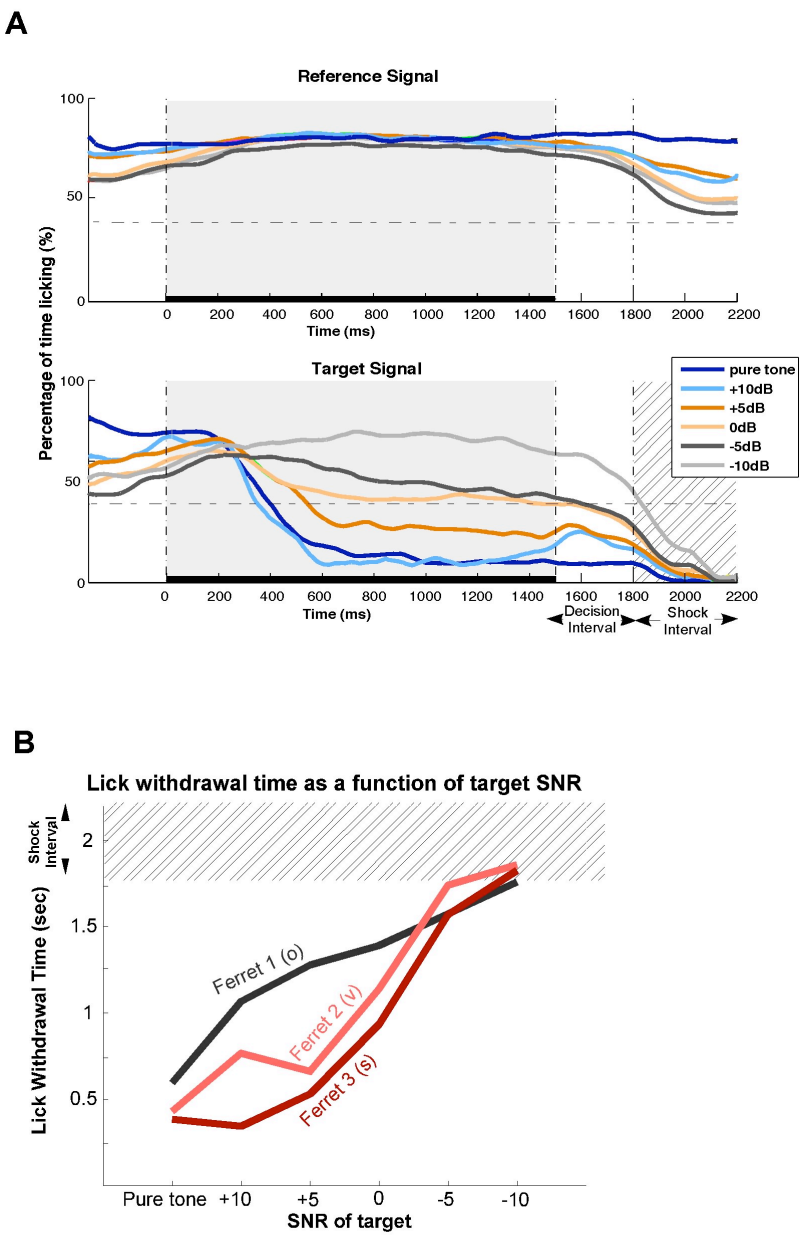

Figure 3.2 Detection of tone in noise in different SNR tasks

(A) Average lick rate of one ferret; lick-rate during *reference* TORCs is relatively flat (top panel) and provides a baseline against which cessation of licking during *target* tone presentation is measured. Dashed horizontal line indicates the lick-rate at half of this baseline. (Bottom panel) (B) Response latency measured in three animals as the interval from onset of target tone to the point at which licking decreases by 50% of maximum

3.3.2 Physiological Results

Neurophysiological recordings were conducted in A1 of two ferrets (#1 and #2 in Fig.3.2B) while they performed a tone detection task with target SNRs ranging from -9 to +15 dB. Patterns of receptive field plasticity (derived from a comparison of STRFs measured during the task condition to those measured during a passive sound presentation condition) were analyzed with respect to variations in two task parameters: (i) the frequency of the target tone relative to the best frequency (BF) of the recorded cells and (ii) task difficulty (i.e., target SNR). All STRF measurements were made from responses to the reference TORCs alone, not during any target presentations (as described in detail in Methods and in (Fritz et al., 2003)).

Ferrets performed two or three tasks in a given recording session, but it was not always possible to maintain recordings from the same cell throughout multiple task conditions. Consequently, most of our STRF measurements are from single cells that were recorded during one task condition and also during its preceding passive state. In a given task, the target tone frequency and SNR were held constant throughout. Neurophysiological data were then pooled from all cells across different recording sessions.

For analysis, the data was subdivided into *near* and *far* cells according to the separation between the each cell's BF (defined in Methods) and the target tone frequency. Cells were labeled as *near* the target if the unit's BF was within 0.6 octaves from the target tone and as *far* otherwise. Apart from giving a roughly balanced population of each type (112 versus 125), the precise choice of this dividing line was arbitrary, and none of the results described below depended critically on its

exact position (See Fig SD-4 in supplementary data). Therefore, units designated as *near* were primarily driven by the target tone, but also partly by the simultaneously presented component of noise in their local spectral vicinity. In contrast, *far* neurons could be viewed as primarily encoding the reference TORC and the masking noise in the target signal. Data were also subdivided into three groups according to the difficulty of the tasks, as parameterized by the target SNR. The three non-overlapping ranges were: high SNR (>=0 dB), mid SNR (0 dB > SNR >= -5 dB), low SNR (< -5 dB), with 93, 57, and 87 single-units in each range, respectively.

STRFs measured were normalized by their individual r.m.s. power (see Methods). As a consequence, differences between the normalized STRFs reflected mostly changes in shape (as opposed to STRF gain). This issue is revisited later in this report where we explore a model that explicitly distinguishes between the gain and shape changes.

3.3.2.1 Patterns of STRF Plasticity in single-units

When an animal discriminates a pure target tone from a TORC reference or from a tone of a different frequency, the induced STRF plasticity in A1 neurons usually consists of an enhancement at the frequency of the target tone and a weaker suppression that reflected the broad spectrum of the reference signal (Fritz et al., 2007b). In the current experiments, the observed pattern of plasticity was roughly similar when the target tone level was high relative to the noise (SNR >= 0 dB) and the BF of the cell's STRF was near the target tone. An example of such STRF plasticity is shown in Fig.3.3A, when a target tone (4.8 kHz) with a relatively high SNR of 0 dB was placed near the BF of the cell (4.3 kHz). During behavior, the unit's

STRF sharpened and its excitatory region strengthened relative to the inhibitory sideband. Afterward, the STRF largely reverted back to its pre-behavior shape. This kind of facilitatory change at target frequency during behavior is typical of results of the pure tone detection experiments reported previously (Fritz et al., 2003). However, in sharp contrast, when the tone was placed far from a unit's BF, the STRF change became suppressive in high SNR tasks. For example, the target tone (2 kHz) in Fig.3.3B (high SNR of 4 dB) was placed more than 2 octaves below the unit's BF (8.2 kHz). The excitatory region of the unit's STRF (near 8 kHz) became substantially suppressed relative to their pre-behavioral levels. As has often been observed in examples in previous plasticity studies (Fritz et al., 2003), this change persisted after behavior was completed. Although we frequently observed persistent changes, there was no systematic trend in persistence versus the type of STRF plasticity.

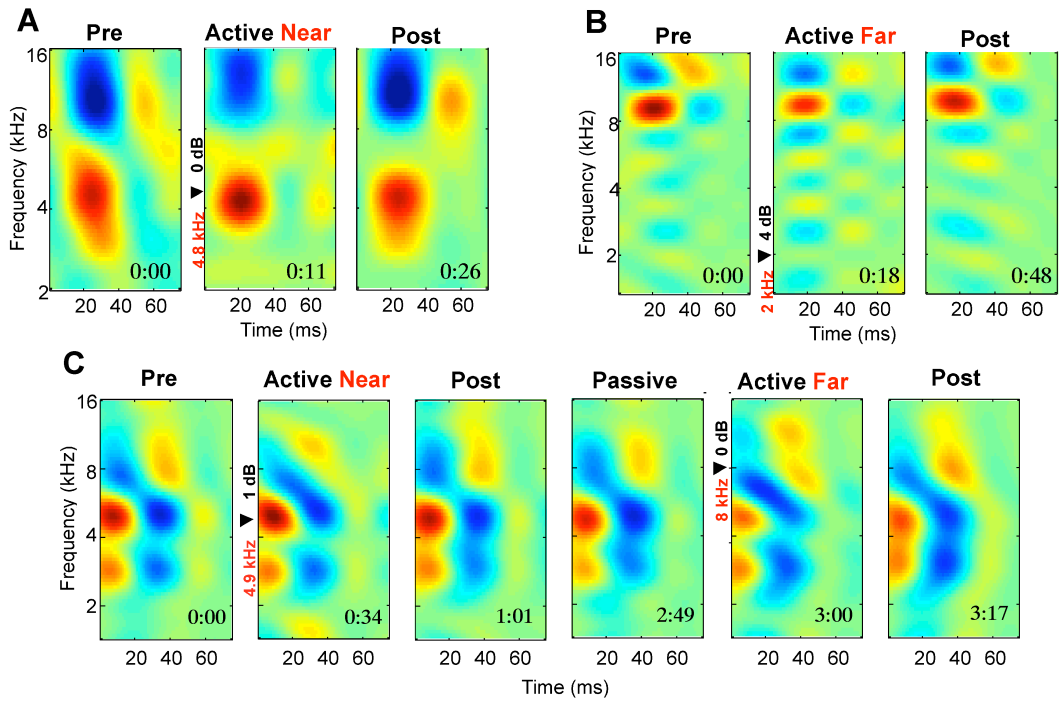

Figure 3.3: Examples of STRF changes in high SNR tasks

This pattern of STRF changes is further illustrated by the sequence of two behavioral tasks shown in Fig.3.3C. Here the unit's pre-behavioral STRF had two excitatory regions near 3 kHz and 5 kHz (the BF). When the high SNR target was placed near the BF (4.9 kHz), the nearby region sharpened and became slightly enhanced during behavior and then returned to its pre-behavioral shape following the task. The task was then repeated but with a tone far from the BF (8 kHz). Consistent with the previous example, the excitatory region in the STRF was suppressed, a change that persisted afterwards.

When the task was more difficult (low SNR), the plasticity pattern changed and STRFs on the whole became more depressed, especially far from the target. Three examples of such single-unit changes are depicted in Figure 3.4. In the first

(Fig.3.4A), the target tone (3.2 kHz) was placed near the BF (4.7 kHz). During behavior, two changes were evident: the excitatory field was depressed, and became more narrowly tuned around the BF and a new inhibitory region appeared below the BF. Following behavior, the STRF partially recovered its broader excitatory field, which remained weak, however, relative to a strengthened post-excitatory inhibitory field. The example in Fig.3.4B illustrates the changes due to a low SNR target tone placed far from the BF. Again, the STRF excitatory region weakened considerably during behavior, while the suppressive sideband below the BF strengthened. Note also the disappearance of inhibition above the BF near the frequency of the target tone (7 kHz) and the partial recovery of the original STRF after the behavior were completed.

Figure 3.4C illustrates these same changes in a sequence of two low SNR tasks in which the tone was placed at two distances: first relatively far from, and then near, the BF (6.3 kHz). As in the previous two examples, the STRF excitatory field was suppressed in both cases and then mostly recovered post behavior. Suppression, however, was stronger in the far than in the near condition (2^{nd} versus 4^{th} panels).

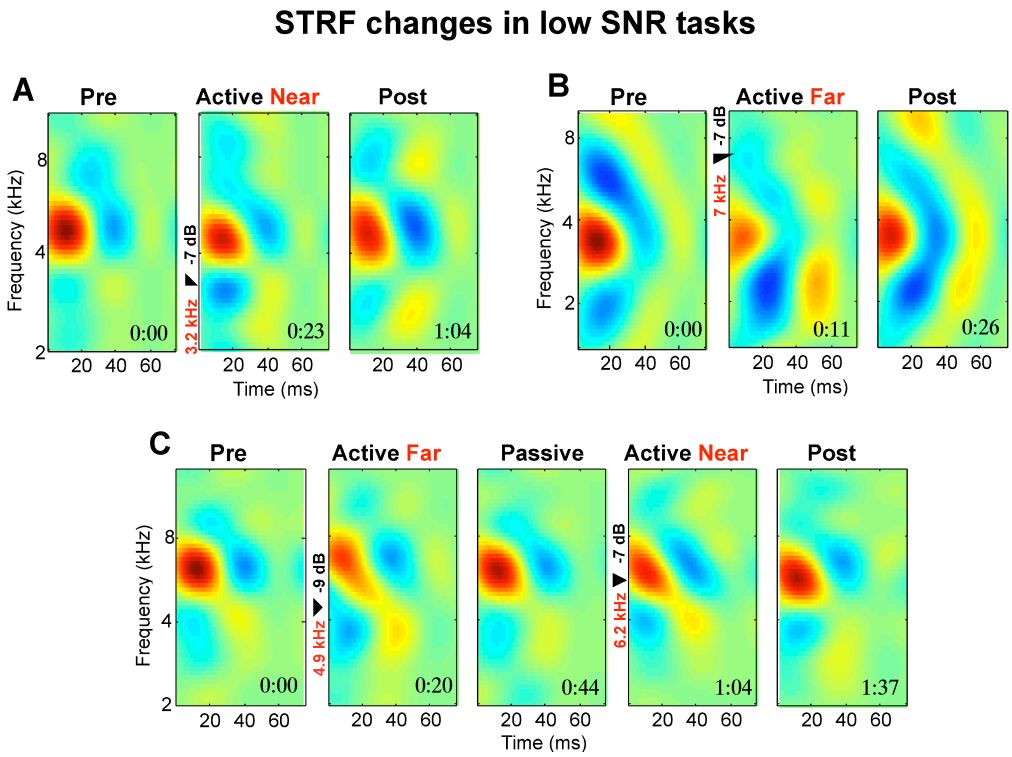

Figure 3.4: Examples of STRF changes in low SNR tasks

3.3.2.2 Population patterns of STRF Plasticity

To obtain a global view of the receptive field plasticity in these tasks, and the factors that influenced the nature of this plasticity, STRF changes were examined in a population of 237 cells from two animals. "Amplitude" change (Δ_{BF}) in the STRF was defined as the maximum difference between the "active" (during task) STRF and the "passive" (preceding the task) STRF measured within a spectrotemporal band +/- 0.2 octaves and 0-25 ms around the BF (as discussed in more detail in Methods). As explained earlier, each STRF was normalized with respect to its r.m.s. power. The results of the population analysis were relatively independent of the exact choice of parameters and manipulations of this spectrotemporal window and normalization.

3.3.2.3 Dependence on task difficulty

STRFs exhibited different overall patterns of change depending on task difficulty (i.e., target SNR), as shown in Figs. 3.3 and 3.4. In Figure 3.5, such STRF changes were compiled and contrasted from all units measured in the different tasks. In Fig. 3.5A, histograms of the Δ_{BF} changes were subdivided into high, mid, and low SNR conditions. Overall, suppression was greater in lower SNR tasks, as evidenced by the increasingly leftward skewed histograms. Suppression was weak in high and mid SNR tasks, and became significant (mean = -13.1 %; $p < 0.05$) only in the low SNR tasks. Using ANOVA Δ_{BF} changes for high and low SNR conditions were found to be significantly different ($p<0.05$). To present this trend in a more visually intuitive manner, the difference between active and passive STRFs ($STRF_{diff}$) of all units were averaged within each SNR group after aligning them at the locations of their Δ_{BF}s, as shown in the three panels of Fig.3.5B. As anticipated from the Δ_{BF} histograms in Fig.3.5A, suppression gradually increased from low to high task difficulty (i.e. from high to low SNR) as indicated by the progressively darker blue region at the origin of each figure in Panel 3.5B.

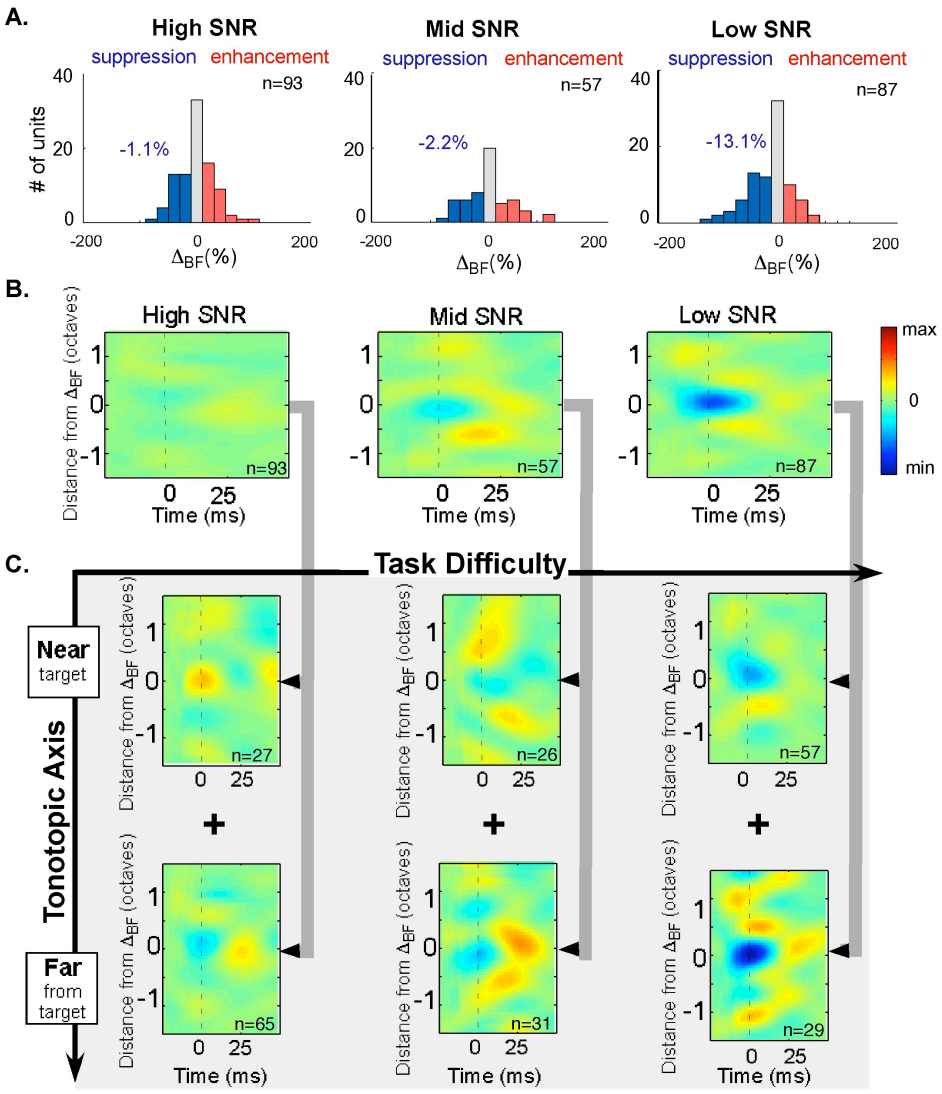

Figure 3.5: Dependence on task difficulty

The histograms and averages of Figs.3.5A and 3.5B include both near and far cells in each SNR condition. In Fig.3.5C the Δ_{BF} changes were grouped according to target proximity in order to highlight the opposite effects that occur within each. Note that in the high SNR tasks the net change across all cells was small and barely noticeable (Fig.3.5B: left panel). However, when plasticity changes were grouped by near and far cells, it became apparent that near cells on average were enhanced (red)

whereas far cells were suppressed (blue). This difference between near and far cells was also seen in the mid and low SNR groups, but this time relative to an overall progressively deeper (more blue) suppression. Figure SD-1 (in Appendix 1) accumulates the data from all three SNR conditions to highlight the dependence of receptive field plasticity on the distance between the target tone and the BF of the STRF, regardless of task difficulty.

3.3.2.4 Dependence on behavioral performance

Fluctuating performance levels in a given task may reflect changes in the attentional and/or motivational state of the animal. To explore how performance correlated with STRF changes, we ranked the performance level for all experiments (as defined by the discrimination rate for behavioral sessions in individual physiology experiments; see Methods) and then computed the average difference between active and passive STRFs for the experiments with best (top third) behavioral performance. Figure 3.6 displays the results from a total of 85 cells in the tone-in-noise detection task, sorted into three groups by SNR level.

The trend of increasing suppression for low SNRs (e.g., as in Fig.3.5) is repeated here, but with an important difference: STRF changes were amplified. For example, in Fig.3.6B, the STRF change in high SNR tasks exhibited a strong net (excitatory) enhancement compared to its weaker counterpart in Fig.3.5B. By contrast, low SNR tasks induced a deeper suppression than seen earlier in Fig.3.5B. Δ_{BF} changes for high and low SNR conditions here were more distinctly different as demonstrated by the divergence in their means ($p<0.01$). Therefore, the near and far cell populations within each of these three tasks (Fig.3.6C) displayed a similar

divergence of enhancement and suppression to the entire neuronal population (Fig.3.5C), except that the changes were more pronounced.

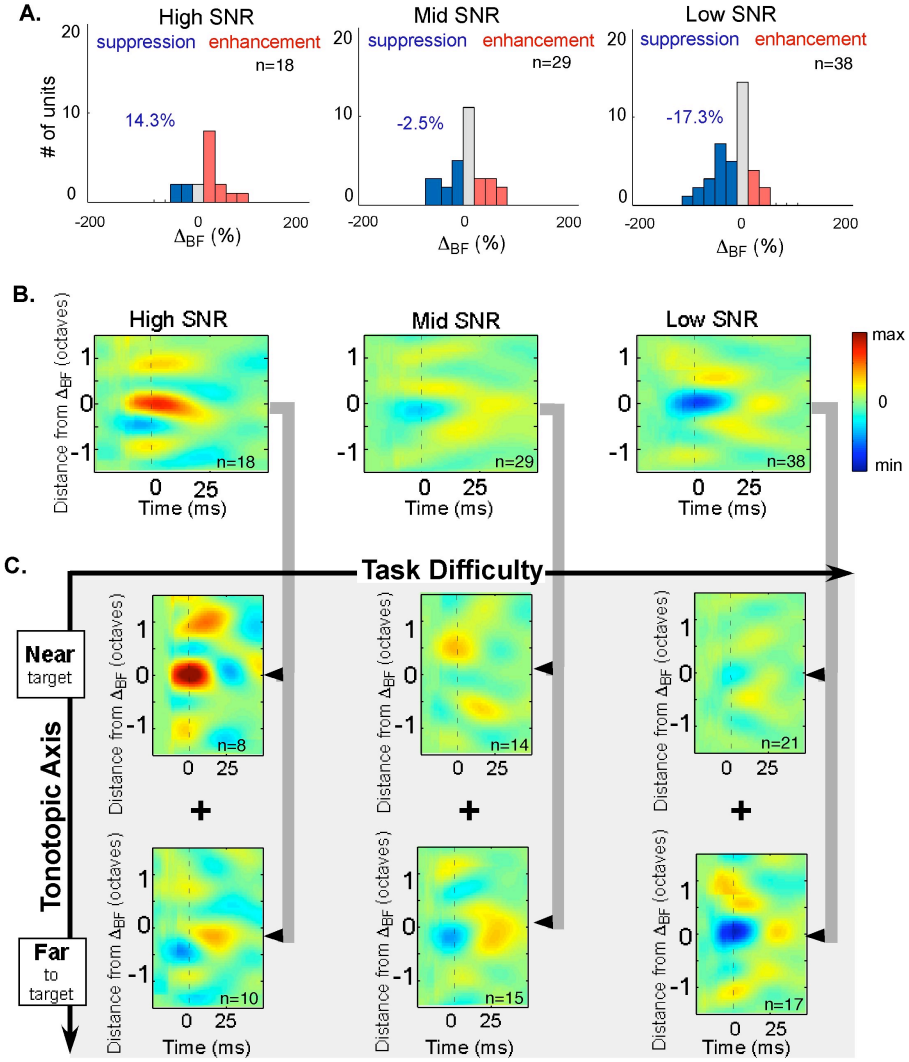

Figure 3.6: Dependence on behavioral performance

To demonstrate further the crucial role of behavior in inducing these changes, STRF changes were measured in 93 units from 3 *naïve* animals using exactly the same stimuli and analysis procedures as those used in the behavioral animals. Some minor changes in the STRFs were observed, these changes however were not

consistent in the absence of behavior, as illustrated in Figure SD-2 in Supplementary Data.

	Task difficulty		
	Easy task	**Intermediate task**	**Difficult task**
All units	Mean: -1.1%	Mean: -2.2%	Mean: -13.3% Significant negative trend ($p<0.05$)
Units of best performance expts.	Mean: 14.3% Significant positive trend ($p<0.05$)	Mean: -2.5%	Mean: -17.3% Significant negative trend ($p<0.01$)
	Tone distance from the BF		
	Near BF	**Far from BF**	
All units	Mean: -3.2%	Mean: -7.4% Significant negative trend ($p<0.05$)	
Units of best performance expts.	Mean: 2.3%	Mean: -13.1% Significant negative trend ($p<0.01$)	

Table3.1: Summary of Δ_{BF} changes controlling for task difficulty, distance of tone from BF, and behavioral performance of the animal: Showing the mean of the distribution of Δ_{BF} changes under the corresponding conditions, a noting the p value for significant trends.

3.3.2.5 Task-related suppression of TORC responses

The experimental technique and behavioral paradigm applied in this study allowed for the measure of the effect of STRF changes on the average PSTH responses to the (reference) TORC stimuli since identical sets and sequences of TORCs were presented to all animals in all SNR tasks. Figure 3.7A contrasts the average TORC responses in the near and far cell populations (red and blue curves, respectively) during the two extreme tasks, the high and low SNR (left and right panels, respectively). This population of cells is the same group selected from sessions with best performance as shown in Figure 3.6. The normalized responses of these groups of cells during the passive epoch preceding the behavioral tasks are

plotted in gray in each panel. Two obvious trends confirm earlier conclusions: (i) responses during behavior were more suppressed in far cells than in near cells, and (ii) suppression strengthened with increasing task difficulty (lower SNRs). Thus, within a given level of task difficulty, far cells were more suppressed than near cells. Furthermore, increasing task difficulty from high to low SNR targets caused a uniform overall suppression of about one *third* in the firing rate (as indicated by the dashed lines of Fig.3.7A).

3.3.2.6 Contributions of gain and shape changes to STRF plasticity

What are the relative contributions of *gain* and *shape* changes to rapid STRF plasticity? It is clear that changes in TORC responses described above were not due to a pure gain change because STRFs also exhibited substantial shape changes (e.g., the six examples in Figs. 3.3 and 3.4), and because the results of Figs. 3.5 and 3.6 were obtained despite the fact that STRFs were normalized to equalize their r.m.s. power (see Methods).

As explained earlier, STRF *power normalization*, which was used in previous publications (Fritz et al., 2003; Fritz et al., 2005), does not completely differentiate between *gain* and *shape* changes. Thus to assess more accurately the relative changes in gain and shape, an alternative measure was computed that explicitly and separately included both gain and shape changes. I define the *active (during) STRF* ($\mathbf{S_d}$) as the sum of a scaled *passive (before-task) STRF* ($\mathbf{S_b}$) and a change in the shape of the STRF, i.e.: $\mathbf{S_d} = g.\mathbf{S_b} + \delta$, where g is the *gain* that reflects the fraction of the STRF that maintained its original shape, and δ is the remaining (orthogonal) *shape change* that could not be captured by scaling $\mathbf{S_b}$ (this δ was used to generate the plots in

Fig.3.7C). To confirm that these results were robust with respect to measurement noise, shape changes using an alternative method developed by were computed (David et al., 2008) (described in more detail in Methods and Appendix 1), and replicated the same trends discussed below.

Figure 3.7B illustrates the distribution of the gain changes computed for the same cells in Fig.3.7A but broken into four groups: high versus low SNR and near versus far. To summarize these data: (i) In a majority of cells (> 66% in high SNR and near STRFs, and >80% in low SNR and far cells), the gain was <= 1 (median of approximately 0.9 and 0.7, respectively) indicating an overall suppression of the gain during behavior. (ii) Increasing task difficulty or distance from target caused an additional small depression of the gain in about 15% of all STRFs. This weak dependence of the gain on task difficulty, however, was not confirmed when the results from all cells in this study were pooled, i.e., including all performance levels (see Figure SD-3A in Appendix 1. where gain distributions remain relatively unchanged with SNR with medians of about 0.7). Finally, I replicated these trends in the gain distributions when using the alternative method of (David et al., 2008) to take noise into account (see Appendix 1 : Figure SD-3B).

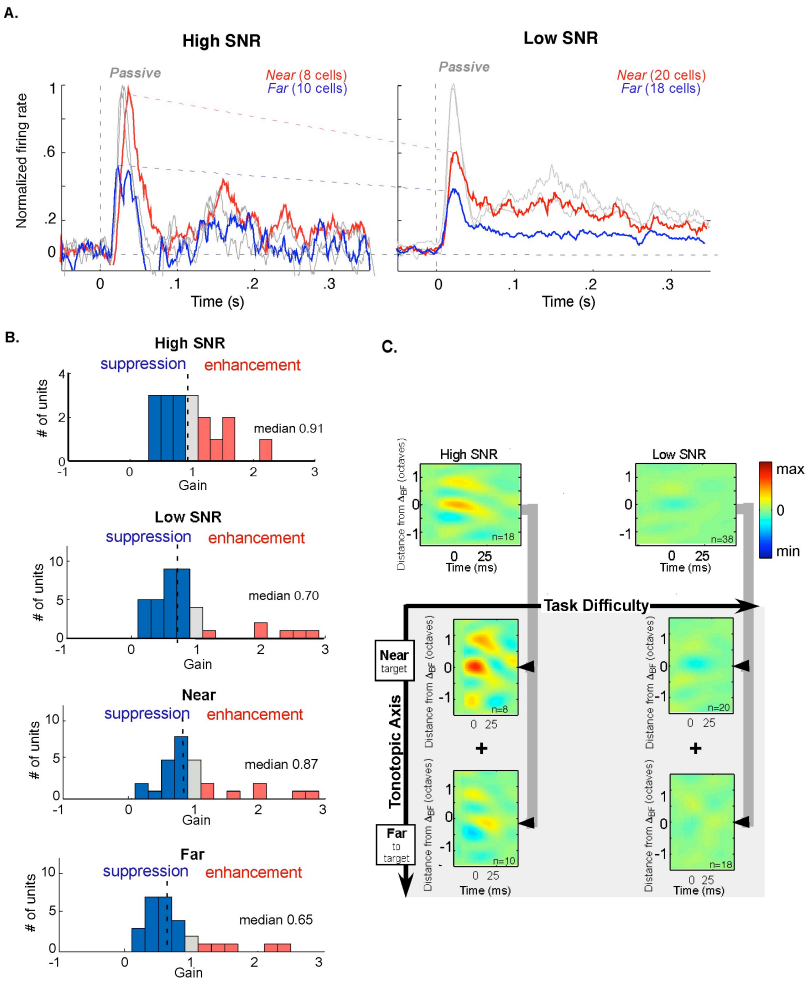

Figure 3.7: Contributions of *gain* and *shape* changes to TORC responses and STRF plasticity. (A) Dependence of PSTH reference responses on task difficulty and BF separation from target tone. PSTH curves were computed from all cells selected for Figure 3.6 during the passive state (faint gray curves), and during the *high SNR* and *low SNR* tasks (left and right panels, respectively). In each panel, responses of *near* (red) and *far* (blue) cells are shown. All responses were normalized relative to their corresponding passive responses (after subtracting out the spontaneous activity). (B) Distribution of STRF *gain* changes during behavior relative to the pre-behavioral state. (C) Contribution of STRF *shape* changes to plasticity was comparable in strength but almost completely positive and focused when the target tone was in a high SNR and near the BF of the cell. All plots are shown relative to the same color scale for all panels in this figure.

The contribution of the pure shape changes were then considered, which reflected STRF changes that remained after accounting for all gain effects. Figure 3.7C illustrates the average δ for the same population of cells that were shown in Figs.3.7A and B. All panels employ the same color scale as Fig.3.6B. Unlike the suppressed gain, (i) the average shape change δ was mostly positive and focused in the near cells during high SNR tasks and (ii) shape changes followed the same trends seen above in Figs.3.5 and 3.6, both with respect to task difficulty (becoming more enhanced in high SNR tasks) and with respect to distance from target tone (near STRFs are enhanced relative to far cells).

Figure 3.8 displays the average *combined* gain and shape (or *net*) changes induced during behavior in high and low SNR tasks, and in near and far cells. The pattern of changes looks similar to that due to shape in Fig.3.7C, except for a depression in all panels reflecting the overall suppression of the gain across all tasks and distances. To summarize, in high SNR tasks, the target induces positive changes in nearby STRFs, thereby enhancing the representation of the target tone, similar to earlier findings with pure-tone targets (Fritz et al., 2003). Decreasing the target tone (low SNR) causes overall gain suppression, especially in far cells, thereby maintaining the enhanced representation of the target tone responses relative to those of the masking noise.

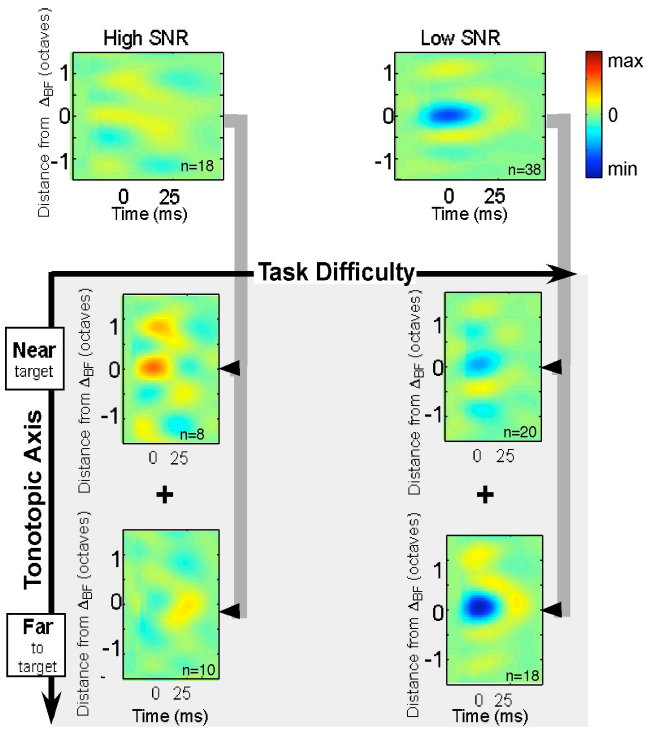

Figure 3.8: **Average STRF difference combining gain and shape changes**

3.4 Discussion

When an animal performs an auditory task, its A1 receptive fields undergo rapid changes that reflect the stimuli and performance of the task (Fritz et al., 2003; Fritz et al., 2007a). This study extends those findings by examining the effects of modulating the difficulty of a tone detection task by embedding it in noise at different SNRs. Behaviorally, increasing task difficulty has been shown to induce compensatory enhancement of attention (Boudreau et al., 2006; LaBerge et al., 1991; Lavie and Cox, 1997; Sade and Spitzer, 1998; Urbach and Spitzer, 1995; Yantis, 1996). Physiologically, this enhanced attention has been linked to increased responses to targets or more suppression of distracter responses (Chen et al., 2008). Either way, these changes enhance target representation and hence facilitate target detection.

The working hypothesis upon embarking on this study was that behaviorally-induced response modulation would serve to counter the detrimental effects of masking noise by maintaining the neural representation of the tone. Interpreted in this light, STRFs adapted differently across a wide swathe of the tonotopic axis relative to the target tone. Cells tuned *near* the target tone frequency displayed an enhanced sensitivity at BF, while those tuned *far* from it became largely suppressed (Figs. 3.5-3.7). These effects were stronger in experiments when performance was best (Figs. 3.6-3.7). While the analysis of STRF plasticity in the current study is centered on cell BF, the results are largely compatible with earlier studies of task-related plasticity in which analysis was centered on target frequency (Fritz et al., 2003; Fritz et al., 2005, 2007b).

3.4.1 Effects of attention on receptive field gain and shape

In studies of visual cortex, attentional effects on neural responses have often been thought to reflect a change in both *gain* and *shape* of spatial (Connor et al., 1997; Luck et al., 1997) and feature receptive fields (David et al., 2008; Maunsell and Treue, 2006). STRF measurements allowed the separation of these two factors and the assessment of their relative contributions. By assuming that STRF changes were the superposition of a global gain change and an orthogonal shape change, the analysis revealed that engagement in the tasks resulted in a substantial (10-30%) *reduction* in STRF gain during behavior (Fig.3.7B). This change was the same regardless of task difficulty, and occurred across most cells (near or far). However, the gain reduction was counterbalanced by an enhancement due to *shape* changes that

was focused and largest in cells with BF near the target tone during high SNR tasks (Fig.3.7C).

It is unclear to what extent this pattern of broad gain reduction and focused shape enhancement was dependent on the specifics of the tone-in-noise task. For example, it is possible that this gain suppression simply related to an increase in overall level of alertness when ferrets became engaged in *any* task (as suggested by Otazu et al. 2009). Or, it could have been specific to our task design or valence (i.e. specific to a conditioned avoidance paradigm as opposed to the appetitive positive reinforcement paradigms more widely used in studies of attention). Finally, it is conceivable that our stimulus design – specifically, holding noise (TORC) levels constant through all SNR conditions (only the level of the target tone was varied), was a reason for the relative constancy of the gain reduction regardless of task difficulty. These changes in gain were not observed in previous studies (Fritz et al 2003; 2005; 2007b) that, unlike the present study, did not include broadband noise in the target. While definitive resolution to these issues will require further experiments that dissociate the contributions of the stimulus structure and the behavioral paradigm to these changes, I nevertheless offer a few conjectures below based on what is already known from the results of previous studies of behaviorally-driven effects in the auditory and visual systems.

3.4.2 Functional significance of rapid plasticity

The diverse pattern of STRF changes described in this report is broadly consistent with the types of plasticity observed in previous studies in which ferrets detected target tone(s) relative to a reference TORC noise (Fritz et al., 2003; 2007b),

or discriminated a target tone relative to reference tone of a different frequency (Fritz et al., 2005). In those experiments, *target* tones induced an enhanced sensitivity, whereas *reference* signals produced mild to strong suppression that reflected the reference spectral shape. Such STRF transformations were interpreted as a "contrast matching filter" that is driven by the spectral difference between *target* and *reference* signals which serves to "amplify" their differential neuronal responses, and hence their *perceptual distance* and discriminability, as illustrated in Figure 3.9A (Fritz et al., 2007b). In the current experiments, not only did the reference stimuli consist of broadband noise, but also the target tone was surrounded by the same broadband noise. Hence the process of extracting the tone component of the target necessitated suppression of responses to this concurrent masking noise, while simultaneously enhancing the sensitivity to the *near* target cells. Figure 3.9B summarizes the broader functional interpretation of these findings in terms of the "matched contrast filter hypothesis" for different SNR tasks.

Such a differential pattern of plasticity in *near* and *far* cells is consistent with our previous findings that significant STRF plasticity occurred *only* when the *behaviorally-relevant* stimuli in the task (*target* and/or *reference* signals) were in the vicinity of the STRF (Fritz et al., 2007b). In the current experiments, the excitatory enhancements induced in the *near* cells stem from their proximity to the target tone region, whereas the strong suppression in the *far* STRFs was due to the *behaviorally-meaningful* broadband masking noise that surrounded the target and drove the responses in those cells. Without this noise, changes in *far* STRFs would have been

much smaller since the target tone was relatively far (> 0.6 Octaves) from the BFs of these cells (e.g., as in (Fritz et al., 2005)).

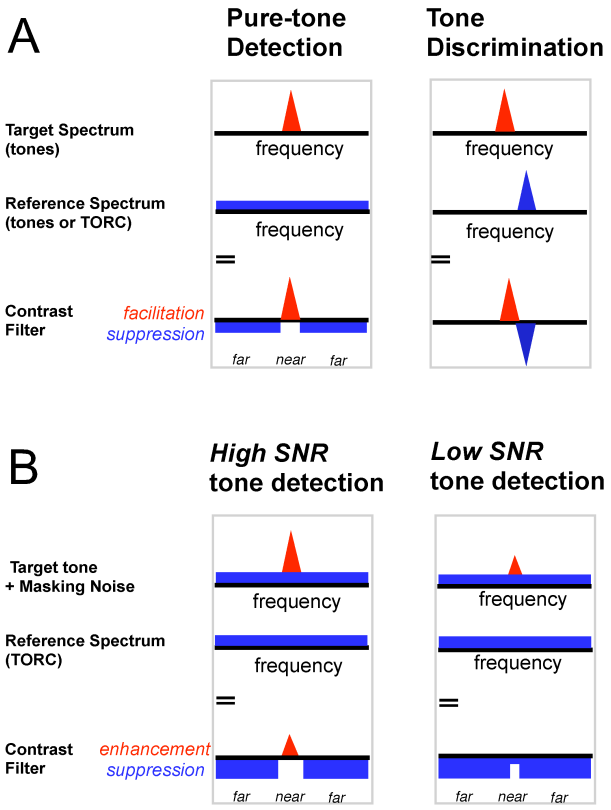

Figure 3.9
Schematic of the "matched contrast filter" hypothesis in different behavioral tasks. (A) Schematics of the target and (*inverted*) reference spectra in two previous behavioral tasks (Tone detection, and Tone discrimination). (B) In tone-in-noise detection tasks, a target tone with varying levels is embedded in noise (TORC) that was of an identical intensity level to the reference.

3.4.3 Relation to attention effects on visual responses

Systematic STRF shape changes described in our experiments occur only when the animals are engaged in behavioral tasks requiring attention to target and reference stimuli, and does not reflect stimulus adaptation such as might be expected to occur during passive presentation of the same stimuli (Elhilali et al., 2007; Fritz et al., 2007b). We have used the term *rapid task-related plasticity* to describe these transformations because they are induced rapidly after the onset of the behavior (occurring within a few minutes, which is the earliest our methods allow us to

measure them). Moreover, although rapid in onset, they often persist for minutes or hours following the conclusion of the task (Fritz et al., 2005). Despite these distinctive properties, the effects may be fundamentally similar to those transiently induced by attentional demands in visual tasks. The contrast matched filter shares many properties with models proposed to describe the effects of attention in the visual system (Compte and Wang, 2006; Connor et al., 1997; David et al., 2008; Luck et al., 1997; Maunsell and Treue, 2006; Womelsdorf et al., 2008).

The different dynamics of the effects may simply reflect the varied design of the experiments rather than the basic underlying neural phenomenon. For instance, an important feature of our experiments is their block-design, in which attention to a specific target (tone) is maintained throughout the task, thus allowing for sustained attentional effects to build up, that we conjecture, may contribute to the strength of receptive field changes during behavior as well as to their post-behavioral persistence. There is also general agreement between our findings and the results of visual attention studies in which attention-induced response modulations have been interpreted as changes in receptive field shapes. For instance, in experiments manipulating selective spatial attention (Connor et al., 1997; Womelsdorf et al., 2008), receptive fields in the retinotopic vicinity of the focus of attention shifted and narrowed, while others far away remained unchanged. In our experiments, STRF shape changes were also largest in the tonotopic vicinity of the target tone (Fig.3.7C). However, further detailed comparison of these two sets of findings may be of limited value because of key differences in the behavioral paradigm and data analysis. First, we included masking stimuli (or effectively, distracters) in our tasks, which

modulated task difficulty and probably caused the suppression in STRFs far from the target tone (see below). Second, we quantified STRF changes in terms of a pure gain and an orthogonal shape-change, a parameterization that differs from the Gaussian fits of the visual receptive fields (Womelsdorf et al., 2008). Finally, during the tone-in-noise task, the strategy of the animal is unlikely to be to selectively attend to the frequency of the target tone. Instead, its strategy may be to discriminate between the target's narrowband structure and the broadband references (TORC).

Finally, there are close parallels between our results and those that examined the effects of task difficulty on the responsiveness of the visual cortex cells in monkey (Boudreau et al., 2006; Chen et al., 2008; Spitzer et al., 1988; Spitzer and Richmond, 1991). In one study, (Boudreau et al., 2006) compared the activity of visual neurons during easy and difficult behavioral tasks in which targets and distracters were cued by their likelihood of occurrence. They observed that during difficult tasks, attending selectively to the likely stimulus (target) caused small increases in the responses near it, but substantial suppression of responses to the (unattended) distracter, results that are analogous to the net effects seen in our experiments (e.g., Fig. 3.6). This pattern of attentional effects has been generally described as a center-surround pattern of "facilitation-suppression" that sharpens the sensory representation of competing stimuli by facilitating responses to the attended stimulus (foreground) and suppressing the rest (background) (Chen et al., 2008).

3.4.4 Enhancement of stimulus representation

Ultimately, STRF changes are interpreted as task-related neural plasticity that serves to enhance the representation of target and reference stimuli so as to facilitate

their discrimination. This view is illustrated in Figure 3.10A which depicts a population of A1 cells arrayed along the tonotopic axis, each with a simplified hypothetical triangular iso-intensity "tuning curve" response reflecting the spectral selectivity of the cell (or the spectral dimension of its STRF). The "initial" or passive state of the A1 is an array of identical STRFs of equal height (green). In a pure-tone detection task, i.e., with no added noise in the target stimulus, the STRFs are enhanced *near* the target tone (red), and are weakly suppressed *far* from it due to the broadband *reference* signals (as in (Fritz et al., 2003)). When the target tone is embedded in noise at a *high SNR*, STRF *gains* become suppressed overall, except *near* the target where they exhibit a focused enhancement (orange). Low SNR tasks yielded a stronger net suppression both *near* and *far* as the positive *shape* enhancement weakened (Figs.3.5-3.7). Figure 3.10B illustrates the finding that STRF transformations also depended upon behavioral performance (as shown in Fig 3.6). During best performance (which was likely associated with higher attention levels), STRF changes preserved the same "sign" of facilitation and suppression, but overall, became stronger and more pronounced.

These patterns of STRF change suggest a scenario in which, engagement in a pure-tone detection or a *high SNR* task where the target tone is salient, leads to an enhanced neural representation and good performance (Fig.3.5). When target-tone *SNR* diminishes, the task becomes harder, and both performance and the target neural representation deteriorate (Figs.3.3 and 3.6). This decrement, however, could be reversed by heightened attention that both restores the enhanced target representation and improves performance (Fig.3.6).

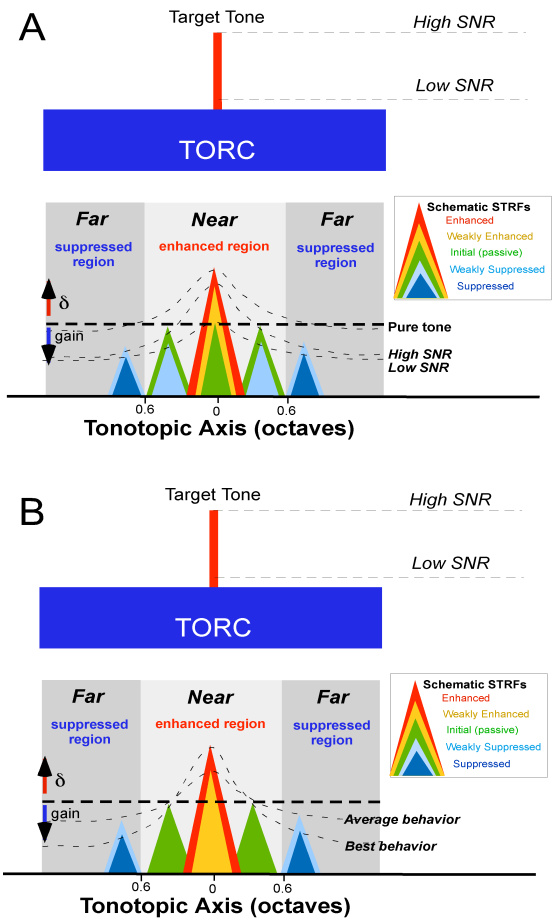

Figure 3.10: Schematic of STRF changes during tone-in-noise detection under different conditions. STRFs distributed along the tonotopic axis relative to the target tone are depicted by triangular "iso-intensity response functions". Colors indicate enhancement or suppression of the STRFs. (A) During pure tone detection tasks, STRFs *near* the tone are facilitated, whereas *far* STRFs are mildly suppressed, effectively enhancing the representation of the target tone. As the masking noise level increases, all STRFs become gradually more suppressed relative to the passive state, thus maintaining the enhanced representation of the target tone. (B) During excellent behavioral performance, STRF changes become more exaggerated while maintaining the same pattern.

3.5 Conclusion

This study investigated the effects of varying task difficulty on dynamic receptive field changes in auditory cortex. Manipulating task difficulty revealed a previously unreported dimension along which plasticity occurs, suppressing the acoustic background while further enhancing the representation of the relevant auditory object. The magnitude of changes correlated with task performance, suggesting a direct relationship between the level of attention and magnitude of plasticity.

Chapter 4: Rapid plasticity in secondary auditory cortex

4.1 Introduction:

The auditory cortex in the ferret consists of a primary auditory field (A1) surrounded by acoustically sensitive areas often referred to as higher order auditory areas (Bizley et al, 2005, Nelken et al 2004b, Kowalski et al 1996). Several subdivisions of auditory areas surrounding A1 have been reported in the cat, primates, and rodents (Merzenich and Brugge 1973, Reale and Imig 1980, Kaas and Hacket 2000, Kajikawa et al 2005, Winer and Lee 2007), usually based on the direction of the tonotopic order, tuning properties, and response dynamics. In the ferret, such fields consist of an anterior auditory field (AAF), and auditory regions extending down the anterior and posterior limbs of the ectosylvian gyrus (AEG and PEG), as shown in Figure 4.1. AAF shares with A1 a high frequency region, and has comparable tuning curves, short latency responses, and strong phase locking to the envelop of the stimulus (Bizley et al. 2006, Kowalski et al. 1996). The AEG fields are poorly tuned, and have higher thresholds and variable latencies. The PEG fields are well tuned exhibiting robust response to tones with a higher percentage of non-monotonic cells when compared to A1. PEG is subdivided into posterior suprasylvian field (PSF) and posterior pseudosylvian field (PPF) fields. These two fields have similar functional properties and projections from A1 and the auditory thalamus. They share a low frequency boundary and only differ in a weak tonotopic gradient from low to high, moving dorso medially in PSF and droso-laterally in PPF (Bizely et al, 2005). Based on their functional properties, and anatomical connections

to A1 and the ventral and dorsal nuclei of the auditory thalamus, these fields have all the characteristics of secondary auditory cortex, and are analogous to A2 area in the cat auditory cortex (Bizely 2005).

This study combines neural responses gathered from both posterior fields in PEG, because of the resemblance in their functional and anatomical properties, in addition to the difficulty of distinguishing between the two areas in the physiological preparation that is used in this study (see methods). Therefore both areas will be referred to in this chapter by the joint area name, posterior ectosylvian gyrus or PEG (Bizley 2005)

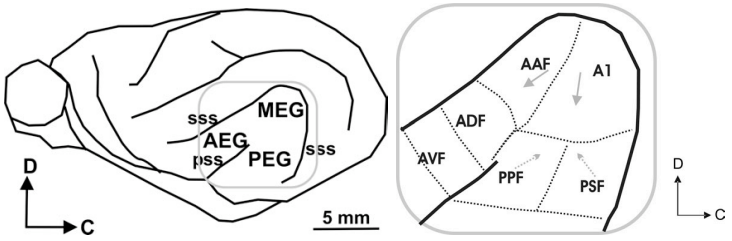

Figure 4.1 Functional Organization of the ferret auditory cortex, (Bizley et al. 2005)

The functional significance of these non-primary fields in all animals remains uncertain despite decades of attempts to ascribe them with properties analogous to those of the visual cortical fields. For example, the distinction between a *what* and *where* auditory pathways in analogy with primate vision (Romanski et al 1999a,1999b, Rauschecker et al 1995), and the reported high selectivity to natural vocalizations (Wang et al 1995, Wang 2000). Whatever their functional role in hearing, the secondary auditory areas display a wide range of complex responses and receptive fields that are highly interconnected with A1 and each other, and have

unique bottom-up inputs and feedbacks with thalamic and midbrain nuclei, and top-down connectivity with numerous cortical regions (Read et al 2002). Consequently, it is expected that these regions exhibit heightened sensitivity to the behavioral state of the animal, and may be strongly influenced by experience and learning. Although the main focus in auditory neuroscience research continues to be A1, several studies into higher auditory areas have confirmed aspects of these hypotheses. For example, long-term operant training can cause frequency specific plasticity and/or plasticity in amplitude tuning in primary and secondary cortical areas (Recanzone et al. 1993; Rutkowski and Weinberger 2005; Polley et al. 2006). Similarly, classical conditioning shifts a greater proportion of receptive fields in secondary cortical areas toward the conditioned stimulus than in A1 (Diamond and Weinberger 1984, 1986; Weinberger et al. 1984). In all these cases, the stimulus-specific plasticity occurred during learning across numerous cortical areas, suggesting that pervasive top-down influences were engaged in the process. Finally, similar stimulus-specific plasticity has been induced in secondary auditory fields in experiments with Nucleus Basalis (NB) stimulation to simulate classical conditioning and operant conditioning protocols (Puckett et al 2007). These studies of plasticity in secondary auditory fields have clearly demonstrated that behaviorally specific plasticity is not limited to A1, and in some reports, that plasticity in secondary auditory areas can be significantly larger than that in A1 (Diamond and Weinberger 1984, 1986). Yet because of the experimental designs, none of these studies could investigate the dynamic changes that take place in these areas during the performance of an acoustic task, leaving an important element of understanding this type of cortical plasticity missing, in addition

to it's value in understanding the development of the representation of behaviorally significant acoustic signals, and the effect of the task demands in real time. This study investigates rapid task related plasticity and the form it takes in secondary auditory cortex, utilizing the experimental paradigm explained in (Fritz et al. 2003, 2005, and 2007, Atiani et. al 2009) with some alteration to the reference stimuli. Single unit responses were gathered from PEG and A1 using the exact same stimuli and experimental paradigm to make a direct comparison between plasticity in both areas.

4.2 Methods

Stimuli:

Stimuli used to probe tuning properties of primary and secondary areas consisted of pure tones, two tone chords, and TORCs(Temporally orthogonal ripple combinations (Klein et al., 2000)). Pure tones were 100ms in length and were randomly generated to cover a range of frequencies specified for each recording session. Two tone chords were generated by adding two pure tones with the same onset time and phase of a 100ms in duration. Each one of these two tone chords was an instance of a set of two tone chords defined to contain all possible two tone combinations from two identical sets of tones specified at the beginning of each recording session. TORCs were randomly chosen from a set of 30 five octave wide broadband noise with a dynamic spectro-temporal profile that is the superposition of the envelopes of 6 temporally orthogonal ripples. A single ripple has a sinusoidal spectral profile, with peaks equally spaced at 0 (flat) to 1.2 peaks-per-octave; the

envelope drifted temporally up or down the logarithmic frequency axis at a constant velocity from 4 Hz up to 48 Hz (Klein et al., 2000; Depireux et al., 2001).

For behavioral experiments, reference sounds were randomly chosen from a predefined set of band pass noise stimuli. The number of noise bands in a given set of reference stimuli depended on the frequency range probed and the bandwidth of the noise band chosen for each experiment. The bandwidth of the noise stimuli was either half, quarter or an eighth of an octave. Each of these noise bands consisted of 10 to 40 tones logarithmically spaced in the narrow frequency band for every individual noise band, and were each labelled by the center frequency of the noise band. A reference stimulus set consisting of a number of these noise bands spanned a frequency range that varied, depending on the experiment, between 3 to 7 octaves, but was held constant between passive and active recordings in each experiment. Target stimuli consisted of a pure tone whose frequency fell within the frequency range covered by the reference stimuli. Each experiment consisted of multiple trials, each trial consisted of a number of references followed by a target (pure tone), except on catch trials in which 7 reference stimuli were presented with no target. The position of the target in the trial was 2^{nd}, 3^{rd}, ….to 7th in the trial. The number of references in each trial was determined based on a lookup table ensuring that a target was equiprobable for every position (2-7) (Frtiz 2003, Heffner and Heffner 1995)

The amplitude of reference and target stimuli was set for a given experiment in the range between 60-75 dB. References and targets were 1.5 seconds long. We played the identical set of reference and target stimuli in two behavioral states; while the animal was passively listening, and while it was engaged in task performance.

Training paradigm and procedure:

Four adult ferrets were trained on the pure tone detection task using a conditioned avoidance procedure (Fritz et al., 2003; Heffner and Heffner, 1995). Ferrets licked water from a spout while listening to a sequence of reference stimuli until they heard a pure tone. Length of reference and target stimuli was always the same, and for most of training and all recording sessions stimulus length was 1.5 seconds. When presented with a target, the animals were trained to briefly stop licking, in order to avoid a mild shock.

The pure tone detection task used here is in line with the task used in (Fritz et al., 2003) substituting the TORCs with the noise band stimuli. Animals were trained on the task until the animal reached criterion, defined as consistent performance on the detection task pure tone targets for two sessions with >80% hit rate accuracy and >80% safe rate for a discrimination rate > 0.65.

Surgery

To secure stability for electrophysiological recording, a stainless steel head-post was surgically implanted on the skull. During surgery, the ferrets were anaesthetized with a combination of Ketamine-Xylazine for induction, and isoflurane (1-2%) for maintenance of deep anesthesia throughout the surgery. Using sterile procedure, the skull was surgically exposed and the head-post was mounted using bone cement, leaving clear access to auditory cortex in both hemispheres. Antibiotics and post-surgery analgesics were administered as needed following surgery.

Post-surgical habituation and training:

After recovery from head-post implantation (2 weeks), the ferrets were habituated to head restraint in a customized Lucite horizontal holder over a period of 1-2 weeks, and then re-trained on the task for an additional 2-3 weeks while restrained in the holder (Fritz et al., 2003). The task-naive control ferrets received no behavioral training on the task, but like the other head-post implanted ferrets also received gradual habituation to head restraint in the holder, before physiological recording commenced.

Neurophysiological recording:

Experiments were conducted in a double-walled, sound-attenuating chamber. Small craniotomies (1-2 mm in diameter) were made over auditory cortex prior to recording sessions that lasted 6-8 hours. We used single and multiple independently moveable electrodes (AlphaOmega) for the recordings. In a typical electrode configuration, there were up to 4 recording electrodes separated by ~500 microns from their nearest neighbor. Single units (typically 1-4 neurons per electrode) were isolated using off-line spike sorting technique with custom-designed MATLAB software. In each individual recording session electrodes were advanced good isolations for multi units were found on the majority of the electrodes. The range of best frequencies in a given experiment varied from 0.5- 2.5 octaves. This allowed for simultaneous exploration of the effect of the target tone frequency on cells whose BFs were at different spectral distances from the target tone. BF was defined as the frequency of the largest excitatory peak in the tuning curve for each cell.

Recordings were confirmed to be A1 neurons based on the presence of distinctive physiological characteristics such as latency and tuning (Shamma et al., 1993; Nelken et al., 2004; Bizley et al., 2005).

Locating secondary auditory areas:

A1 was located using a combination of: 1- an approximate location measured 12 mm anterior to the back ridge of ferret's skull, and 8mm from the middle ridge of the skull, 2- the neural response properties, as A1 neural responses have a short latency14-24 ms, and phase locking to the onset of tones and the envelop of amplitude modulated tones or envelop of broad band stimuli, 3- a clear tonotopic gradient that changes from high frequencies to low frequencies on the dorso-ventral axis. The posterior fields, PPF, and PSF in the ferret auditory cortex were located by first confirming the tonotopic gradient of A1, tracing the change in BF from high to low frequencies until the gradient is reversed and the frequencies start increasing. This reversal in the tonotopic gradient coincides with change in the response properties of neurons in that area where responses are characterized by longer latencies and longer sustained responses coupled with poor locking to the onset of pure tones, and the envelop of amplitude modulated tones or broad band noise. The combination of the reversal of the tonotopic gradient and the change of response properties are used as indicators that the neurons recorded from are located in PEG(PPF and PSF) (Bizley et al., 2005).

Data Analysis:

Single unit responses were isolated using an offline spike sorting program. Change in neural response during the performance of the task was assessed by

comparing the response to the same stimuli in two behavioral states: while the animal was passively listening and while the animal was actively engaged in task performance. Model of combined gain and tuning shape changes introduced in Chapter 3 was used to define changes in responses during behavior in terms of two different components: global gain change in the response of the neuron, and an orthogonal tuning shape change; i.e. $\mathbf{S_d} = g.\mathbf{S_b} + \boldsymbol{\delta}$. The equation is manipulated to study the changes in response to the noise band at the BF, noise band at the frequency of the tone, and the change in response to the target tone, substituting S with Nbf, Nt, and T respectively. The gain or *g* term in the equation was measured using *gain fitting STRF model* (David et al., 2008). The model measured the average tuning curve for an experiment from the responses to the nosie bands presented in the passive pre-behavioral, and active (during the performance of the task) epochs. This average tuning curve was then used to scale the passive and active tuning curves to match the averaged one. The ratio of the scalars computed during behavior and passive was defined as the change in gain of the neuron.

4.3 Results

4.3.1 Passive response properties of PEG:

Studies of secondary auditory areas in animal models like the rat (Pandya 2007), the cat (Tian et.al 1998) and the ferret (Bizley 2005) report long latency onset response, long sustained response, higher level thresholds, and higher percentage of units with non-monotonic level functions. Similarly responses gathered from PEG in this study show long latency response for neurons that range from 30-80ms, and

response durations that last from 50ms to 200ms. Fig.4.2A shows an example of a PEG cell's response to short pure tones (100ms) of frequencies ranging from 125 to 16000Hz all presented at 70dB level. This unit responds with a minimum latency of 40ms to frequencies around 500Hz, and with maximum response to frequencies 250 Hz with a 50ms latency and sustained response that lasted till about 150ms.

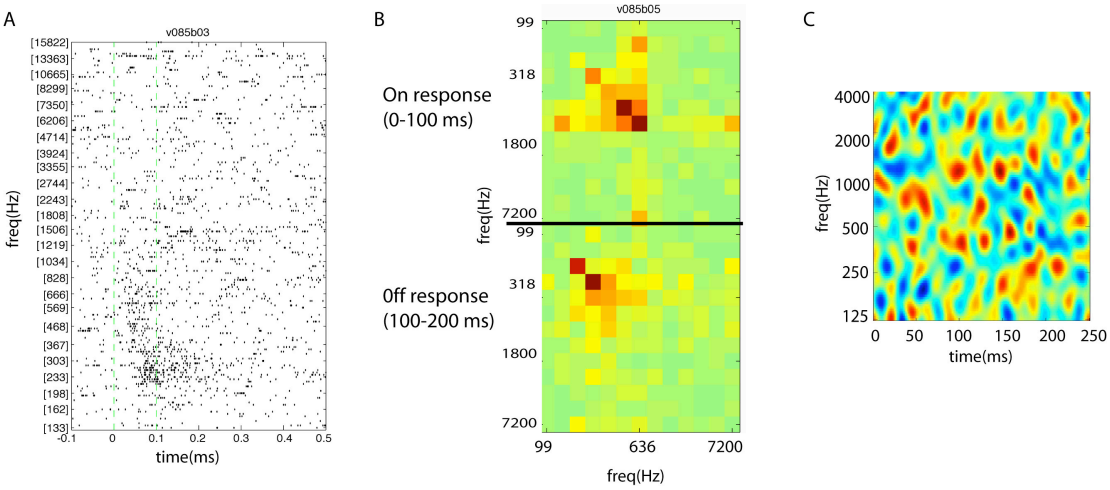

Figure 4.2: example of passive neural responses in PEG

A: raster capturing a secondary cell's response to pure tones that ranged from 125Hz to 16kHz. **B**: Heat map capturing the response of the cell to two tone chords, chords paired tones ranging from 99Hz 7200Hz. The upper part of the heat map shows the on response of the cell, during the first 100ms after the onset of the sound. The lower part of the heat map, captures the response in 100to 200 ms after the onset of the sound, which is the first 100ms after the offset of the sound. **C**: is a low yeild STRF of this cell measured from the responses to TORCs.

Fig 4.2B shows a heat map for this cell's response to two tone chords. This stimulus consisted of two tones paired from a predetermined set of two tones chords (see Methods). The heat map in this figure illustrates a nonlinear response to the two tone combinations, where the response to two tone chords does not reflect the sum of response of the individual tones. Primary auditory cells' response to two tones chords

can be approximated by a linear relationship between the response to the first and the second tone in the complex (see example in Fig 4.3B). Fig 4.2C illustrates the STRF measured from the same cell's response to TORCs. This is a very low yield STRF and doesn't contain information about the spectrotemporal properties of the neuron, a result to PEG cell's poor phase locking to the envelope of the TORCs, rendering the measurement of the spectrotemporal properties of the neuron via reverse correlating with the spectra of the TORCs useless for this purpose.

Fig 4.3 illustrates the responses of a primary cell in A1 to the same stimuli used in the example displayed in Fig4.2. Primary cells have sharp onset responses to pure tones with a short onset response of around 18 ms and a short response duration of about 20ms. This cell like many primary cells in A1 has very low sound thresholds, in this example it's threshold is 30dB. Fig 4.3B shows a characteristic response of primary cells to two tone chords where in this example the cell is tuned to about 1200Hz, and responds to 1200Hz no matter what other frequency the tone is paired with. This cell's response to these chords is a demonstration of a linear like response and confirms the tendency of primary neurons towards linear response properties. This is emphasized further by the high yield STRF illustrated in fig 4.3C which shows the spectrotemporal tuning properties of this cell, and is another indication of mostly linear response for this primary cell.

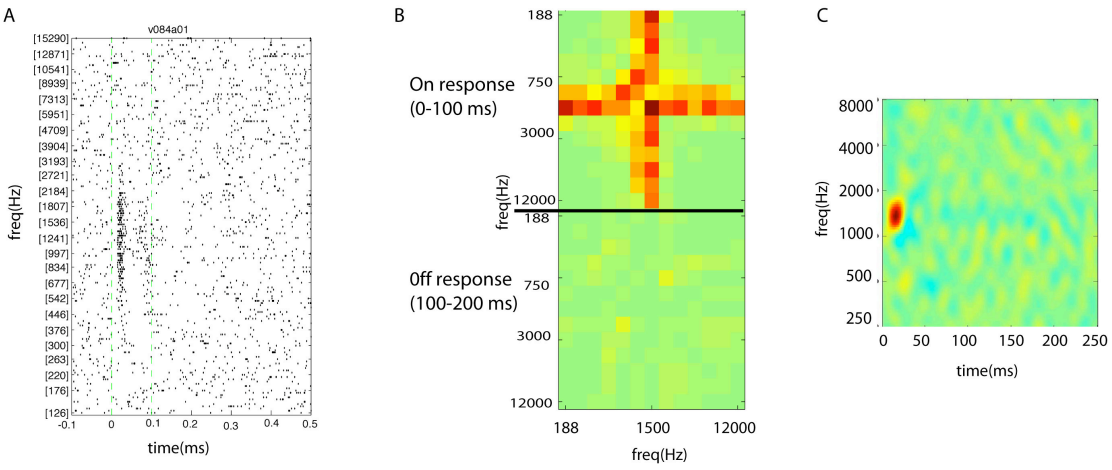

Figure 4.3: example of passive neural responses in A1

A: raster capturing a primary cell's response to pure tones that ranged from 125Hz to 16kHz. **B**: Heat map capturing the response of the cell to two tone chords, chords paired tones ranging from 188Hz 12000Hz. The upper part of the heat map shows the on response of the cell, during the first 100ms after the onset of the sound. The lower part of the heat map, captures the response in 100to 200 ms after the onset of the sound, which is the first 100ms after the offset of the sound. **C**: is a high yield STRF of this cell measured from the responses to TORCs

Poor phase locking of PEG neural responses prevents a reliable measurement of STRFs using the reverse correlation method. The poor phase locking to TORC envelops doesn't necessarily mean the absence of a response to TORCs, as some of the units in PEG respond with a substantial increase in the firing rate to TORCs, but these units fail to consistently phase lock to the envelop of the TORC producing a low yield on STRF measurement from these responses, and rendering this measure of tuning useless for our purposes in this study.

TORCs have been the primary set of stimuli that we used to study spectrotemporal tuning properties and consequently rapid plasticity of these properties during the performance of acoustic tasks. This required the development of

a new stimulus set that allows for the reliable measurement of tuning properties in both A1 and PEG. This study used a set of band pass noise stimuli. Noise bands were half, quarter or an eighth of an octave in spectral width. Reference stimuli were drawn from a predetermined set of these band pass noise stimuli (see Methods). The target stimulus, a pure tone, was fixed in frequency for a given experiment, and was varied from one experiment to another. Animals learned to lick during the reference stimuli and stop licking when they detected the target in order to avoid a mild shock. Figure 4.4 illustrates a schematic of a trial. Each behavioral session consisted of many trials that had 2 to 6 references followed by a target tone except on catch trials, where there was no target and a trial consisted of seven references.

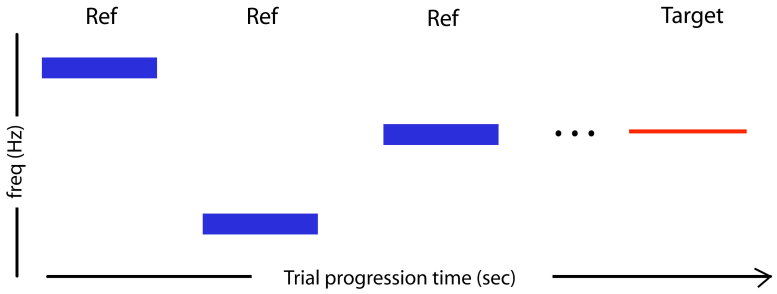

Figure 4.4 Schematic of a behavioral trial

4.3.2 Plasticity in Secondary Auditory Cortex (PEG)

Neural responses were gathered from four behaving ferrets. In three of these ferrets neural responses were recorded from PEG. Another ferret was used to record from A1. In two of the ferrets where PEG responses were gathered, A1 responses were gathered from them as well. Neural responses from these two areas were gathered in two behavioral states; during passive listening, and during active engagement in the task. Results from these experiments are presented in a

comparison framework. Task related changes are reported in PEG and compared to changes in A1.

While ferrets performed one or two behavioral tasks in a given recording session, it was seldom possible to maintain recordings from the same cell throughout multiple task conditions. Consequently, most of our measurements are from single cells that were recorded during one task condition and its preceding passive state.

4.3.2.1 Patterns of plasticity in single units in PEG:

When an animal discriminates a target tone from a TORC reference or from a tone of a different frequency, neural receptive fields are altered to enhance the frequency of the target tone and suppress the reference signal. This enhancement was in the cell's response to a certain frequency measured through reverse correlating with the spectrum of the stimulus, which directly translates into improvement in the phase locking to that frequency in the envelop of the TORCs. Here since PEG neurons don't phase lock in response to sound onset, or to the envelop of broad or narrow band modulated stimuli, TORCs can no longer be used to measure the spectrotemporal tuning properties of cells in PEG. As explained above, the reference set of band pass noise elicited robust responses from the two areas, this allowed for the measurement of spectral tuning properties in both areas. Tuning curves were measured by averaging over the time axis of the rasters of neural responses. Therefore the plasticity we report in this study will be measured in terms of changes in firing rate in response to target tone and reference noise bands. We look at firing rate to noise bands across frequencies probed in the experiment, specifically firing rate to noise bands at the BF of the neuron, and firing rate to noise band that falls near the

target tone. In addition to changes in the response to reference noise bands changes in firing rate to the target tone.

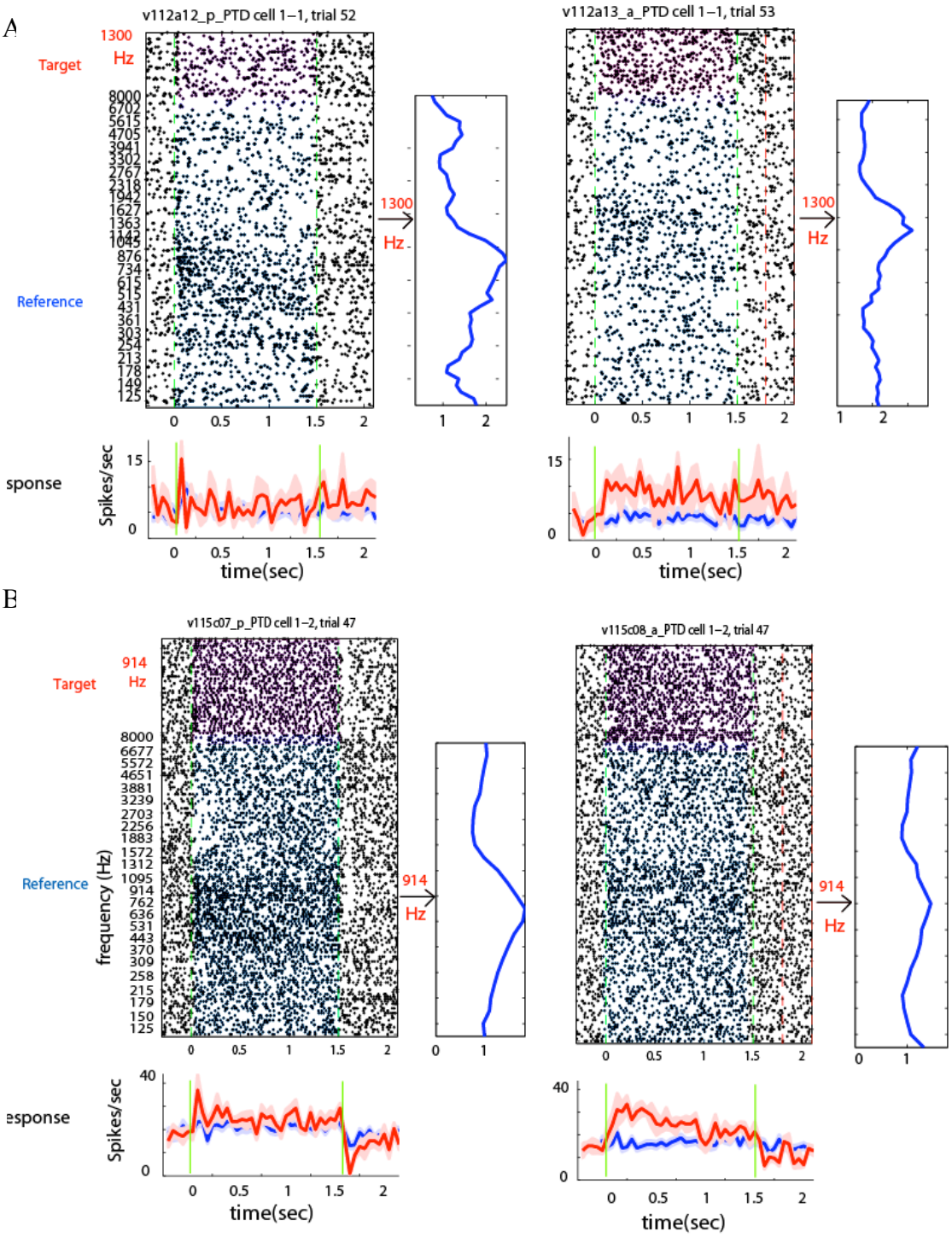

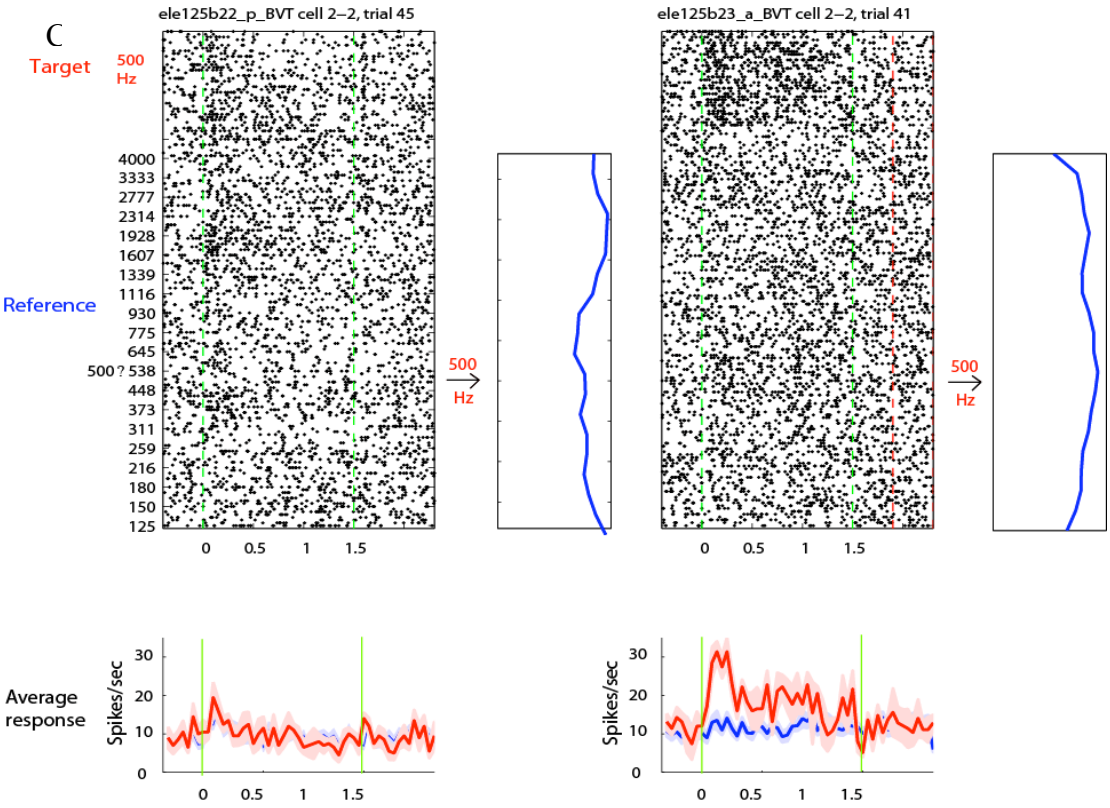

Figure 4.5: Examples of task related changes in PEG

A number of changes were observed in the response properties of neurons in the PEG. Overall there was an increase in cell's firing rate to the target tone during the performance of the task. In addition to a decrease in the response to the noise bands at and around the BF during behavior, some cells displayed a shift in tuning towards the frequency of the target tone during the performance of the task. For example, in Fig4.5A this cell responded to noise bands with center frequencies ranging from 400Hz to 1900Hz as is clear in the passive raster of this cell's response. The cell responded with a higher sustained response between 500Hz and 1100Hz and a maximum response to the noise band centered at 1000Hz (BF of the cell) as is clear from the tuning curve measured by averaging the responses to different noise bands over the duration of these stimuli. In this example the tone was placed at 1300Hz,

relatively near the BF. During the passive listening state the cell responded to the target with a weak onset response and a return to the spontaneous baseline firing rate for the remaining duration of the sound, as illustrated by the PSTH of the tone response marked in red. During the animal's active engagement in the task a shift took place in the tuning curve from a maximum response at around 1000Hz towards noise bands with frequencies closer to the target tone. This shift manifested itself in a significant reduction in the response to the noise bands at the BF, and an increase in the response to the noise bands around the frequency of the target tone. The response to the target tone during behavior increased significantly from its pre behavior passive firing rate, this increase is most evident during the sustained response to the tone. For the example illustrated in Fig 4.5 B the tone is placed at 900Hz near the best frequency of the cell, while the animal is passively listening. This cell responded well to the noise bands with center frequencies ranging from 400Hz to 1200Hz, with a peak in the response to the noise band centered at 914Hz which is designated as the BF of the cell. The cell exhibited a weak onset and a weak sustained response to the target tone. During behavior the overall tuning of the cell didn't change, with a small decrease in the magnitude of response to the reference which is mostly visible in the response to the noise bands around the BF of the cell. The response to the target on the other hand increased significantly compared to the passive cell's response to the same tone. In the example in Fig 4.4 C during the passive listening state the cell's responded weakly to references between 1600Hz and 2200Hz with a maximum response around 1900Hz (BF). We placed the tone at 500Hz about two octaves away from the BF. The response to the target tone was characterized by a weak onset

response to the target tone followed by a return to the spontaneous firing rate during the sustained portion of the response. During behavior the cell's weak response to the noise bands around the BF becomes weaker and there was a very slight increase in the response to the noise bands around the frequency of the tone, compared to this week change in the response to the noise bands, the response to the target tones during behavior increases significantly from its pre behavior passive firing rate.

4.3.2.2 Patterns of plasticity in single units in A1

A1 cells are characterized by a sharp onset response to pure tones and high phase locking to envelop of narrow band or broad band stimuli. We used the same stimuli used while recording from PEG neurons. Cells in A1 responded with a sharp onset response to pure tone and noise bands that fell with in the receptive field of the cell. Pattern of plasticity in tuning and firing rate of the cells were mixed. Some cells showed increased firing rate response to the target tone, and an enhanced response to the noise bands near the target tone. But an equivalent number of cells exhibited an opposite trend, where the response to the target tone was suppressed during the performance of the task, and the response to the noise bands that are close to the target tone was suppressed as well. One trend that was observed in most A1 neurons was a suppression of the response to the noise bands at the BF of the cell. Fig 4.6 A illustrates an example of an A1 cell that responded to noise bands between 1500Hz and 8000 Hz with a maximum response around 6000Hz. The cell also responded to a target tone at 4400Hz with a large onset response and a sustained response that significantly differed from the base firing rate of the cell. During behavior there was a suppression to the cell's response to noise band that were far from the BF while the

response to the noise bands near the BF and the target were strengthened. There was also an increase in the cell's sustained firing rate to the target tone, while there was a mild decrease in the onset response.

Fig 4.6 B shows another example of A1 cell where the tone was placed near the BF of the cell. This cell responded robustly to noise bands between 600 and 1300Hz with a maximum response to noise bands around 900Hz. The cell responded with a robust onset response to a target tone of 1200Hz and no sustained response that differed from the base line firing rate of the cell. During behavior there was an over all suppression of the response to the reference stimuli, where the firing rate to the noise bands around the BF decreased to baseline levels in the sustained portion of the response. The response of the cell to the target tone during behavior was characterized with a reduction in the onset firing rate to the tone. There was no difference in the sustained firing rate of the cell; it remained at base line during behavior.

Fig 4.6 C displays a third example of an A1 cell where the target tone (1000Hz) was placed more than two octaves away from the BF of the cell. This cell responded to noise bands ranging from 125 to about 4000Hz with a BF of 150Hz. The cell response to the target tone didn't differ from the baseline given that the tone was placed well out of the receptive field or frequency range of response of the cell. During behavior responses to the noise bands near the BF of the cell dropped significantly leaving a very small (almost negligible) response to the noise band at 200Hz, and there was no change in the cell's response to the target tone.

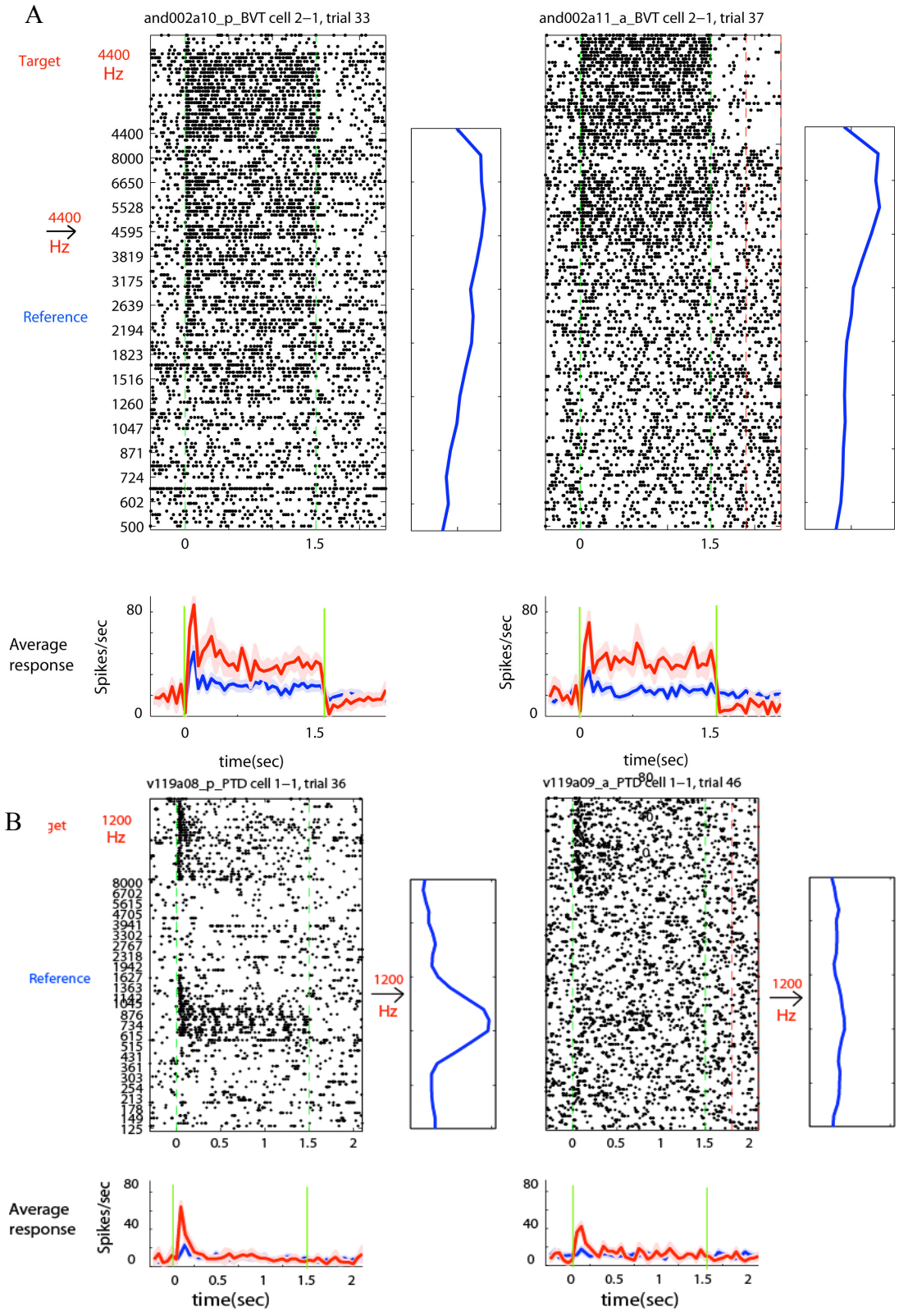
A
and002a10_p_BVT cell 2–1, trial 33
and002a11_a_BVT cell 2–1, trial 37
Target
4400 Hz
4400
8000
6650
5528
4595
3819
3175
2639
2194
1823
1516
1260
1047
871
724
602
500
4400 Hz
Reference
0
1.5
Average response
Spikes/sec
80
0
time(sec)
B
v119a08_p_PTD cell 1–1, trial 36
v119a09_a_PTD cell 1–1, trial 46
1200 Hz
8000
6702
5615
4705
3941
3302
2767
2318
1942
1627
1363
1142
1045
876
734
615
515
431
361
303
254
213
178
149
125
Reference
1200 Hz
0
0.5
1
1.5
2
Average response
Spikes/sec
80
40
0
time(sec)

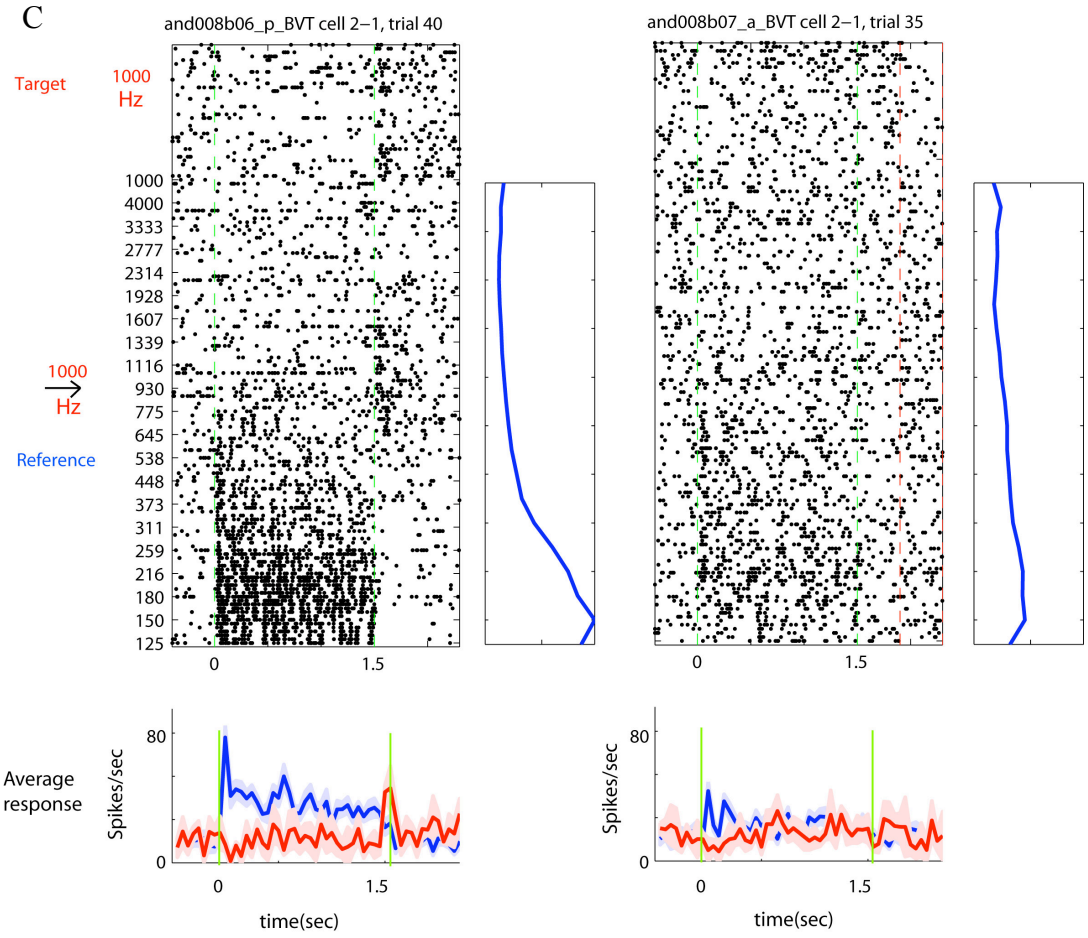

Figure 4.6: Examples of task related changes in PEG

4.3.2.3 Population Patterns of plasticity

To assess the population patterns of plasticity, responses of 81 cells from PEG and 62 cells from A1 were pooled. The PSTHs for responses to the target and the reference stimuli were averaged for the passive state and the active behavior state for cells from A1 and PEG separately, as illustrated by the right panels of Fig4.7, where the average PSTH for the response to the tone in the passive state is illustrated in light red and the average PSTH for the tone responses during behavior is illustrated in dark red. In A1 responses to the target experienced a decrease on average during behavior,

where there was a clear decrease in the onset response to the target when compared with the passive response. There was also a smaller drop on average in the sustained response to the tone during behavior when compared with the sustained response to the tone in the passive state. In PEG, neurons exhibited an average increase to in the response to the tone during behavior as clearly illustrated by the average active PSTH when compared with the average passive PSTH. The average PSTH response to the target tone captures a consistent trend of plasticity in PEG during the performance of the task where the engagement in the task resulted in an increase in the firing rate in response to the target in many cells. This was different from the population trend in A1, where the cells exhibited a mild suppression on average for the sustained response during behavior and a more apparent suppression to the onset response (Fig 4.7)

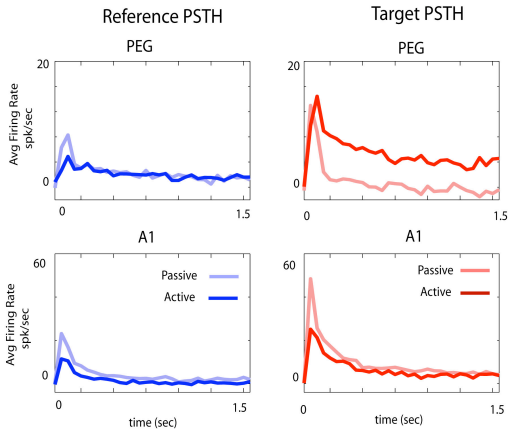

Figure 4.7: Average Population PSTH for reference and target

The PSTH for response to all noise bands was averaged across the population of neurons in PEG and A1, as illustrated in the left panels in Fig4.7, where the passive average population PSTH is illustrated in the light blue and the active PSTH

population average is illustrated in the dark blue for both areas. The average PSTH for the response to the noise bands show a small suppression in the PSTH response to the reference during behavior that was apparent in both the average in PEG and A1. To investigate what noise bands specifically contributed to the suppression seen in the average response, the PSTH of the response to two specific noise bands were generated; PSTH for noise band at the BF of the cell, (BF is defined as the center frequency of the noise band that elicits the maximum response by the cell) and the noise band that the frequency of the tone falls with in, or as will be called, the noise band at the tone. Population PSTH of responses to these two noise bands were averaged for the passive and active states, for cells in PEG and cells in A1 separately. Fig 4.8 shows the population mean for these PSTHs where the left panels show the population average PSTH for the noise band at the BF, with the average passive PSTH illustrated in light green and the active average PSTH illustrated in dark green. These average PSTHs show a clear suppression in the response to the noise bands at the BF of the cell. This suppression is seen for responses in PEG and A1. The average PSTHs for the noise band at the tone show some, though less pronounced than the suppression seen at the BF. This difference in the suppression is apparent in both areas, though it is much more pronounced in PEG, where the responses to noise band at tone exhibit a mild suppression, especially in the sustained part of the response. It is unclear whether this is a real difference in the response of the two areas, or whether this is due to the fact that the average response to the noise band at the tone in the passive state is very small to start with. To answer this ambiguity and investigate the

source of suppression witnessed in the response to the reference during behavior, changes for each cell were assed and pooled in the section below.

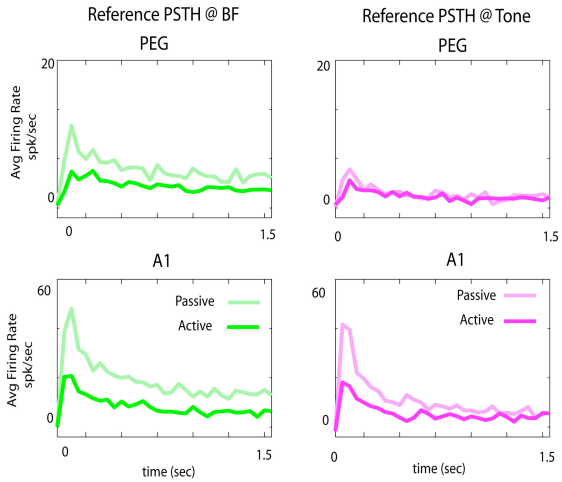

Figure 4.8: Average population PSTH for noise band at BF and at tone

4.3.2.4 Changes in gain, tuning and target responses

The suppression revealed in the averages of PSTH response to the reference sounds, which become more pronounced in the average PSTH response to the noise bands at the BF invokes the question of whether this suppression is due to change in the global gain of the response of the cell or whether it is a frequency specific change that doesn't require change in the gain of the cell's response. To answer this question the model developed in chapter 3 (Atiani et al 2009) is utilized. The *active (during) tuning curve* ($\mathbf{N_d}$) is defined as the *passive (before-task) tuning curve* ($\mathbf{N_b}$) scaled by the change in the gain of the response ***g*** added to frequency specific changes that are not captured by the change in gain, i.e.: $\mathbf{N_d} = g.\mathbf{N_b} + \boldsymbol{\delta}$, where g is the *gain* and $\boldsymbol{\delta}$ is the remaining change in the tuning curve that was not be captured by scaling $\mathbf{N_b}$ by the gain. The gain change was measured for each cell in PEG and A1 (see Methods).

Figure 4.9 illustrates the distribution of the gain change in the population of PEG and A1 cells.

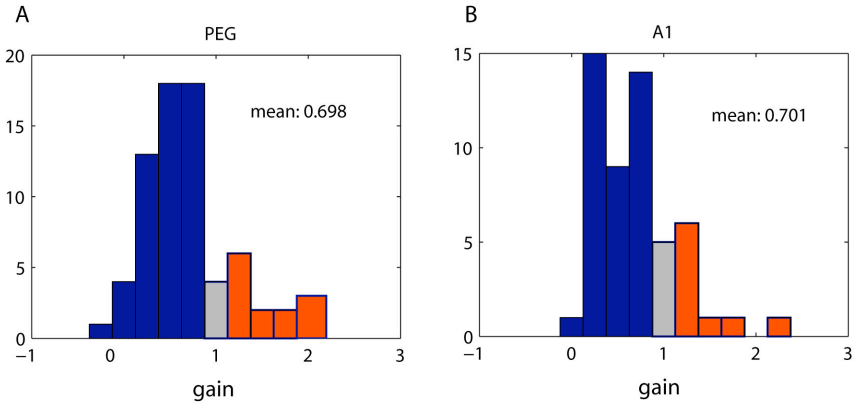

Figure 4.9 : Gain changes in PEG and A1

The distributions of change in gain in PEG and A1 are similar with an average gain value of 0.7 in both populations, indicating a 30% drop in the gain of the cells on average during behavior. Three quarters of the cells in A1 and PEG exhibited a drop in gain. The remaining quarter of the cells maintained or increased their gain. We used the value of gain change for each cell to measure the changes in shape of tuning curves that are not accounted for by the global gain change.

By definition $\mathbf{N_b}$, and $\mathbf{N_d}$ are tuning curves and therefore are functions of frequency. These frequency functions are in essence the average firing rate to the noise bands that span the frequency range of the tuning curve. Given this aggregate nature of the tuning curve measurement, it is possible to apply the same equation defined above to the firing rate of individual noise bands of frequencies of interest; which are in this case the noise band at the BF and the noise band at the tone. Therefore the equations can be altered to reflect these changes:

$$\mathbf{N}bf_{\mathbf{d}} = g.\mathbf{N}bf_{\mathbf{b}} + \delta\mathbf{N}bf \ldots (1)$$

where $\mathbf{N}\boldsymbol{bf}$ is the average firing rate of the cell to the noise band at the BF. So the cell's firing rate to the noise band at the BF during behavior is therefore defined as the firing rate to the noise band at the BF before behavior scalled by the global gain change in the firing of the cell, in addition to $\boldsymbol{\delta Nbf}$, which is the changes at BF that are not captured by the change in gain.

Similarly to apply this model to the noise band at the tone, the equation becomes:

$$\mathbf{N}t_{\mathbf{d}} = g.\mathbf{N}t_{\mathbf{b}} + \boldsymbol{\delta Nt} \quad \ldots (2)$$

where $\mathbf{Nt}$ is the average firing rate to the noise band at the tone, and where $\boldsymbol{\delta Nt}$ represents the changes in the tuning curve at the tone that are not captured by the gain change.

Adapting the model above to be used on specific sections of the tuning curves, and therefore having the variables be described in terms of firing rate, allows for applying the same model to the cells' responses to the target tone itself. And while the responses to the target tone fall outside the boundaries defined for the equation above, the basic principle of the equation, which defines the changes as combined global change and specific localized change, can be extended to be used on the responses to target tone. Therefore $\mathbf{T_d}$ is defined as the cell's firing rate in response to the tone *during* the performance of the task, and $\mathbf{T_b}$ as the cell's response to the same target tone as the animal was listening passively *before* the task, The response to the target tone during the performance of the task is affected by the change in global gain of the response, which affects the response to the tone as it affects the response to the reference noise, and a second term: $\boldsymbol{\delta t}$ that is by definition the change in the response that is not captured by the gain change; i.e. $\boldsymbol{T_d} = g.\boldsymbol{T_b} + \boldsymbol{\delta t}$ … (3)

Equations 1,2, and 3 were used to measure δN_{bf}, δN_t and δ_t for each cell in PEG and A1. The value of δ was deemed significant if it was at least twice as large as the standard error of the signal. Figure 4.10 shows the distributions of the δN_{bf}, δN_t and δ_t for the populations of cells in PEG and A1. The distributions of δN_{bf} in both PEG and A1 are negatively shifted, indicating there is an additional decrease in the firing rate at the BF that is not captured by the gain drop measured, and illustrated in Fig4.9. This negative trend is significant in PEG and A1, a t-test shows that there is no difference in the distributions of δN_{bf} in PEG and A1. The distributions of δN_t are centered at zero for both A1 and PEG, indicating that while some δN_t took negative or positive values for different cells, the population average shows no change for the noise bands at the tone that wasn't captured by the change in gain. Nevertheless the zero centered distributions of δN_t in PEG and A1 are significantly different from the negatively shifted distributions for δN_{bf} in both areas ($p=0.0039$ in A1, $p=0.0094$ in PEG). This indicated that the changes at the noise bands at the tone were slightly more positive than those at the BF.

The distributions of δ_t contain the most striking result of this study, where the distributions of δ_t show that 75% of cells in PEG exhibited an increased firing rate to the target tone during behavior, compared with 48% of cells in A1. As a consequence, the distribution of δ_t in PEG is positively shifted with a median of increase of 2.8 spikes per second. The distribution of δ_t was centered around zero with slight shift to the negative that was not significant. Applying a t-test on the distributions of δ_t and δN_t in both PEG and A1 reveals that the change in the firing rate to the target tone

was significantly different than that to the noise band at the tone in PEG (p=0.0004), where as the same test applied to A1 indicates that the change in response to the target tone and the noise band at the tone are not significantly different in A1.

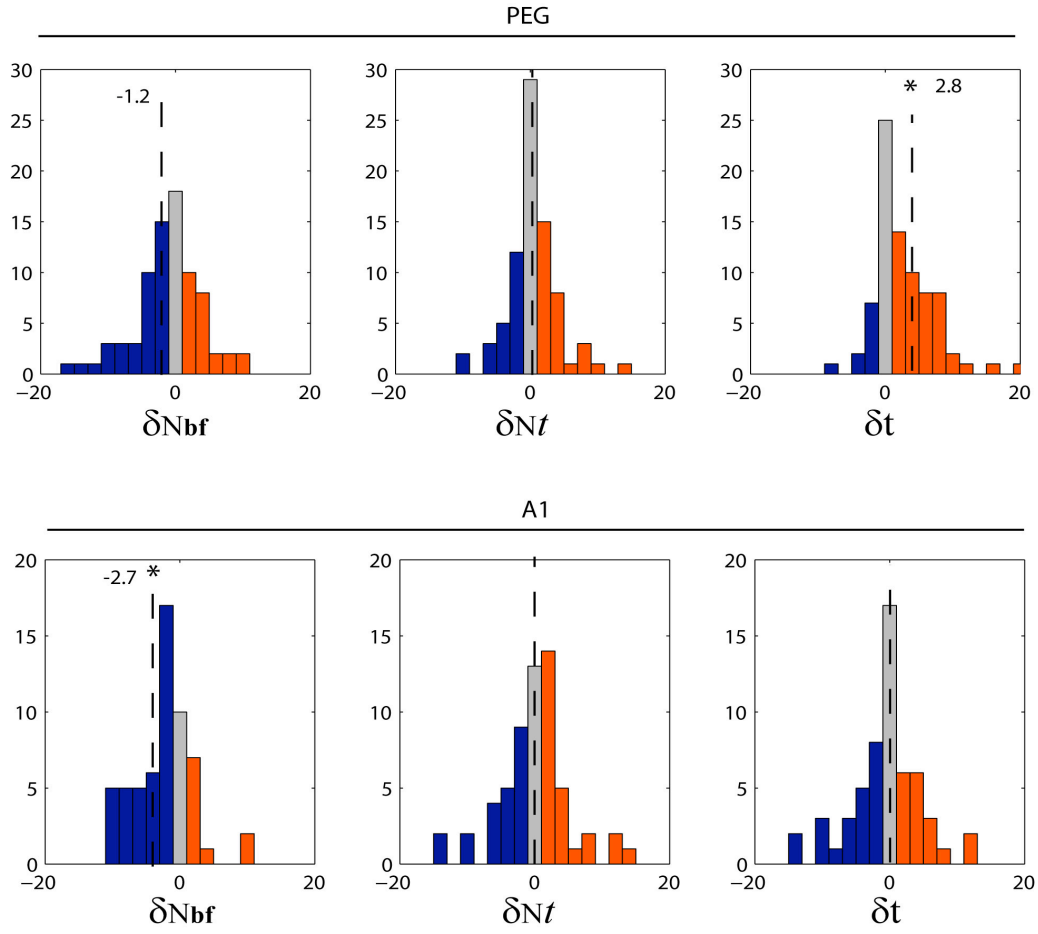

Figure 4.10: Distributions of shape changes (δ) in PEG and A1

Figure 4.11 illustrates similar distributions as in Figure 4.10, but only with the cells that had significant values of **δN*bf*,** **δN*t*,** and **δ*t***. Taking only the significant values of **δ** provides a different view of the data, where the negative trend in the **δN*bf*** seen in Fig 4.10 no longer holds, and the distributions of **δN*bf*** are centered around zero indicating that most of the changes at the BF were captured by the change in global gain (distributions illustrated in Fig 4.9).

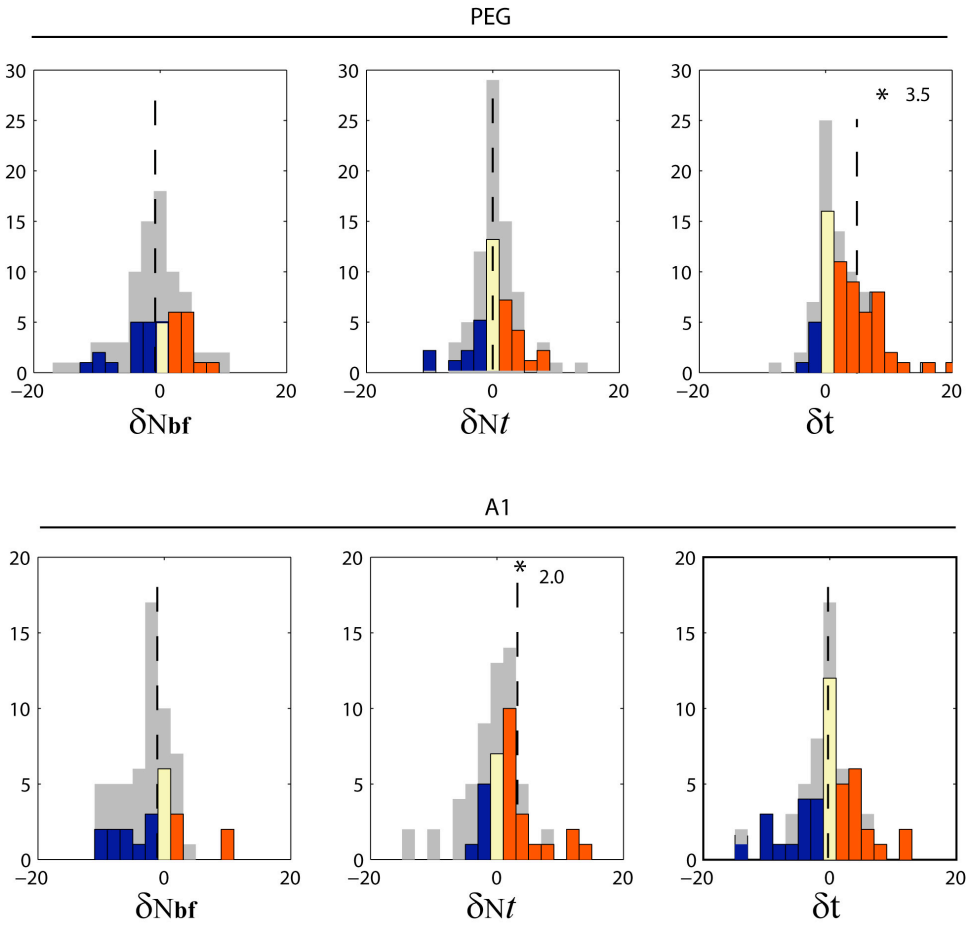

Figure 4.11: Distributions of *significant* shape changes (δ) in PEG and A1

Another difference revealed when looking at the significant values of the **δ** is that the distribution of **δN*t*** in A1 became positively shifted, a shift that is significant ($p<0.05$). This also made the distributions of **δN*bf*** and **δN*t*** significantly different in A1, confirming the trend seen in Fig 4.10. The positive shift in **δN*t*** indicates that in A1 cells's response to the noise band at the tone was not fully captured by the gain change, and that cells in A1 responded with a relative increase in firing rate to the noise band at the tone, and that increase on a population level was significantly different ($p=0.0006$) from these cells' responses to the noise band at BF. There was

no similar effect in PEG, where the distributions of δN_{bf} and δN_{t} were not different ($p=0.16$) indicating that the change in gain response of the cell captured changes in the firing rate of PEG cells to the noise bands at the BF and at the tone. The significant values of δt emphasized the positive trend seen in the distributions in Fig 4.10, where out of the cells in PEG that showed significant δt ($n=62$), 83% had a positive δt value, i.e showed an increase in the relative firing rate to the target tone during the performance of the task, compared to 51% of the cells in A1, where the distribution of δt was centered on zero.

4.4 Discussion:

Receptive fields in A1 undergo changes in their spectrotemporal properties to better the performance the task at hand (Fritz et al., 2003; Fritz et al., 2007a). This study aimed to expand the investigation of rapid plasticity into higher order auditory areas. Here neural responses were gathered from awake behaving ferrets as they performed an acoustic task requiring them to distinguish between two classes of sounds, band pass noise stimuli presented at different frequencies which they learned are safe to lick the water spout when they were heard, and pure tone of the same duration which required them to stop licking the water spout right after its end. The experimental paradigm we used in this study is similar in design to the that used to study plasticity in A1, however a couple of things were changed in this study; first the reference stimuli in this study is one of a set of band pass noise stimuli which are much narrower in their spectral bandwidth than the TORCs that were used as reference in previous work (Fritz et al. 2003, 2005, 2007, Atiani et al. 2009). This set

of stimuli was chosen because it elicits robust responses from A1 and PEG cells where TORCs become less reliable in producing a high yield STRF in PEG because of the change in its temporal properties.

The second difference in this study is that the neural responses were collected in the passive state to the same stimuli played during the performance of the task. In previous studies in A1 the stimuli played in the passive condition was the reference stimuli only, in order to measure an STRF for the passive state, the target tone was not played to the animal in the passive state. That was convenient as the changes measured during those experiments were changes in the spectrotemporal properties of the cells for which only a high yield STRF was necessary. It became apparent after the completion of those studies that the studies were not able to account for any changes in the response to the target tone itself. Therefore in the present study responses to the reference and the target were collected in the passive and the active behaving states, which allowed for measuring the task related plasticity in response to the target tone as well as changes in tuning properties.

4.4.1 Response indicators of plasticity

There are many response measures that are useful indicators of plasticity, and the choice of response measures is often dictated by the nature of the behavioral task, experimental paradigm, the stimuli, and the cortical area under investigation. For instance, tuning curve BFs and bandwidths have been among the most commonly used measures in experiments studying plasticity using pure tones to measure the tuning curves for neurons in various auditory fields. Other measures used were rate-level non-monoticity with level-detection tasks in A1 (Polley et al 2004,2006), and

modulation transfer functions for rate-discrimination tasks (Kilgard and Merzenich 1998, Bao et al 2004). Previous studies from our lab have extensively relied on the STRF estimated from responses to TORCs as a measure of the tuning properties of the neurons, and task related (Klien 2000). This is one of a host of measures that have been developed over the last decade to estimate the spectral and dynamic properties of response areas in AI and some other auditory (DeCharms et al 1998, Escabi and Schreiner 2002, Theunissen et al 2000, Miller et al 2002). TORCs are highly effective stimuli in A1 because of the fidelity of the response of cells and the high phase locking to the envelop of stimuli that they exhibit, making STRFs are a great measure of small changes in temporal precision and phase locking that the cell's exhibit during the performance of the task. Changes that do not always correlate with an increase or a decrease in the firing rate of the cell.

And while they are highly effective in A1, the use of TORCs and STRFs cannot be readily extended to other auditory cortical areas like PEG where responses are temporally sluggish, and do not phase-lock to the modulations in the spectra of TORCs, resulting in low yield STRFs. Substituting TORCs with band pass noise allowed for the measure of tuning curves for both A1 and PEG cells. And while not as convenient as STRFs in measuring the temporal properties of the cells, this new set of stimuli provided an alternative to measuring the spectral tuning properties of these cells by eliciting a robust response from neurons in both areas. However unlike STRFs, tuning curves in this case are a direct measurement of the firing rate of these cells, and therefore by virtue of using this new stimuli set, we are looking at a different indicator of plasticity, an indicator that is heavily reliant on changes in firing

rate, unlike previous studies that relied on the changes in the temporal precision and phase locking normalizing changes in firing rate.

4.4.2 A different form of plasticity:

The results from this study show a significant distinction in the form and magnitude of plasticity that PEG and A1 neurons exhibit. PEG neurons showed a significant increase in the firing rate to target tone during the performance of the task. Cells in A1 didn't exhibit a similar pattern; the population of cells in A1 showed no significant change in the firing rate response to the target tone during behavior. The lack of significant change in the firing rate to the tone in A1 during the performance of the task is a result of response properties of primary cells in A1 which are characterized by temporal precision and phase locking to stimuli's envelop, since A1 uses spike timing rather than firing rate as the main mechanism to encode sound (DeCharm and Merzenich 1996). Previous studies of rapid plasticity in A1 confirms that changes in tuning reported during behavior are due to changes in the phase locking rather than changes in the firing rate (Fritz et al 2003, 2005, and 2007, Atiani et al 2009). Therefore the results of this study indicate that PEG neurons exhibit a different form of plasticity one that is characterized by change to the firing rate of the neuron, rather than to their spike timing or phase locking. This indicates also a transformation in the mechanism of coding in secondary auditory cortex, where cells encode stimuli by different firing rates. And while firing rate can only relatively encode stimuli, relative representation of a signal with in what's behaviorally relevant in an environment is adequate to distinguish relevant parameters and stimuli.

4.4.3 The significance of plasticity in higher order areas

Studies in visual cortex have often described task related changes in terms of changes in gain and shape of receptive fields or to reflect changes in gain only (Connor et al., 1997; Luck et al., 1997; Maunsell, 2004; Maunsell and Treue, 2006). The model of change that was used this chapter and the previous chapters allowed for the distinction between the contributions of change in gain or shape of to the observed plasticity. Separating the contributions from global gain change and frequency specific changes showed that the engagement in this task resulted in 30% reduction in the gain of the response of cells both in A1 and PEG. This is consistent with our results from the previous chapter, in addition to the results from Otazu et al.(2009) reporting that engagement in a task results in a reduction in firing rate of cells in A1. Results from this study show also that there are no significant shape changes in the tuning curves on a population level at the BF in A1 and PEG, indicating that most of the changes in firing rate for the noise band at the BF are captured by the global change in the gain observed. Change in the gain of the cell's response also captured the changes in the response to the noise band at the tone for PEG cells, where neurons in PEG responded in a similar manner to all reference noise bands, whether located at the BF or the tone. That was not the case for A1 cells where changes to the noise band at the tone was not fully captured by the change in the global gain, A1 cells exhibited a relative increase in their response to noise bands at the tone, responding differently to the noise bands at tone than the noise band at the BF. Similar to results from Fritz et al. (2003), cells in A1 enhance the representation of the frequency of the tone, which was manifested by an increase in the phase locking to the frequency of

the tone in the envelop of the TROCs in Fritz et al. 2003, and in this study it is manifested by increase in the firing rate to the noise band at the frequency of the tone, but not to the frequency of other noise bands in the reference. On the other hand the population in A1 showed no average increase in the firing rate to the target tone, where most of PEG cells showed an increase in the response to the target tone. This difference in the change in response to the target was the most pronounced difference in the responses of cells in A1 and PEG, where the vast majority of neurons in PEG (83%), showed a significant increase in the firing rate to the target tone. The lack of average change to the target on a population level in A1 might be due to the fact that the target tone has no modulations or temporal structure which meant most A1 cells responded with a high onset response, and a weak or no sustained response.

The combination of the increase in the response to the tone in PEG with the lack of response to the noise band at the tone indicate the development of a separate representations of the target tone from noise band that has similar frequency component as the tone in PEG. The fact that the tone and noise band at the tone have similar frequency components indicated that the development of the new representation of the target tone during behavior might rely less on the physical characteristics of the stimuli, like the frequency, and more on the behavioral significance of the sound which becomes relevant only during the performance of the task. On the other hand, the difference in the response to the noise band at the tone from that at the BF, indicates that the mechanism underlying plasticity in A1, relies more on the physical features of the sound than PEG, where the performance of the task resulted in an enhancement in the representation of the physical features that are

shared by the tone, and that are present in the noise band at the tone. This transformation in the representation of the target and reference sound from A1 to PEG can be a step towards the development of distinct behavioral representation of the two sound classes that is observed during behavior in frontal cortex (Fritz et al submitted), where frontal neurons do not respond to the reference or target in the passive listening state, and responds with a large increase in the firing rate to the target tone while having no change in the response to the reference sounds.

4.5 Conclusion:

Neural responses were gathered from primary and secondary auditory cortex of the ferret while animals were engaged in the performance of auditory discrimination task. The comparison between plasticity in A1 and PEG showed that PEG neurons exhibit a form of plasticity that is different from that in A1. This form of plasticity further enhances the distinction between the reference and target by increasing the firing rate to the target tone during the performance of the task, creating an increase in the separation between the representation of the two classes of stimuli involved in this task, and providing a step towards distinct behavioral representation of these two classes of sound in executive areas of frontal cortex.

Chapter 5: Tuning properties of Local field potential in primary auditory cortex

5.1 Introduction:

System neuroscience research has utilized extracellular recordings as one of the primary measures of neural activity and computation. These recordings convey two types of signals: first is the spike signal containing the action potentials of the neurons in the vicinity of the electrode tip. The spike signal is obtained by high pass filtering the recorded voltage and isolating the spike form the high-passed signal by thresholding. These spikes are the output of a number of single neurons that fall close to the recoding site, and therefore this signal is referred to in this study as multi single units (MSU). The second and less understood signal is the local field potential (LFP). This signal contains low frequency fluctuations in the electric potential generated by local and more remote neurons. The LFP signal is obtained by low pass filtering the recorded voltage.

While the biophysical origin of the spike signal is well understood (Hodgkin and Huxley, 1952, Holt and Koch 1999) less is known about the biophysical origin of the LFP. It is suggested that the LFP signal represents the combined activity of neurons distributed over a relatively large area of cortex surrounding the recording site (Mitzdorf, 1985). LFP mainly reflects the dendritic activity with in an area of 250 to 500μm around electrode tip (Kruse and Eckhorn 1996, Katzner et al. 2009), reflecting intracortical processing as well as inputs from other brain areas (Mitzdrof, 1985; logothetis 2003). Many studies have reported on the functional significance of the LFP in different contexts, such as motor intentions (Scherberger et al 2005),

visual attention (Womelsdorf et al 2006) and visual object representation and selectivity (Kreiman et al 2006). Additional interest in LFP has been fueled by functional magnetic resonance imaging (FMRI) where LFP seems to be a better predictor of the BOLD signal used in these studies than spiking activity (logothetis et al. 2001, Kayser et al. 2004). While studying the LFP signal has demonstrated potential in many different contexts, the goal of this thesis is the study of rapid plasticity in auditory cortex. Understanding the imprint of rapid plasticity on the LFP signal can provide important insight into the mechanisms underlying this type of plasticity on the level of the neural network in auditory cortex. However an important prerequisite is to understand the tuning properties of the LFP signal. Does it exhibit tuning properties similar to that of the MSU? And what insights does that provide about the processing taking place in auditory cortex? The goal of this chapter is to investigate the spectrotemporal tuning properties of the LFP signal in addition to the tuning of different frequency bands of LFP; alpha (8-12Hz), beta (12-25Hz), gamma (25-100Hz), and high gamma (100-300Hz). The tuning properties of the LFP and its component frequency bands are studied in comparison to those of the MSU from the same recording site.

The MSU and LFP responses were recorded from primary auditory cortex (A1) of awake, passively listening ferrets. Responses to pure tones (narrow band), band pass, and broad band stimuli were recorded. To account for the possibility of contamination of the LFP signal by the spiking activity, the LFP signal was corrected by removing events in the LFP that correspond to nearby spiking events. The tuning

properties (best frequency (BF), preferred spectral and temporal modulation) of spiking activity and different LFP frequency bands were compared.

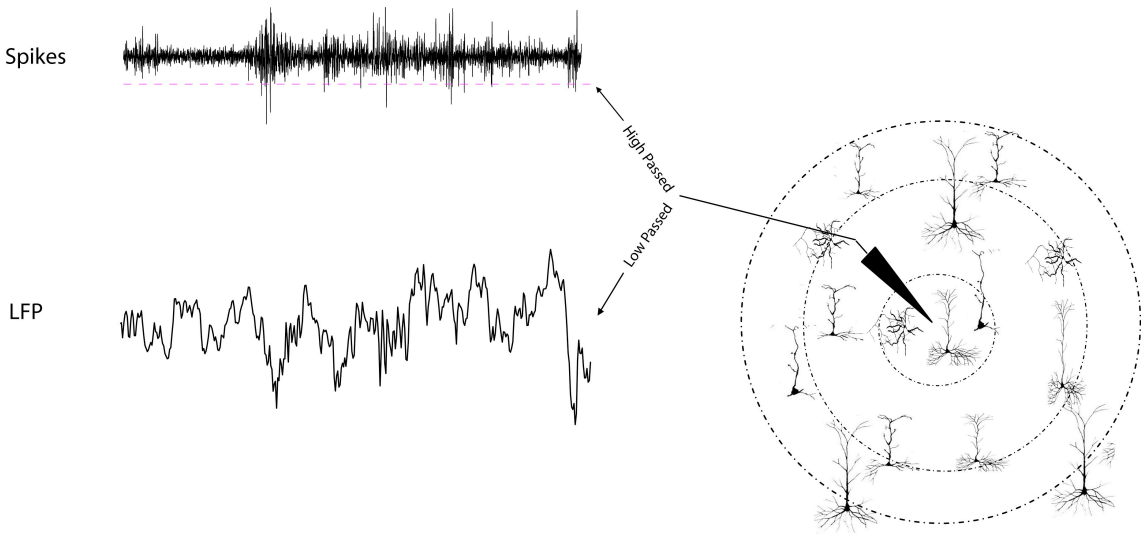

Figure 5.1 Schematic of a recording site and the signals extraction

5.2 Methods

Stimuli:

Responses to narrow band, bandpass, and broad band stimuli were gathered. Narrow band stimuli consisted of 100ms tones, presented one tone at a time with a inter stimulus interval that ranged from 0.8 to 1.2 sec. Bandpass stimuli were quarter of an octave noise burst that consisted of 20 tones logarithmically spaced within the quarter of an octave spectral band. Noise bands were 1.5 seconds long and were presented one noise band at a time, with an interstimulus interval of 1.2 seconds. Noise bands in a given experimental session were presented at different center frequencies to span 3 to 8 octaves. Broad band stimuli consisted of temporally orthogonal ripple combinations (TORCs). Each of the 30 TORCs was a 5 octave wide

broadband noise with a dynamic spectro-temporal profile that is the superposition of the envelopes of 6 temporally orthogonal ripples. A single ripple has a sinusoidal spectral profile, with peaks equally spaced at 0 (flat) to 1.2 peaks-per-octave; the envelope drifted temporally up or down the logarithmic frequency axis at a constant velocity from 4 Hz up to 48 Hz (Depireux et al., 2001; Klein et al., 2000; Kowalski et al., 1996; Miller et al., 2002).

Surgery

Animals were implanted with a steel head post to allow for stable recording. While under anesthesia (ketamine induced and maintained under isoflurane), the skin and muscles on the top of the head were retracted from the central 4 cm diameter of skull. Several titanium set screws were attached to the skull, a custom metal post was glued on the midline, and the entire site was covered with bone cement. After surgery, the skin around the implant was allowed to heal. Analgesics and antibiotics were administered under veterinary supervision until recovery. After recovery from surgery, a small craniotomy (1-2 mm diameter) was made over auditory cortex.

Neurophysiology

Single unit activity was recorded using tungsten microelectrodes (1–5 MΩ, FHC, Bowdoin, ME) from head-fixed animals in a double-walled sound-attenuating chamber. During each recording session, one to four electrodes were positioned by independent microdrives, and activity was recorded using a commercial data acquisition system (Alpha-Omega, Alpharetta, GA). For most recordings, a 60 Hz notch filter was used to remove ambient noise. Because low frequency components of extracellular recordings tend to contain substantially more power than high frequency

components, the analog signal was filtered into low (1–1000 Hz) and high frequency (300–6000 Hz) bands before digitization. The low frequency band was digitized with a 3125 Hz sampling rate, and the high frequency band was digitized with a 25000 Hz sampling rate. The separation of spikes and LFP frequency bands is a standard procedure used by commercial data acquisition systems and outside of experimental control. The analysis described below could also be performed on a single signal, appropriately band-pass filtered to extract spike and LFP bands. Upon identification of a recording site with single units, a sequence of random tones (100 ms duration) was used to measure latency, and spectral tuning. Responses to band pass stimuli and broad band stimuli were also measured.

LFP and spiking activity measurement

Spiking activity was extracted from the high frequency (300–6000 Hz) component of the recorded electrophysiological signal, $r_h(t)$, using two different methods. For the first, multiple single unit spiking activity (MSU) was identified by the time when the recorded potential underwent a rapid decrease during a single time step (1/25000 Hz = 0.04 ms)

$$S_{MSU}(t) = \begin{cases} 1, & r_h(t) - r_h(t-1) < -n\sigma, \\ 0, & \text{otherwise}, \end{cases}$$

so that nonzero values of $s_{MSUn}(t)$ indicated the likely occurrence of a spike at time t if the decrease from the previous time bin was greater than a threshold, $n\sigma$. The value of σ was the standard deviation of $r_h(t)$, and n was a scaling term that specified a sensitivity threshold. This thresholding procedure is a common first step in spike

sorting algorithms. After threshold spiking events were identified, the events were binned at 300 Hz, to match the sampling rate of the LFP signal.

The specific choice of threshold (or even the definition of spike events) may vary across experiments, the logical choice being the threshold used for spike sorting (in previous studies using the same experimental procedures, $n = 4$ was used, (Fritz et al 2003)). Smaller values of n are more permissive and identify a larger number of spiking events while larger values are more conservative.

The raw local field potential (LFP), $L_0(t)$, was extracted from the electrophysiological recording by low-pass filtering (<300 Hz, linear-phase FIR, duration 100 ms) of the low frequency component of the recorded electrophysiological signal (Kayser et al 2007, Gieselmann et all 2008, Norena et al 2008).

Spike decoupling

The signals $L_0(t)$ and $r_h(t)$ existed in entirely different frequency bands and thus were orthogonal (i.e., linearly uncorrelated). However, extracting single or multiunit activity from $r_h(t)$ involved nonlinear computations that could reintroduce linear correlation between them. This coupled component was identified by measuring their cross covariance

$$c_{sl}(\tau) = \langle (L_0(t) - \langle L_0 \rangle_t)(s(t-\tau) - \langle s \rangle_t) \rangle_t.$$

In order to remove all spike-coupled features from the LFP signal, a filter was generated that made the best (i.e., minimum mean-squared error) prediction of the LFP from the spike signal. (David el al 2010)

To remove the spike-coupled components from the LFP signal, the spike-LFP filter was convolved with the spike signal to predict the LFP and the prediction was

subtracted from the raw LFP signal to produce a signal with no correlation with local spiking activity (David el al 2010)

Measuring different frequency bands of LFP:

The LFP signal was divided into 4 different frequency bands: alpha (8-12), beta (12-25 Hz), gamma (25-100Hz), and high gamma (100-300Hz). The alpha and beta frequency bands of the signal were measured by filtering the signal with a band pass zero phase FIR filter with frequency pass area that corresponds to the frequency edges of alpha and beta sub bands. The gamma and high gamma components were computed by filtering the raw LFP signal into the frequency bands corresponding to the gamma and high gamma ranges, the output was then low pass filtered to obtain the envelop of these high frequency signals.

Tuning measurement:

Heat maps of binned MSU rasters and LFP voltage were generated to compare the tuning of both signals. Similarly heat maps were generated for the alpha, beta, gamma and high gamma frequency bands. For the broad band stimuli we measured the spectro temporal receptive field (STRF) for the MSU by reverse correlating the spikes with the dynamic spectra of the stimulus. For the LFP a full cycle was considered an LFP event and these series of events were reverse correlated with the dynamic spectra of the stimulus to measure the LFP STRF. To compare the tuning of the MSU with the different parts of the LFP signal measured in this study, a tuning curve was measured by generating a power spectrum for the LFP signal and averaging the energy in the frequency bands corresponding to the alpha, beta, gamma and high gamma bands. These tuning curves were then centered by the best

frequency of the MSU, and averaged across the population of cells studied. For STRFs the tuning curve was measured by taking a spectral cross section at the latency of the maximum of the LFP, gamma and high gamma STRFs, These tuning curves were centered at the BF of the MSU STRF and averaged across the population of cells studied. Spectrotemporal tuning of MSU, LFP, gamma and high gamma STRFs were studied by measuring the modulation transfer functions (MTF) for each of these STRFs, taking the two dimensional Fourier transform. The preferred spectral and temporal modulation for each STRF was estimated by measuring the center of mass for the temporal and spectral dimension of the MTF.

5.3 Results:

5.3.1 Local field potential responses to narrow band stimuli:

Neural responses to pure tones (100ms) were gathered from primary auditory cortex of the ferret. Neural signal was divided into two components, high passed part of the signal, which after thresholding captured the spiking activity of the neurons in the vicinity of the recording site (MSU). The second part of the neural signal, is the local field potential (LFP), obtained by low passing the same neural signal.

MSU responses to pure tones in A1 have been well studied and reported on in the literature (Phillips et al. 1988, Shamma et al 1993, Mendelson et al. 1997 Eggermont et al. 1998, Bizley et al 2005). A1 neurons respond with high fidelity to pure tones with frequencies falling with in its receptive field. Figure 5.2A shows a heat map capturing this site's MSU response to pure tones ranging in frequency from 125 Hz to 16000Hz, with a maximum response to tones around 2300Hz, which is

marked as the best frequency (BF) of the MSU. This site like most of A1 neurons responds with a sharp onset response around 18ms to the tones falling with its receptive field.

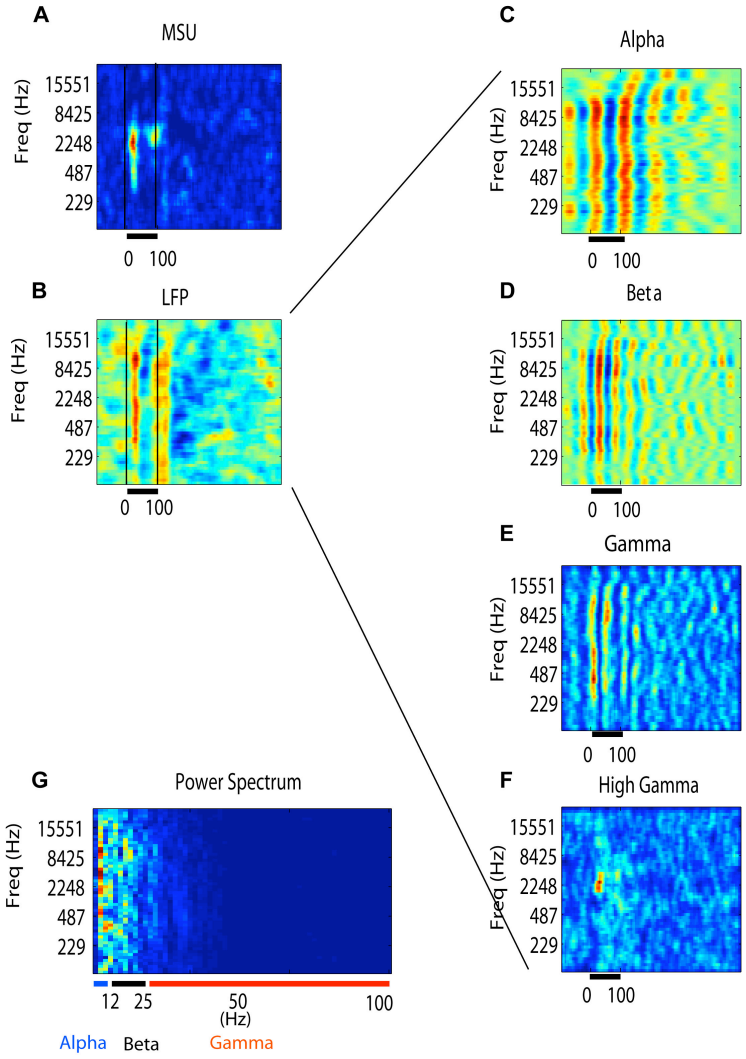

Figure 5.2: Example of MSU and LFP responses narrow band stimuli

The heat map of the LFP of this site, illustrated in Figure 5.2B has deflection in voltage around 18ms after the onset of the tones. The frequency range that elicited the initial deflection in the LFP was larger than that which elicited action potentials from the neurons as apparent in figure 5.2A. This trend in the LFP response was

common in the population of 144 recordings analyzed, where the LFP exhibited a response to a wider range of frequencies than the MSU. To investigate the LFP response further, four frequency bands of the LFP were extracted: alpha (8-12Hz), beta (12-25Hz), gamma (25-100Hz), high gamma (100-300Hz). A heat map was generated for each of the LFP frequency bands as shown in figure 5.2C,D,E, and F. Close inspection of tuning of the four frequency bands shows that the wider tuning observed in the LFP signal is mainly the contribution of the alpha and beta bands, as these bands contain most of the energy in the LFP (Fig 5.2G). The heat maps of the alpha and beta bands show a large frequency range of response like the aggregate LFP signal. The gamma band for this recording site has energy in a broad range of frequencies though less than that in the alpha band (fig 5.2E). The high gamma band on the other hand responded to the frequencies that elicited response in the MSU, making it the one frequency band of LFP in this example that has similar frequency tuning as the MSU.

5.3.2 Narrow band stimuli: Population summary of tuning properties

The population tuning trends for the four different LFP frequency bands were assessed by measuring a frequency tuning curve for each. The BF of each site was defined as the frequency that elicited the maximum response for the MSU. The tuning curves from the four frequency bands were centered at the MSU BF and the population of BF centered tuning curves was then averaged for each frequency band. Figure 5.3 shows the average tuning curves for the four frequency bands centered at the MSU BF. In response to narrow band stimuli, the alpha band exhibit tuning to wider range of frequencies than the MSU resulting in poor tuning on average when

compared with the MSU. The beta frequency band exhibited better tuning than the alpha band. The gamma and high gamma bands show even better tuning, with the high gamma band having the closest correspondence among all frequency bands to MSU frequency tuning.

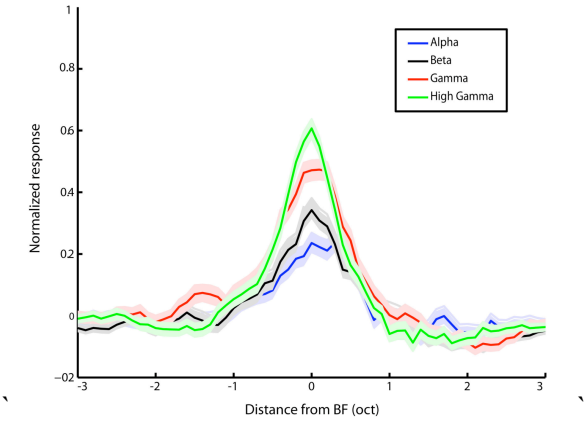

Figure 5.3: Narrow namd stimuli, average LFP frequency bands' tuning

5.3.3 Local field potential responses to bandpass stimuli:

Band pass noise stimuli were generated by adding 20 tones logarithmically spaced with in a quarter of an octave spectral band, creating a spectrally denser stimulus than pure tones. The interaction between the tones gives this stimulus a temporal structure that varied from band to band. Each noise band was presented for 1.5 sec. And by presenting a number of noise bands spanning the frequency range in question (3 to 6 octaves), the tuning of these recording sites was probed. A heat map was generated for MSU, LFP, and the four frequency bands of the LFP studied. Figure 5.4A shows a heat map capturing the MSU response to noise bands ranging in frequency from 250 to 4000Hz. The MSU responded well to frequencies around 1000Hz, with a maximum onset and sustained response. This is marked as the BF of this recording site.

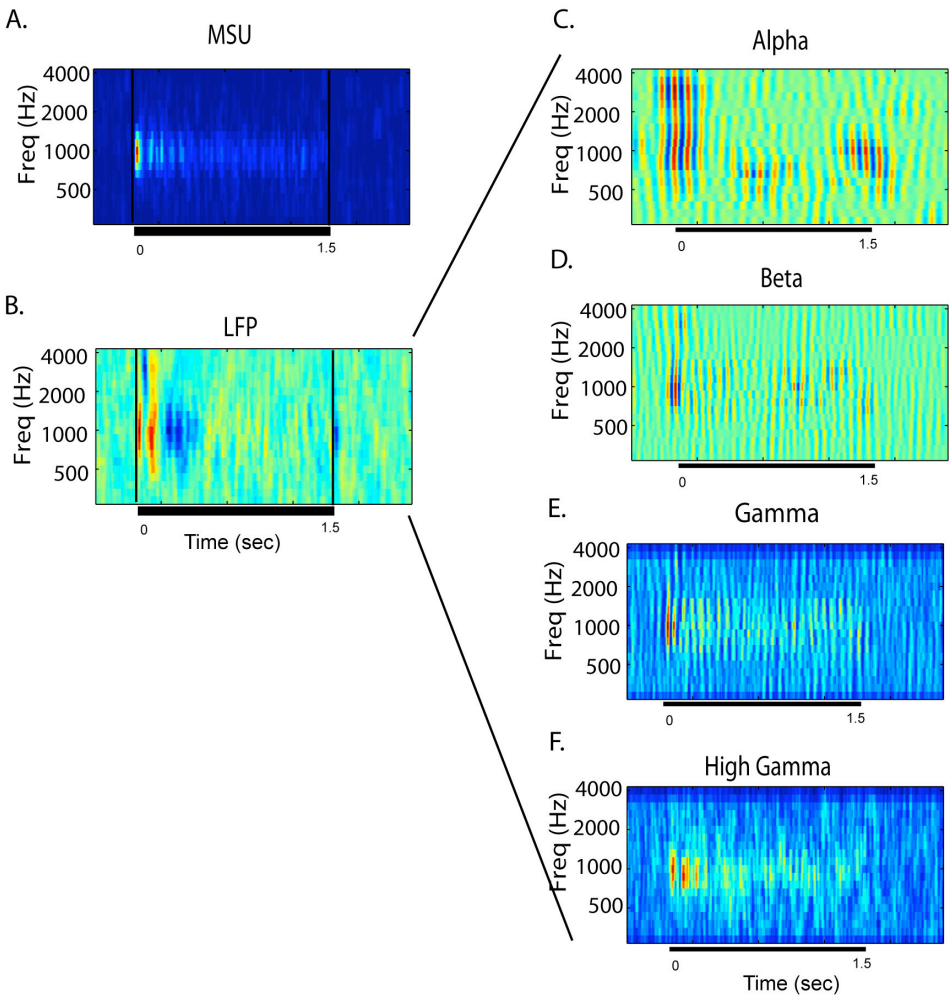

Figure 5.4: Example of MSU and LFP responses band pass stimuli

The heat map of the local field potential of this site, shown in Figure 5.4 B has large deflection in voltage right at the onset of the noise bands. Like the LFP response to pure tones this deflection in voltage comes in response to noise bands with a wide range of frequencies larger than the frequency range that elicited MSU response. The LFP responded in this example is to a frequency range that spanned 3 octaves, while quite larger than the MSU response, the LFP response to band pass noise spanned a considerably smaller range than the example presented in 5.2 where the LFP

responded to tones spanning the range of 6 octaves. In this example the long duration of the stimulus allows for the investigation of whether the LFP exhibits sustained activity. The sustained activity is clearly visible in the MSU heat map (fig5.4A), in comparison the LFP heat map (Fig 5.4B) doesn't show any apparent sustained activity.

The LFP signal was divided into four different frequency bands: alpha (8-12Hz), beta (12-25Hz), gamma (25-100Hz), high gamma (100-300Hz), the heat map for each of these frequency bands is illustrated in figure 5.4 C,D, E and F. Comparing the heat maps of the four frequency bands, the alpha bands captured the wide response seen in the aggregate LFP signal where here as well, the alpha band response spans 3 octaves, and goes beyond the frequencies that elicit a response in the MSU. The response of the alpha band is mainly an onset and an offset response, where most of the energy in the heat map is concentrated around the onset and offset of the sound. The beta band in this example is considerably more tuned than the alpha band response, yet here like in the alpha response the beta band exhibits only an onset response to the sound. The gamma and high gamma bands are better tuned than the first two bands as they responded to the same frequencies that elicited a response from this site's MSU. Moreover these two frequency bands also respond with onset and sustained activity to the noise bands. The sustained activity of the high gamma band in particular comes very close to that of the MSU.

5.3.4 Bandpass stimuli: Population summary of tuning properties

Tuning curves for the four frequency bands for each site were measured from the onset and sustained response, centered at the MSU BF and averaged across the

population of 71 recordings analyzed. Figure 5.5 shows the averages of the centered tuning curves for each of the four frequency bands. On average the frequency bands' response to band pass noise was more tuned than that to the pure tone. The gamma and high gamma bands exhibit best tuning among the four frequency bands when compared to the MSU BF. The alpha and beta bands' average tuning, while worse than that of the gamma and high gamma, shows considerably better tuning than alpha and beta bands' average response to pure tones (fig 5.3).

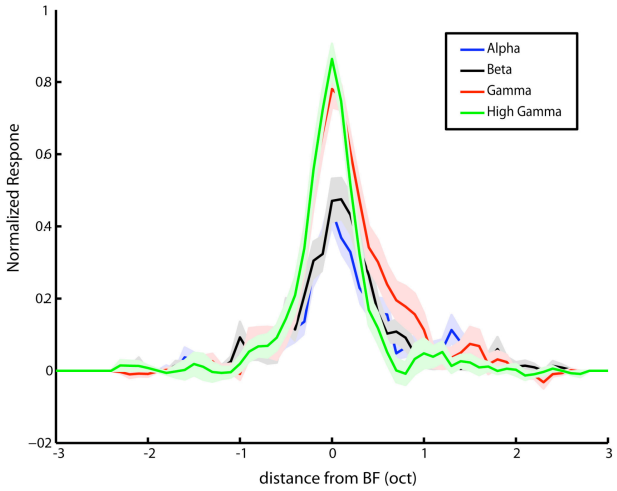

Figure 5.5: Band pass stimuli, average LFP frequency bands' tuning

5.3.5 Local field potential responses to broad band stimuli:

STRFs were measured for the LFP and MSU signals. Figure 5.6A shows an example of an STRF estimated from the MSU response to TORCs. This recording site has a BF around 750Hz with a latency of 21 ms. Fig5.6B is the STRF measured from the LFP response to TORCs from the same site. Both LFP and MSU STRF for this recording site had a maximum response around 750Hz, indicating that both signals have similar frequency tuning. The latency of the maximum response of the

LFP STRF is shorter than that of the MSU STRF by a few milliseconds. An inhibitory area at a latency of 35 ms follows the excitatory area illustrated in the LFP STRF, which is absent from the MSU STRF. A closer look at the LFP MSU shows that the spectral bandwidth of the excitatory area in the LFP STRF is a bit larger than that in the MSU STRF. Temporal and spectral tuning properties of both MSU and LFP STRFs were further explored by taking the two dimensional Fourier transform of both STRFs measuring the modulation transfer function (MTF) for each. The measured MTFs show clear differences in the spectro-temporal properties of the LFP and MSU STRFs. The MSU STRF in this example was tuned to wide range of spectral modulations that range from 0.2 cyc/oct to 1.4 cyc/oct, and while it responded best to low temporal modulation of 4Hz. Comparing that with the MTF of LFP STRF we see a different spectrotemporal tuning pattern, where the LFP STRF is tuned to a lower spectral modulation, as most of the energy in the MTF in Fig 5.6D indicated preferred spectral modulation of about 0.2cyc/oct. Whereas the LFP STRF responds well to a wide range of temporal modulations.

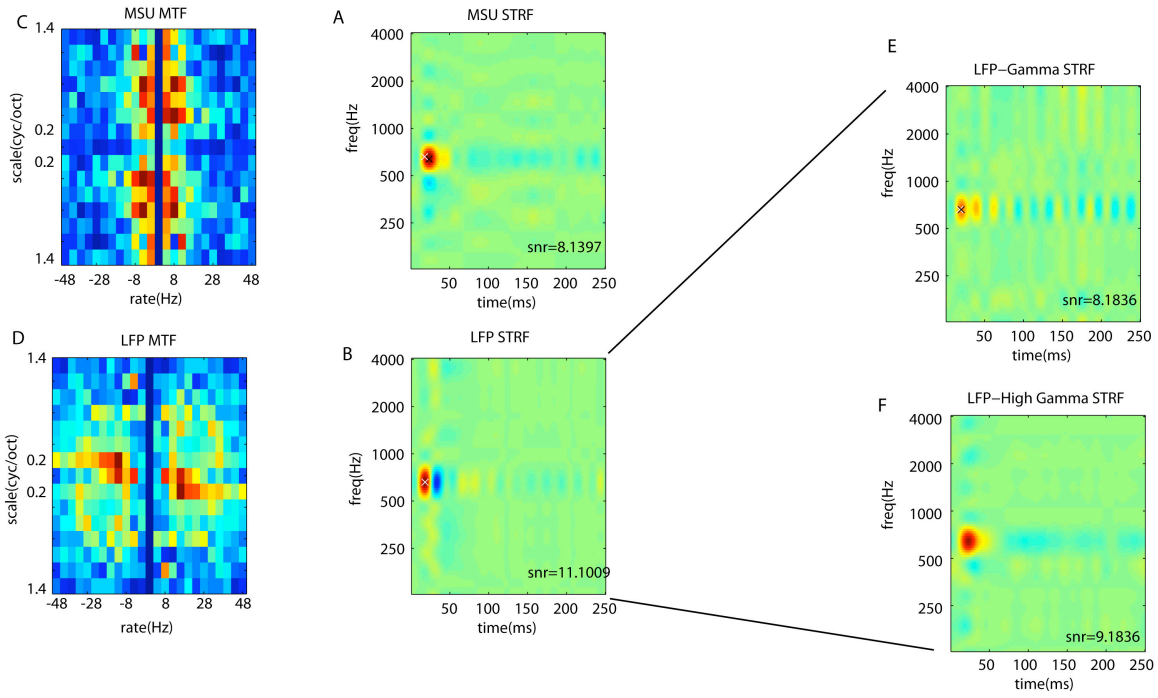

Figure 5.6: Example of MSU and LFP responses to broad band stimuli

The LFP signal was filtered into the gamma and high gamma components of the LFP. There was no attempt at extracting the alpha and beta frequency ranges from the LFP because the TORCs have oscillations that range from 4 to 48. A1 neurons are characterized by their phase locking to stimuli modulated at frequencies that cover this range. Therefore most of the energy in the LFP response fall with in the alpha and beta range, making difficult to separate the intrinsic oscillations of the areas we are studying from those that are directly evoked by the stimulus. Therefore we limit our investigations to a the upper range of the gamma band (50-100Hz)_and the high gamma band (100-300Hz). After filtering the LFP signal we measured the STRF for the gamma and high gamma bands displayed in Fig5.5 E, F respectively. The gamma band STRF has a similar BF as the MSU and LFP STRFs' BF. However the gamma band shares temporal dynamics that are closer to those of the LFP STRF in this

example. The high gamma STRF on the other hand, resembles the MSU STRF in it's BF and spectro-temporal tuning. These tuning properties were investigated for each set of STRFs measured from each recording site available. They were then pooled and averaged to assess the population trends.

5.3.6 Broadband stimuli: Population summary of tuning properties:

The extent to which the LFP BF matched the MSU BF was assessed by taking a spectral cross section of the STRF at the latency of the maximum response creating a frequency tuning curve for the site measured from the response to broadband stimuli (TORCs). Similar frequency tuning curves were created from the gamma and high gamma STRFs. These tuning curves were then normalized by their maximum, centered at the location of the BF of the MSU and averaged. Fig 5.7 shows the averaged tuning curves for the LFP, gamma and high gamma STRFs centered at the MSU BF. The LFP response to broad band stimuli was best tuned to the MSU when compared with the LFP response to narrow band and band pass stimuli (Fig 5.7). Yet like the previous two sections the high gamma signal has the best resemblance to the frequency tuning of the MSU STRF. This is further emphasized when looking at the population summary of the spectral and temporal tuning of the raw LFP signal and the high gamma Fig 5.7, C and D.

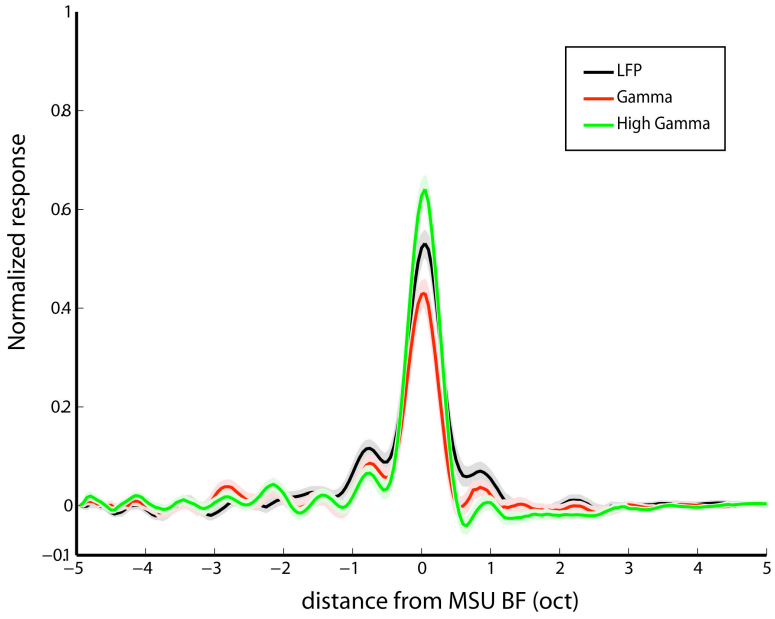

Figure 5.7: Broad band stimuli, average tuning of LFP

Preferred spectral and temporal modulation of the LFP, high gamma and MSU STRFs were estimated by measuring the center of mass for spectral and temporal dimension of the MTF (see methods). Fig 5.8A plots the preferred spectral modulation for the LFP STRF against that of the MSU STRF. Most of the points in our population fall off the diagonal line, showing a clear preference towards higher spectral modulations in the MSU STRFs when compared with the LFP STRF. This trend was significant with a $p<0.001$. Fig 5.8B shows a similar plot where the preferred temporal modulation of the LFP STRFs were plotted against that of the MSU STRFs. While a lot of examples were consistent with the one in Fig 5.6 in that the LFP STRFs were tuned to wider range of the temporal modulations than the MSU LFP, that trend is not significant in the population of recordings 443 recordings analyzed. Fig 5.8B shows that the temporal tuning of the recording sites analyzed

changed considerably between the LFP and the MSU STRFs but that changes were not systematic.

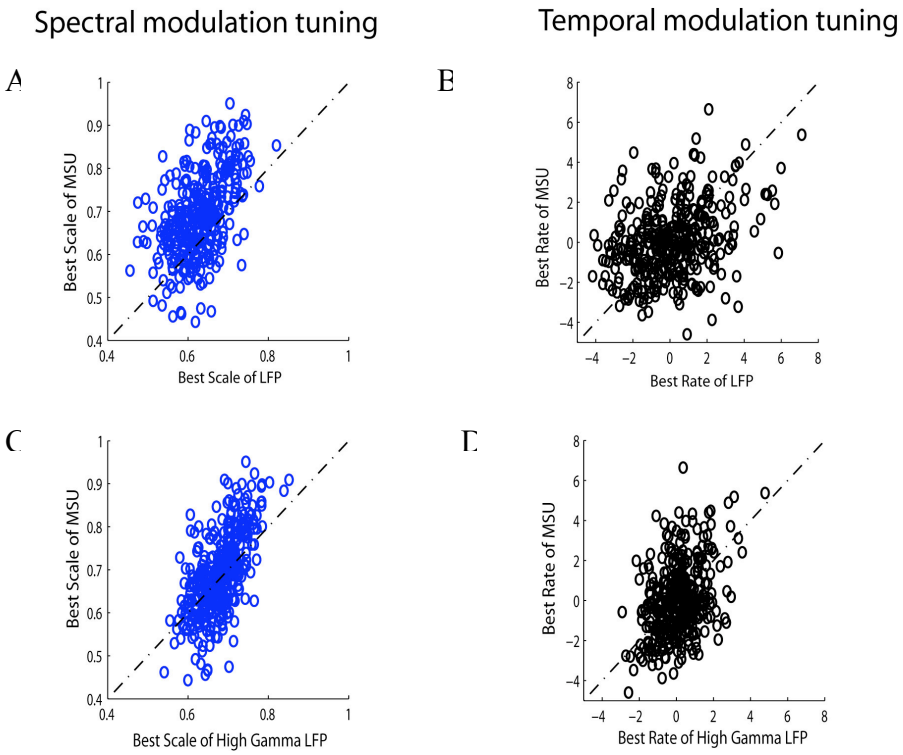

Figure 5.8: Population LFP and MSU spectral and temporal tuning

Fig 5.7C D replace the LFP STRF spectro-temporal tuning with the high gamma STRF spectro-temporal tuning and compares that to the MSU STRF. The preferred spectral tuning of the high gamma STRF came much closer to that of the MSU STRF than that of the aggregate LFP STRFs. The significant tuning trend to lower spectral tuning in the LFP STRF does not hold when we look at the high gamma STRF. This is demonstrated on a population level by having more points in the plot packed around the diagonal line in Fig5.8C than that in Fig5.8A. For the temporal tuning, while the LFP STRFs didn't show a significant trend towards preference for higher temporal modulations, there was still a considerable difference between the LFP and the MSU temporal tuning. This difference is smaller when the

high gamma temporal tuning is compared with the MSU, and while there are differences between the two sets, those differences are considerably smaller.

5.4 Discussion:

The MSU and the LFP signals are different imprints of activity of the cortical tissue studied. While MSU tuning properties in A1 have been studied extensively, the same cannot be said about the LFP signal. The results above show that there are similarities and difference in the tuning properties of MSU and LFP. The LFP responses to pure tones showed that the LFP signal is tuned to a larger range of frequencies than the MSU. A deflection in the potential occurred in response to a wide range of frequencies, most of which didn't elicit action potentials from neurons at the same site. LFP responses to band pass noise were better tuned than those to pure tones, and LFP STRFs measured from LFP response to broad band stimuli exhibited very similar tuning to the MSU STRFs. This trend of improved tuning of the LFP confirms the findings that spectrally denser stimuli elicit a better tuned LFP response from A1 neurons (Noreña et al 2008). A study of the frequency bands of the LFP demonstrated that most of the energy in the LFP response is located in the alpha band and to a lesser extent the beta band, and that the poor tuning described above is the mostly the contributions of these frequency bands. The LFP response on average was better tuned in response to noise bands than to pure tones. Yet similar to the response to pure tones the energy contributed by the alpha and beta bands dominated the LFP response, and the alpha and to a lesser extend the beta band captured the large range of frequency response seen in the LFP. It was also observed that the

responses of the alpha and beta bands were mostly limited to the onset of the sound and failed to capture the sustained response seen in MSU responses. The STRFs measured from the LFP exhibited frequency tuning that came very close to that of the MSU STRF (Fig5.7), which indicated that the response of the alpha and beta frequency bands to broad band stimuli were well tuned in response to broad band stimuli. The gamma and high gamma frequency bands were both well tuned in response to all the stimuli presented. These two bands however had far less energy than the alpha and beta bands. The gamma, and to a larger extent, the high gamma band's response corresponded very closely to the MSU activity, be it in response to narrow band, band pass or broad band stimuli.

5.4.1 Alpha and beta:

Studies in the visual system have described similar tuning properties of the lower bands of the LFP (Siegel and König 2003, Kayser and König 2004). Studies of brain rhythm in human research describe the alpha and beta oscillations as resting state oscillations that are disrupted by engaging in an intentional task (Laufs et al 2003, Vázquez Marrufo et al.2001). This hypothesis of the resting state role of the alpha and beta bands when combined with the results above showing the concentration of the energy in alpha and beta during the onset and sometimes the offset of the sound seems to suggest that alpha and beta frequency bands play a gating role. The poor tuning and transient aspect of these low frequencies of LFP suggest that a process, which is characterized by low frequency oscillation can be driven by a very wide range of stimuli, (in this case, driving the system with a wide range of frequencies). The transient nature of this process can be linked to findings from

human studies that report the reduction in the amplitude of the alpha rhythm with sensory stimulation (Ray and Cole 1985, Klimesch 1996). And while it widely thought that the desynchronization in alpha and beta rhythms are indication of the disengagement of areas that are not required for the active task, this view doesn't explain our results given that the animal is passively listening without any engagement in a task. These low frequency transient components of the LFP might be processes that drive bottom up attention, and while we the scope of this study doesn't provide substance to support this claim, some evidence in recent EEG and MEG studies suggests that the low frequency oscillations might be involved in sensory awareness (Palva et al 2005)

5.4.2 Gamma and high Gamma:

The tuning properties of the gamma and high gamma frequency bands of the LFP are more similar to those of the MSU than the alpha and beta frequency bands. The high gamma band activity in particular follows closely the tuning properties of the MSU of the same recording site. Similar results have been reported by studies of LFP in the visual and auditory system (Liu and Newsome 2006, Kayser et al 2007, Gielsemann and Thiele 2008). ECoG (electrocorticography) studies often use the high gamma frequency band to approximate the combined spiking activity of neurons in the vicinity of the recording site. Different frequency bands of the LFP are reported to reflect the combined activity of different size areas of the cortical tissue or the length of the axonal, dendritic projections. The high frequency of the high gamma band suggest that high gamma is the sum of activity over a relatively small area of cortex, something on the scale of a few columns which should have tuning properties

that are very close to MSU of the recording site. Therefore the finding that the high gamma has the closest correspondence to the MSU confirms this view of the high gamma and provide further basis to using the high gamma frequency band to approximate the activity of neurons in the vicinity of the recording site.

5.5 Conclusions:

In A1, the LFP has similar frequency tuning to nearby multiunit activity. Alpha and beta bands in the LFP signal are poorly tuned and are mostly triggered by the stimulus onset, suggesting that they do not reflect MSU activity.

Gamma and high gamma bands in the LFP signal are better tuned. These two frequency bands capture the sustained response of MSU, and their frequency tuning closely corresponds to that of the MSU.

STRFs measured from LFP have BFs that generally correspond to BFs of STRFs measured from MSU. However LFP STRFs are tuned to a lower spectral modulation frequency than MSU.

Chapter 6: Conclusions

6.1 Thesis Overview

One of the goals of neuroscience research today is to understand the dynamic nature of the brain, the processes that allow intelligent organisms to live optimally and adapt to the changing environment in real time. In this thesis we expanded the investigation of one mechanism that underlies the ability to dynamically respond to a changing environment. Rapid plasticity as we describe in this thesis is one type of plasticity described in literature, yet it is a very critical one to understand given our interest in the dynamic nature of our brains.

In this thesis I expand on the already existing body of research of rapid plasticity to understand the neural mechanisms underlying this type of plasticity in two different directions; I first looked into the effects of manipulating task difficulty on rapid plasticity; as the task difficulty increases both performance and the target neural representation deteriorate, because the separation in spectro-temporal space between the references sound (TORCs in this case) and the target sound (low levels of tone embedded in one of the TORCs) becomes very small. Neurons in auditory cortex responded by suppressing the representation of the noise and enhancing the representation of the signal. The level of suppression and enhancement varied according to the difficulty of the task and the animal's of engagement in the task. For easier tasks the spectro-temporal difference between the reference and the target was large enough that it follows to a certain extent the pattern described in pure tone detection (Fritz et al 2003) in cells that are near the target tone. In far cells' response

was suppressed. This suppression was necessary because unlike previous studies the noise in this case is also present in the target sound as well as the reference. As the task becomes more and more difficult, that spectro-temporal difference between the reference and the target sounds becomes smaller and smaller, overall suppression of responses was observed, suppression that was less pronounced for cells near the frequency of the tone and much more pronounced for cells that are far. This decrement, however, was reversed by active engagement in the task and heightened attention that both restored the enhanced signal representation and improves performance of the animal.

In chapter 4 we also expanded the investigation of rapid plasticity into higher order auditory areas of the ferret auditory cortex. The aim was to link our understanding of the neural mechanisms underlying this type of plasticity in A1 to that observed in frontal cortex during the performance of the task. The investigation was conducted within a comparison framework, to study plasticity in PEG in reference to A1.

PEG neurons exhibited a form of plasticity that is different from that in A1. This form of plasticity further enhances the distinction between the reference and target by increasing the firing rate to the target tone during the performance of the task, creating an increase in the separation between the representation of the two classes of stimuli involved in this task, and providing a step towards distinct behavioral representation of these two classes of sounds in executive areas of frontal cortex. This increased distinction between the classes can be thought of as one more step in building the cortical representation underlying different sound categories in

the auditory system. Frontal executive areas have a binary like representation of the two sound classes the animals are actively discriminating in the task (Fritz et al submitted). These two distinct responses can be thought of as the two far ends of a categorical distinction curve (one that hasn't been fully investigated yet). The enhancement in the response to the target sound that I report in PEG can be one more step towards forming this binary response that is more directly coupled to animal's behavior in executive and motor areas.

In chapter five results from a study of the tuning properties of the LFP in A1 are reported. This study is a necessary prerequisite to our aim to understand the imprint of plasticity in the LFP signal. This is important because the LFP signal carries much more information than evoked potentials in general. Since as a signal it combines components of the input to the cortical area recorded from, sub threshold process in neurons in that area, and a part of the output signal integrated across a relatively large patch of cortex. And while it is difficult to separate these components of the LFP signal, it is still very insightful to contrast the sum of these components (that can be thought of as aggregate input) with the output of the same area (the spikes). The LFP signal responds to a much larger frequency range than the MSU when probed with pure tones. The LFP signal becomes more and more tuned as the density of the stimulus increases. The tuning properties of a number of frequency components of the LFP signal were investigated (alpha, beta, gamma and high gamma) finding that the alpha and beta bands are poorly tuned, while the gamma and high gamma are much better tuned. The gamma and to a greater extent the high gamma frequency bands capture the sustained response of the spiking activity, and

the alpha and beta frequency bands are onset transient processes. The spectro-temporal tuning properties of the LFP were studied finding that LFPs are tuned to lower spectral modulation. This result fits well with the general view of the nature of the LFP signal as a signal that combines the activity from a larger area of cortex than the MSU which means that it relatively responds to a larger range of frequencies.

6.2 Future Directions

I studied rapid plasticity in this thesis, focusing on specific projects that expand our knowledge in this area of research. And while these projects have shed the light on the neural mechanisms underlying rapid plasticity in different areas of the ferret auditory cortex, it is safe to say that these projects have just scratched the surface. A lot more needs to be studied in rapid plasticity in general, and with in the paradigm used in this thesis. Specifically further exploration of the functional significance of higher order auditory areas, and their role in the development of representation and perception of sound. Rapid plasticity becomes a tool in this line of research rather than an end of its own, as the representation of sound in higher order areas is expected to be more tied to their behavioral significance than their physical characteristics, which makes utilizing behavior and looking at the response through the lens of plasticity a critical tool to understanding the functional properties of these areas.

Another direction that requires extensive further research in plasticity is LFP's signature of plasticity. This direction has the potential of expanding our understanding of these rapid changes on a network level, and can help provide many

more insight into changes in the cortical network dynamics underlying plasticity in response properties observed and ways it this knowledge can be exploited to build dynamic systems for audition.

Appendix 1

Supplementary data for chapter 3

STRF changes as a function of BF-target distance

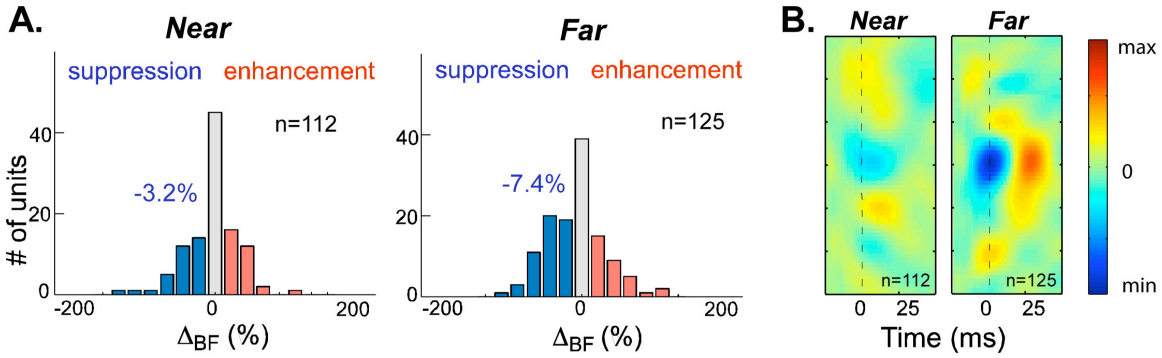

Figure SD-1

Dependence of STRF amplitude changes on distance of BF from target tone frequency. (Data accumulated from all tasks). (A) Histogram of amplitude changes (Δ_{BF}) for 112 *near* and 125 *far* STRFs. Suppression was strongest in the *far* cells as reflected by the negatively skewed histogram (mean of -7.4%; $p < .01$). (B) Average STRF change was mostly suppressive in the *far* cells. In each panel, the $STRF_{diff}$ between the pre-task and during-task STRFs for each cell was computed, aligned to others at the point of maximum change (Δ_{BF}), and then averaged across all cells.

Lack of STRF changes in naïve animals

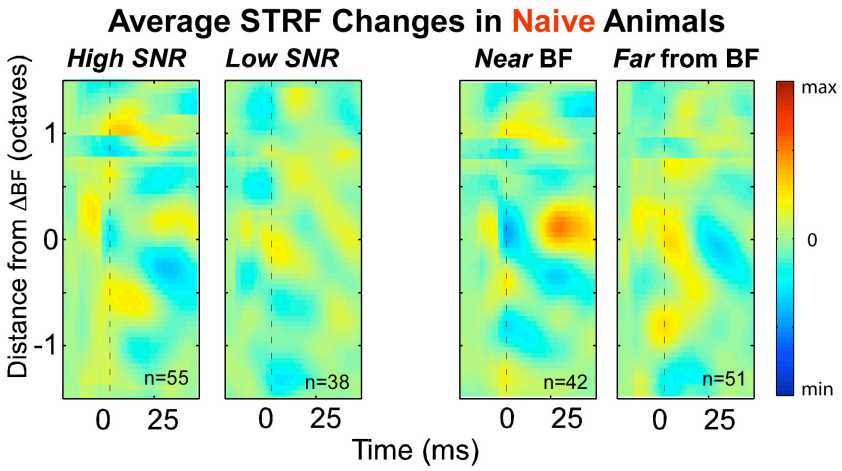

Figure SD-2

There were no observable STRF changes in the naïve animals. The average $STRF_{diff}$ was computed for all four conditions (*high SNR, low SNR, far, near)*. All show very weak, or no significant, effects compared to those seen during behavior in the trained animals (Figs. 3-6). All color scales are the same as those in Figs.5 and 6.

Analysis of gain effects in STRF changes

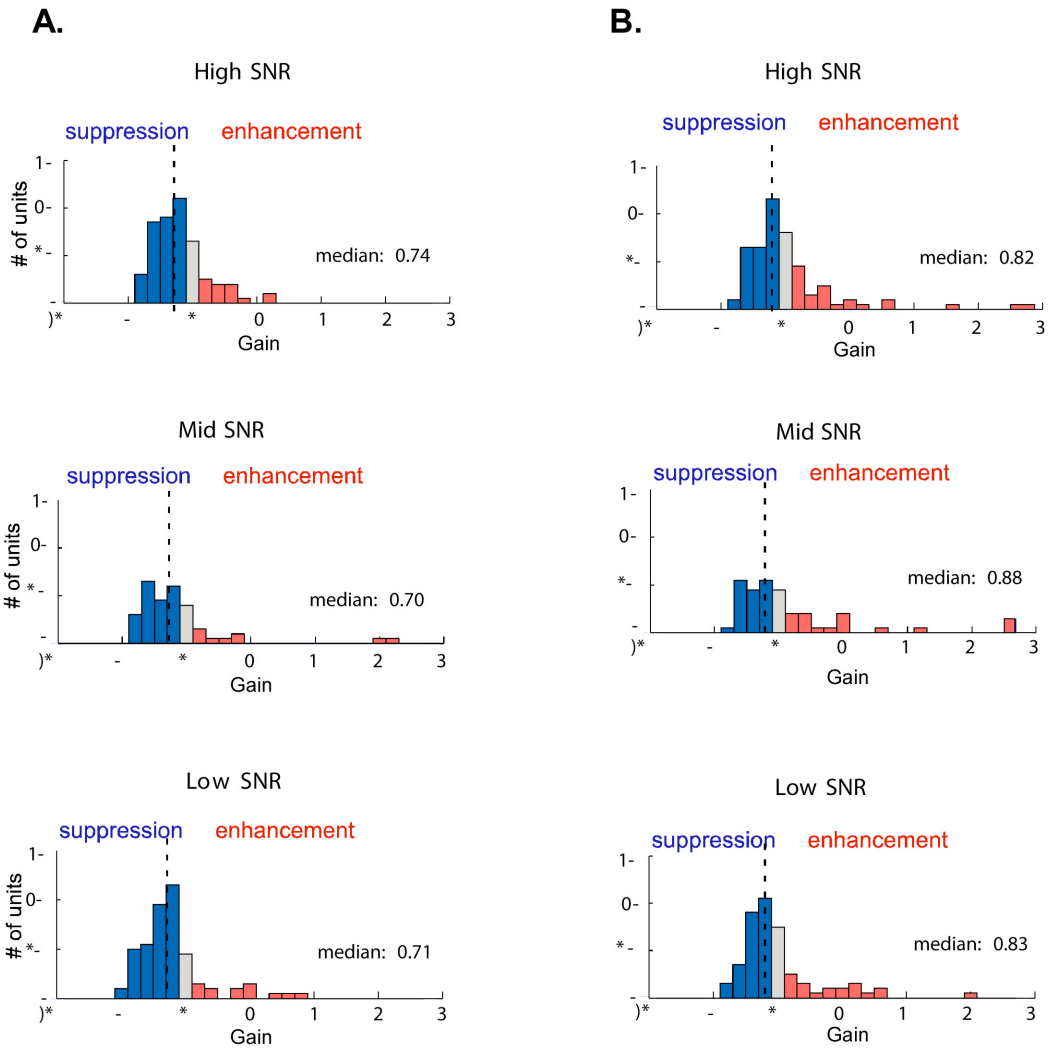

Figure SD-3

(A) Distribution of gain factors from all STRFs in this study, i.e., including *all* acceptable performance levels. Gains (g) were sorted according to task difficulty. The three distributions were not significantly different from each other, and have a comparable mean of about 0.7, regardless of task difficulty. (B) Gain and shape changes measured using the method due to David et al. (2008). The results are comparable to those shown in Figs.7, with only a small dependence on task difficulty

and distance of STRF from target. The gain and shape changes here are comparable to those shown in (A) above and in Fig.7C, except that the gain is consistently less attenuated, causing shape changes to range from positive (high SNR) to slightly negative (low SNR).

Different method of designating near and far yields similar results

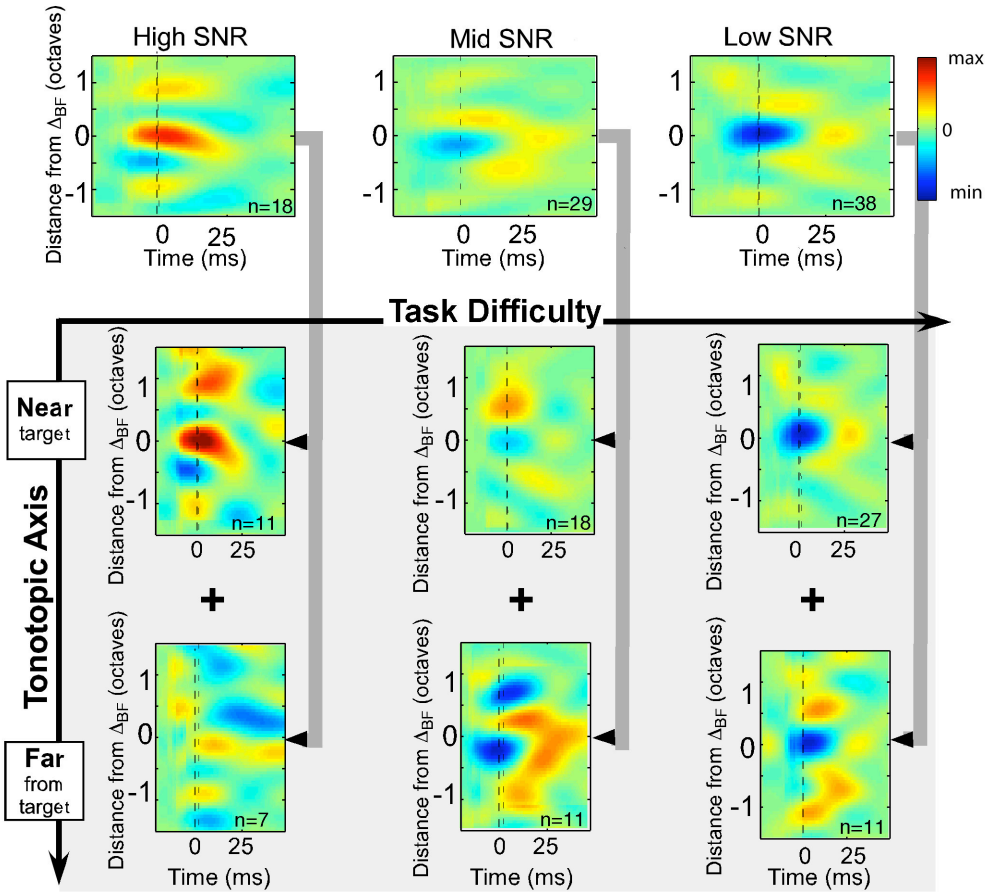

Figure SD-4

Distributions of Δ_{BF} and population average of $STRF_{diff}$ for high mid and low SNR, which is separated in the contributions of near and far cells. All data were measured in experiments with best behavior, and were presented exactly as in Figure 6 except

for designation of near and far. Here the near and far label for each cell was determined relative to its STRF width. We first computed for each STRF its Hilbert envelope, and then selected the boundary between near and far at the distance where this envelope drops to 60% of the peak of the STRF. Some cells changing their near/far designation relative to Figs 2L & 3L, the majority (84%) did not, and the averages therefore remained similar.

No systematic changes in STRF bandwidths

We explored the effect of task performance on other STRF parameters such as *bandwidth*. We defined the bandwidth to be the width of *excitatory* area around the BF peak, measured between frequencies where the amplitude decreases to 20% of the BF peak. In many single-units, there was a significant sharpening of this excitatory region during performance, as illustrated in Fig.3. However, when population data were examined across all tasks and conditions, we found only a weak consistent trend of narrowing BW in the near cells as the tasks became less difficult (mean bandwidth sharpening low SNR 0.02 oct, mid SNR -0.035 , high SNR -0.071 in the near cells). However, this trend was not significant.

REFERENCES

Atiani, S., Elhilali M., David S.V., Fritz J.B., Shamma S.A.(2009). Task difficulty and performance induce diverse adaptive patterns in gain and shape of primary auditory cortical receptive fields. Neuron. February 12;61(3):467-80.

Bao, S., Chang, E.F., Woods, J., Merzenich, M.M., Temporal plasticity in the primary auditory cortex induced by operant perceptual learning. Nature Neuroscience . 2004.

Bendor, D., Wang, X., (2007). Differential neural coding of acoustic flutter within primate auditory cortex. Nature Neuroscience. 2007 10,763-71.

Bizley, J.K., Nodal, F.R., Nelken, I., and King, A.J. (2005). Functional organization of ferret auditory cortex. Cereb Cortex *15*, 1637-1653

Bizley, J.K., Nodal, F.R., Bajo, V.M., Nelken, I., King, A.J., Physiological and anatomical evidence for multisensory interactions in auditory cortex. Cerebral Cortex. 2007 17, 2172-89

Blake DT, Strata F, Churchland AK, Merzenich MM (2002) Neural correlates of instrumental learning in primary auditory cortex. Proc Natl Acad Sci USA 99: 10114-10119.

Blake, D.T., Heiser, M.A., Caywood, M, Merzenich, M.M. (2006). Experience-dependent adult cortical plasticity requires cognitive association between sensation and reward. Neuron, October 19;52(2):371-81.

Boudreau, C.E., Williford, T.H., and Maunsell, J.H. (2006). Effects of task difficulty and target likelihood in area V4 of macaque monkeys. Journal of Neurophysiology *96*, 2377-2387.

Brosch, M., Schulz, A., Scheich, H., Processing of sound sequences in macaque auditory cortex: response enhancement. J Neurophysiology. 1999 82,1542-59.

Brown MIrvine DR, Park VN (2004) Perceptual learning on an auditory frequency discrimination task by cats: association with changes in primary auditory cortex. Cereb Cortex 14: 952-965.

Brugge, J.F., Merzenich, M.M. (1973). Responses of neurons in auditory cortex of the macaque monkey to monaural and binaural stimulation. Journal of Neurophysiology. November;36(6):1138-58.

Calhoun, B.M., Schreiner, C.E., Spectral envelope coding in cat primary auditory cortex: linear and non-linear effects of stimulus characteristics. European Journal of Neuroscience. 1998 10,926-40.

Connor, C.E., Preddie, D.C., Gallant, J.L., and Van Essen, D.C. (1997). Spatial attention effects in macaque area V4. J Neurosci *17*, 3201-3214.

David, S.V., Hayden, B.Y., Gallant, J.L..(2006). Spectral receptive field properties explain shape selectivity in area V4. Journal of Neurophysiol. 96(6):3492-505.

David, S.V., Malaval, N., Shamma, S.A.(2010). Decoupling action potential bias from cortical local field potentials. Comput ational Intelligence and Neuroscience. 2010:393019

deCharms, R.C. and Merzenich, M.M. Primary cortical representation of sounds by the coordination of action-potential timing, Nature **381** (1996), pp. 610–613

deCharms, R.C., Blake, D.T., Merzenich, M.M., Optimizing sound features for cortical neurons. Science. 1998 280,1439-43.

Depireux, D.A., Simon, J.Z., Klein, D.J., and Shamma, S.A. (2001). Spectro-temporal response field characterization with dynamic ripples in ferret primary auditory cortex. Journal of Neurophysiology *85*, 1220-1234.

Diamond, D.M., Weinberger, N.M., Physiological plasticity of single neurons in auditory cortex of the cat during acquisition of the pupillary conditioned response: II. Secondary field (AII). Behavioral Neuroscience. 1984 98,189-210.

Diamond, D.M., Weinberger, N.M., Classical conditioning rapidly induces specific changes in frequency receptive fields of single neurons in secondary and ventral ectosylvian auditory cortical fields. Brain Research. 1986 372,357-60.

Durrant, J.D. and Lovrinic, J. H.. Bases of hearing science. Williams and Wilkins,baltimore, third edition, 1995

Edeline, J.M., Weinberger, N.M.(1993) Receptive field plasticity in the auditory cortex during frequency discrimination training: selective retuning independent of task difficulty. Behavioral Neuroscience. February;107(1):82-103.

Edeline, J.M, (1999). Learning-induced physiological plasticity in the thalamo-cortical sensory systems: a critical evaluation of receptive field plasticity, map changes and their potential mechanisms. Progress in Neurobiology. February;57(2):165-224.

Efron, B., and Tibshirani, R. (1993). An introduction to the bootstrap (New York: Chapman & Hall).

Eggermont JJ Representation of spectral and temporal sound features in three cortical fields of the cat. Similarities outweigh differences. J Neurophysiol 80:2743–2764. 1998

Eggermont J. J. Between sound and percpetion: reviewing the search for a neural code. Hearing Research, 157:1–42, 2001.

Elhilali, M., Fritz, J.B., Chi, T.S., and Shamma, S.A. (2007). Auditory cortical receptive fields: stable entities with plastic abilities. J Neurosci *27*, 10372-10382.

Engineer, N.D., Percaccio, C.R., Pandya, P.K., Moucha, R., Rathbun, D.L. and Kilgard, M.P. (2004) Environmental enrichment improves response strength, threshold, selectivity, and latency of auditory cortex neurons. J. Neurophysiol., 92: 73–82.

Escabi, M.A., Schreiner, C.E., Nonlinear spectrotemporal sound analysis by neurons in the auditory midbrain. J Neuroscience. 2002 22,4114-31.

Fritz, J., Shamma, S., Elhilali, M., and Klein, D. (2003). Rapid task-related plasticity of spectrotemporal receptive fields in primary auditory cortex. Nature Neuroscience *6*, 1216-1223.

Fritz, J.B., Elhilali, M., and Shamma, S.A. (2005). Differential dynamic plasticity of A1 receptive fields during multiple spectral tasks. J Neurosci *25*, 7623-7635.

Fritz, J.B., Elhilali, M., David, S.V., and Shamma, S.A. (2007a). Does attention play a role in dynamic receptive field adaptation to changing acoustic salience in A1? Hearing Research *229*, 186-203.

Fritz, J.B., Elhilali, M., and Shamma, S.A. (2007b). Adaptive changes in cortical receptive fields induced by attention to complex sounds. Journal of Neurophysiology *98*, 2337-2346.

Gerstein and Kiang (1964). Response of single units in auditory cortex. Experimental Neurology. July;10:1-18

Gieselmann MA, Thiele A. Comparison of spatial integration and surround suppression characteristics in spiking activity and the local field potential in macaque V1. *European Journal of Neuroscience*. 2008;28(3):447–459

Heffner, H.E., and Heffner, R.S. (1995). Conditioned Avoidance. In: Methods in Comparative Psychoacoustics, G.M. Klump, and W. Stebbins, eds. (Basel: Birkhäuser), pp. 79-94.

Hodgkin, A.L., and Huxley, A. A. (1952). A quantitative description of membrane current and its application to conduction and excitation in nerve. Journal of Physiology 117, 500-544.

Holt, G.R., and Koch, C. (1999). Electrical interactions via the extra-cellular potential near cell bodies. Journal of Computational Neuroscience. 6, 169-184.

Irvine, D., Brown, M., Martin, R., Park V (2004) Perceptual learning and cortical plasticity. In: Auditory cortex: towards a synthesis of human and animal research (Konig R, Heil P, Budinger E, Scheich H, eds), pp 409-428. Hillsdale, NJ: Erlbaum

Ito, M., and Gilbert, C.D. (1999). Attention modulates contextual influences in the primary visual cortex of alert monkeys. Neuron *22*, 593-604.

Jenkins, W.M., Merzenich, M.M. (1987) Reorganization of neocortical representations after brain injury: a neurophysiological model of the bases of recovery from stroke. Progress of Brain Research. 71:249-66.

Kaas, J.H., Hackett, T.A.(2000). Subdivisions of auditory cortex and processing streams in primates. Proceedings of National Academy of Sciences U S A. Oct 24;97(22):11793-9.

Kajikawa, Y., de La Mothe, L., Blumell, S., Hackett, T.A. (2005). A comparison of neuron response properties in areas A1 and CM of the marmoset monkey auditory cortex: tones and broadband noise. Journal of Neurophysiology. January; 93(1):22-34.

Kandel, E. R., Schwartz J. H., and Jessell T. M. (2000). editors. Principles of neural science. McGraw-Hill, New York, fourth edition.

Kanwal, J.S., and Rauschecker, J.P. (2007).Auditory cortex of bats and primates: managing species-specific calls for social communication. Frontiers in Bioscience. May 1;12:4621-40.

Katzner, S., Nauhaus, I., Benucci, A., Bonin, V., Ringach, D.L., Carandini, M. (2009). Local origin of field potentials in visual cortex. Neuron. January 15;61(1):35-41.

Kayser, C., König, P. (2004). Stimulus locking and feature selectivity prevail in complementary frequency ranges of V1 local field potentials. European Journal of Neuroscience. January;19(2):485-9.

Kayser, C., Petkov, C.I., Logothetis, N.K.(2007). Tuning to sound frequency in auditory field potentials. Journal of Neurophysiology. September;98(3):1806-9. Epub 2007 Jun 27

Kemp, S. (1984). Reaction time to a tone in noise as a function of the signal-to-noise ratio and tone level. Perception & Psychophysics *36*, 473-476.

Kilgard, M.P., Merzenich, M.M.,Plasticity of temporal information processing in the primary auditory cortex. Nature Neuroscience. 1998 1,727-31.

Klein, D.J., Depireux, D.A., Simon, J.Z., and Shamma, S.A. (2000). Robust spectrotemporal reverse correlation for the auditory system: optimizing stimulus design. Journal of Computational Neuroscience *9*, 85-111.

Klimesch W, Memory processes, brain oscillations and EEG synchronization, *Int. J. Psychophysiol.* **24** (1996), pp. 61–100

Kowalski, N., Depireux, D.A., and Shamma, S.A. (1996). Analysis of dynamic spectra in ferret primary auditory cortex. I. Characteristics of single-unit responses to moving ripple spectra. Journal of Neurophysiology *76*, 3503-3523.

Kreiman, G., Hung, C.P., Kraskov, A., Quiroga, R.Q., Poggio, T., DiCarlo, J.J.(2006).Object selectivity of local field potentials and spikes in the macaque inferior temporal cortex. Neuron. February 2;49(3):433-45.

Kruse , W. & Eckhorn, R. (1996) Inhibition of sustained gamma oscilations(35-80Hz) by fast transient responses in cat visual cortex. Proceeds of National Academy of Science USA, 93, 6112-6117

LaBerge, D., Brown, V., Carter, M., Bash, D., and Hartley, A. (1991). Reducing the effects of adjacent distractors by narrowing attention. Journal of Experimental Psychology *17*, 65-76.

Laufs, H., Krakow, K., Sterzer, P., Eger, E., Beyerle, A., Salek-Haddadi, A., Kleinschmidt, A.(2003).Electroencephalographic signatures of attentional and cognitive default modes in spontaneous brain activity fluctuations at rest.

Proceedings of National Academies Science U S A. September 16;100(19):11053-8. Epub 2003 Sep 4.

Lavie, N., and Cox, S. (1997). On the efficiency of visual selective attention: efficient visual search leads to inefficient distractor rejection. Psychological Science *8*, 395-396.

Liu, J., Newsome, W.T.(2006) Local field potential in cortical area MT: stimulus tuning and behavioral correlations. Journal of Neuroscience. July 26;26(30):7779-90.

Logothetis, N.K., Pauls, J., Augath, M., Trinath, T., Oeltermann, A.(2001). Neurophysiological investigation of the basis of the fMRI signal. Nature. July 12;412(6843):150-7.

Logothetis, N.K. (2003). The underpinnings of the BOLD functional magnetic imaging signal. Journal of Neuroscience 23, 3963-3971

Luck, S.J., Chelazzi, L., Hillyard, S.A., and Desimone, R. (1997). Neural mechanisms of spatial selective attention in areas V1, V2, and V4 of macaque visual cortex. Journal of Neurophysiology *77*, 24-42.

Maunsell, J.H., and Treue, S. (2006). Feature-based attention in visual cortex. Trends in Neurosciences *29*, 317-322.

Maunsell, J.H.R. (2004). The role of attention in visual cerebral cortex. In: The Visual Neurosciences, L.M. Chalupa, and J.S. Werner, eds. (Cambridge MA: MIT Press), pp. 1538-1545.

McAdams, C.J., and Reid, R.C. (2005). Attention modulates the responses of simple cells in monkey primary visual cortex. J Neurosci *25*, 11023-11033.

Mendelson, J. R., Schreiner , C. E., Sutter, M. L.(1997). Functional topography of cat primary auditory cortex: response latencies. Journal of Computational. Physiology 181: 615-633

Merzenich, M.M., Brugge, J.F. (1973). Representation of the cochlear partition of the superior temporal plane of the macaque monkey. Brain Research. February 28;50(2):275-96.

Middlebrooks, J.C., Dykes, R.W., Merzenich, M.M.(1980) Binaural response-specific bands in primary auditory cortex (AI) of the cat: topographical organization orthogonal to isofrequency contours. Brain Research. Jan 6;181(1):31-48.

Miller, L.M., Escabi, M.A., Read, H.L., and Schreiner, C.E. (2002). Spectrotemporal receptive fields in the lemniscal auditory thalamus and cortex. Journal of Neurophysiology *87*, 516-527.

Mitzidorf, U. (1985). Current source-density method and applicationin cat cerebral cortex: investigation of evoked potentials and EEG phenomena. Physiology Review 65, 37-99.

Moore B. C. J., editor. Hearing. Handbook of Perception and Cognition. Academic Press, San Diego, second edition, 1995

Motter, B.C. (1993). Focal attention produces spatially selective processing in visual cortical areas V1, V2, and V4 in the presence of competing stimuli. Journal of Neurophysiology *70*, 909-919.

Navalpakkam, V., and Itti, L. (2008) Top-down attention and the role of task difficulty. Trends in Neurosciences (in press).

Nelken. I.(2004a) Processing of complex stimuli and natural scenes in the auditory cortex Current Opinion in Neurobiology, 14:474–480.

Nelken, I., Bizley, J.K., Nodal, F.R., Ahmed, B., Schnupp, J.W., and King, A.J. (2004b). Large-scale organization of ferret auditory cortex revealed using continuous acquisition of intrinsic optical signals. Journal of Neurophysiology *92*, 2574-2588.

Noreña AJ, Gourévitch B, Pienkowski M, Shaw G, Eggermont JJ. Increasing spectrotemporal sound density reveals an octave-based organization in cat primary auditory cortex. *The Journal of Neuroscience*. 2008;28(36):8885–8896

Nudo, R.J., Wise, B.M., SiFuentes, F., Milliken, G.W. (1996). Neural substrates for the effects of rehabilitative training on motor recovery after ischemic infarct. Science. June 21;272(5269):1791-4.

Ohl, F.W., Scheich, H. (1996). Differential frequency conditioning enhances spectral contrast sensitivity of units in auditory cortex (field Al) of the alert Mongolian gerbil. European Journal of Neuroscience. May;8(5):1001-17.

Ohl, F.W., Scheich, H., Freeman, W.J. (2001). Change in pattern of ongoing cortical activity with auditory category learning. Nature, Aug 16;412(6848):733-6.

OTazu, G.H., Tai, L.H., Yang, Y., Zador, A.M.(2009). Engaging in an auditory task suppresses responses in auditory cortex, Nature Neuroscience 2009 May;12(5):646-54

Palmer A. R., Winter I. M., and Stabler S. E.. Advances in Speech, Hearing and Language Processing, chapter Responses to simple and complex sounds in the cochlear nucleus of the guinea pig. JAI Press, London, 1995.

Palva J.M. Phase synchrony among neuronal oscillations in the human cortex (2005), Journal of Neuroscience. 25, 3962–3972.

Pandya, P.K., Rathbun, D.L., Moucha, R., Engineer, N.D., Kilgard, M.P. (2008). Spectral and temporal processing in rat posterior auditory cortex. Cerebral Cortex. Feb;18(2):301-14.

Phillips DP, Judge PW, Kelly JB, Primary auditory cortex in the ferret (*Mustela putorius*): neural response properties and topographic organization. Brain Res 443:281–294, 1988

Pickles, J.O. (1975). Normal critical bands in the cat. Acta Oto-Laryngologica *80*, 245-254.

Polley, D.B., Heiser, M.A., Blake, D.T., Schreiner, C.E., Merzenich, M.M., Associative learning shapes the neural code for stimulus magnitude in primary auditory cortex. Proc National Academy of Sciences 2004 101,16351-6.

Polley, D.B., Steinberg, E.E., Merzenich, M.M., Perceptual learning directs auditory cortical map reorganization through top-down influences.J Neuroscience. 2006 26,4970

Puckett, A.C., Pandaya, P.K., Moucha, R., Dai, W., Kilgard, M.P.(2007). Plasticity in the rat posterior auditory field following nucleus basalis stimulation. J Neurophysiol. Jul;98(1):253-65.

Rauschecker, J.P., Tian, B., Hauser, M., Processing of complex sounds in the macaque nonprimary auditory cortex. Science. 1995 Apr 7;268(5207):111-4.

Ray W.J. and Cole H.W. (1985). EEG alpha activity reflects attentional demands, and beta activity reflects emotional and cognitive processes, *Science* 228, pp. 750–752.

Read, H.L., Winer, J.A., Schreiner, C.E.(2002). Functional architecture of auditory cortex. Current Opinion Neurobiology. August;12(4):433-40.

Reale, R.A., Imig, T.J. (1980). Tonotopic organization in auditory cortex of the cat. Journal of Comparative Neurology. July 15;192(2):265-91.

Recanzone, G.H., Schreiner, C.E., Merzenich, M.M., Plasticity in the frequency representation of primary auditory cortex following discrimination training in adult owl monkeys. Journal of Neuroscience. 1993 13, 87-103.

Recanzone, G.H., Sutter, M.L.(2008). The biological basis of audition. Annual Review of Psychology.59:119-42.

Romanski, L.M., Tian, B., Fritz, J., Mishkin. M., Goldman-Rakic, P.S., Rauschecker, (1999) J.P., Dual streams of auditory afferents target multiple domains in the primate prefrontal cortex. Nature Neuroscience. 2, 1131-6.

Romanski, L.M., Bates, J.F., Goldman-Rakic, P.S.(1999). Auditory belt and parabelt projections to the prefrontal cortex in the rhesus monkey. J Comparative Neurology. 403,141-57.

Rutkowski, R.G., Weinberger, N.M.(2005). Encoding of learned importance of sound by magnitude of representational area in primary auditory cortex. Proc National Academy of Sciences U S A. 102,13664-9.

Sade, A., and Spitzer, H. (1998). The effects of attentional spread and attentional effort on orientation discrimination. Spatial Vision *11*, 367-383.

Scherberger, H., Jarvis, M.R., Andersen, R.A. (2005). Cortical local field potential encodes movement intentions in the posterior parietal cortex. Neuron. 2005 April 21;46(2):347-54.

Schreiner, C.E. (1995) Order and disorder in auditory cortical maps. Current Opinion in Neurobiology. August;5(4):489-96.

Shamma, S.A., Fleshman, J.W., Wiser, P.R., and Versnel, H. (1993). Organization of response areas in ferret primary auditory cortex. Journal of Neurophysiology *69*, 367-383.

Siegel, M., König, P.(2003). A functional gamma-band defined by stimulus-dependent synchronization in area 18 of awake behaving cats. J Neuroscience. May 15;23(10):4251-60.

Spitzer, H., Desimone, R., and Moran, J. (1988). Increased attention enhances both behavioral and neuronal performance. Science (New York, N.Y *240*, 338-340.

Spitzer, H., and Richmond, B.J. (1991). Task difficulty: ignoring, attending to, and discriminating a visual stimulus yield progressively more activity in inferior temporal neurons. Experimental Brain Research. *83*, 340-348.

Sur, M., Garraghty, P.E. and Roe, A.W. (1988) Experimentally induced visual projections into auditory thalamus and cortex. Science, 242: 1437–1441

Sutter, M,L,.(2005) Spectral processing in the auditory cortex. International Review in Neurobiology. 70:253-98.

Tian, B., Rauschecker, J.P., Processing of frequency-modulated sounds in the cat's posterior auditory field. J Neurophysiology. 1998 79,2629-42

Theunissen, F.E., Sen, K., Doupe, A.J., Spectral-temporal receptive fields of nonlinear auditory neurons obtained using natural sounds. J Neuroscience. 2000 20,2315-31.

Urbach, D., and Spitzer, H. (1995). Attentional effort modulated by task difficulty. Vision Research *35*, 2169-2177.

Vázquez Marrufo, M., Vaquero, E., Cardoso, M.J., Gómez, C.M. (2001). Temporal evolution of alpha and beta bands during visual spatial attention. Brain Research. October 12(2):315-20.

Wang, X., Merzenich, M.M., Beitel, R., Schreiner, C.E., Representation of a species-specific vocalization in the primary auditory cortex of the common marmoset: temporal and spectral characteristics. J Neurophysiology. 1995 74,2685-706.

Wang, X., On cortical coding of vocal communication sounds in primates. Proc National Academy of Sciences 2000 97, 1843-9.

Weinberger, N.M., Hopkins, W., Diamond, D.M.(1984). Physiological plasticity of single neurons in auditory cortex of the cat during acquisition of the pupillary conditioned response: I. Primary field (AI). Behavioral Neuroscience. April 98(2):171-88.

Weinberger, N.M.(2007). Associative representational plasticity in the auditory cortex: a synthesis of two disciplines. Learning and Memory. January 3;14(1-2):1-16.

Winer, J.A., Lee, C.C.(2007). The distributed auditory cortex. Hearing Research. July;229(1-2):3-13.

Whitefield, I.C. and Evans, E.F. (1965), Responses of Auditory cortical neurons to stimuli of changing frequency. Journal of Neurophysiology. July;28:655-72.

Whitfield, I.C.(1980). Auditory cortex and the pitch of complex tones. Journal of the Acoustical Society of America. February; 67(2):644-7

Womelsdorf, T., Fries, P., Mitra, P.P., Desimone, R.(2006).Gamma-band synchronization in visual cortex predicts speed of change detection. Nature. February 9;439(7077):733-6.

Yantis, S. (1996). Attentional capture in vision. In: Converging operations in the study of selective visual attention, A. Kramer, M. Coles, and G. Logan, eds. (Washington, DC: American Psychological Association), pp. 45–76.

Yost, W. A (2000). fundamentals of hearing: An introduction. Academic Press, San Diego, fourth edition,